INVESTIGATING DENITRIFICATION FROM TWO MISSOURI CLAYPAN SOILS

A Dissertation

presented to

the Faculty of the Graduate School

at the University of Missouri

In Partial Fulfillment

of the Requirements for the Degree

Doctor of Philosophy

---

by

FRANK E. JOHNSON II

Dr. Robert Lerch, Dissertation Co-Advisor

Dr. Peter P. Motavalli, Dissertation Co-Advisor

December 2020

The undersigned, appointed by the dean of the Graduate School, have examined the dissertation entitled

INVESTIGATING DENITRIFICATION FROM TWO MISSOURI CLAYPAN SOILS

Presented by Frank E. Johnson II

A candidate for the degree of

Doctor of Philosophy

And hereby certify that, in their opinion, it is worthy of acceptance.

_____

Co-advisor, Professor Robert Lerch

_____

Co-advisor, Professor Peter Motavalli

_____

Professor Kristen Veum

_____

Professor Peter Scharf

ACKNOWLEDGEMENTS

I would like to acknowledge and give a big thanks to those who have helped me throughout my doctoral degree program here at the university. Without their continued support, I would not have been able to be as successful. The faculty and staff at the University of Missouri have been generous with their support in the classroom, offices, and laboratories. I would like to give a special thanks to my dissertation co-advisors, Dr. Robert Lerch and Dr. Peter Motavalli, who constantly supported me and were my biggest advocates throughout this entire dissertation process. I would like to acknowledge the staff of the Cropping Systems and Water Quality Research Unit of the USDA-ARS, specifically Ed Winchester and Elizabeth Spiegel. This project would not have been successful without them. I would also like to thank Dr. Kristen Veum and Dr. Peter Scharf for their continued support, and graciously offering their advice, and time and patience to be a part of my graduate committee. Lastly, I would like to thank my friends and family for all of their support. My parents, Frank and Yvonne Johnson, sister, Jonquilla Holmes, brothers, Jai and Rajah Johnson, grandparents, and a host of aunties and uncles have always been in my corner and reminded me that I can achieve anything. As I dealt with personal struggles, Johnnie Williams, Jennifer Casper, Alaysia Brown, Christian Aguirre and Dr. Isais Smith were there to comfort me and remind me that I would be successful throughout the matriculation of this doctoral program.

TABLE OF CONTENTS

LIST OF TABLES

LIST OF FIGURES

INVESTIGATING DENITRIFICATION FROM TWO MISSOURI CLAYPAN SOILS

Frank E. Johnson II

Robert Lerch, Dissertation Co-Advisor

Peter P. Motavalli, Dissertation Co-Advisor

ABSTRACT

Denitrification in agricultural soils is responsible for a majority of anthropogenic nitrous oxide (N_2O) production, and N_2O is a major greenhouse gas with a global warming potential ~300 times that of carbon dioxide. The objectives of this research were to: 1) compare multiple RNA-based sequencing methods for quantifying denitrification genes in soil; 2) relate denitrification gene abundance in soil to actual and potential denitrification rates in claypan soils; 3) measure actual and potential soil denitrification rates from claypan soils and understand how landscape position influences denitrification; and 4) upscale the estimates of denitrification to the field scale to understand its importance to the N budget in row crop fields. The research sites consisted of two claypan soil fields in Central Missouri. Several sets of soil cores were collected in triplicate in two landscape transects across both fields and N_2 and N_2O production were measured using a gas flow soil core incubation system. In addition, soil denitrification potential, under non-limiting conditions, was determined on 90 m-grid samples collected from the fields.

Potential and actual denitrification rates were not significantly different between fields, but potential denitrification rates were greater by almost two-fold in the toeslope position ($p < 0.10$) compared to the backslope and summit positions across, fields. In one

field, actual denitrification rates were greater in the summit landscape position while rates were greater in the backslope position in the other field. Actual denitrification in these fields predominantly resulted in N_2 emissions and N_2O accounted for a minor portion of the total flux. Although the high smectitic clay content of upland soils provides environmental conditions suitable for high N_2O flux rates, these results suggested that denitrification rates are higher in the toe-slope position due to accumulation of soil C from long-term sediment deposition. Therefore, long-term erosion patterns rather than current or recent crop management systems controlled observed spatial patterns of denitrification on these claypan fields.

One set of cores was analyzed for extractable soil RNA, and *nos*Z gene abundance using three methods: real-time quantitative polymerase chain reaction (RT-qPCR); droplet digital polymerase chain reaction (ddPCR); and nanostring sequencing techniques at two depths (0-15 cm and 15-30 cm). There were significant differences in soil RNA quantities between the two depths, with an average of 54.51 mg RNA kg soil^{-1} at 0-15 cm and 14.20 mg kg^{-1} at 15-30 cm. The low soil RNA concentrations in the subsoil prevented quantification of the *nos*Z gene abundance, and suggested low overall microbial activity below 15 cm depth in these claypan soils. Abundance of *nos*Z in the surface soil showed that ddPCR resulted in significantly greater gene copy estimates than those of RT-qPCR and nanostring sequencing ($p < 0.10$). There were no statistical differences between *nos*Z abundance when comparing RT-qPCR and nanostring sequencing. Variability of *nos*Z abundance was very minimal in both RT-qPCR and nanostring technologies. Landscape variability of the gene copy estimates in these two

fields were not similar to the actual denitrification measurement pattern. These results suggest more research should be conducted to establish the molecular sequencing technique best suited to measure genes involved in denitrification from soil samples or that gene prevalence may not effectively predict denitrification, and on these two Missouri claypan soils, most of the biological community and activity are in the top 15 cm of the soil profile.

Actual denitrification, along with other parameters for soil volumetric water content, and soil temperature were used to model and upscale estimates for denitrification at the field scale. Soil O_2, temperature, and volumetric water content (VWC) were measured at a depth of 10 cm depth at three landscape positions within each field and were used to establish a relationship between VWC and soil O_2 content. It was assumed conditions for denitrification were a soil O_2 content $\leq$5% and a soil temperature $\geq$15^{o}C, and flux estimates were corrected using a Q_{10} value of 2. For each field, daily and annual denitrification estimates were calculated for years grown under corn or wheat, due to N fertilizer application. Daily total denitrification (N_2O+N_2) estimates ranged from 0.39 kg N $ha^{-1}d^{-1}$ to 0.87 kg N $ha^{-1}d^{-1}$. The highest annual denitrification estimates were for Field 1 in 2016, in which 9.26 kg N ha^{-1} were estimated. Denitrification accounted for up to 7.6% of total applied N.

There are many facets to denitrification. This study highlights the complex relationship between denitrification and other soil characteristics. Denitrification was more strongly related to differences in soils across landscape position rather than crop management, and served as a major N-loss pathway in both fields. These results will aid

in our understanding of denitrification and demonstrates the need for denitrification mitigation strategies.

CHAPTER 1: INTRODUCTION AND OBJECTIVES

1.1 Literature Review

1.1.1 Importance of Nitrogen, Food Security

Nitrogen (N) is an important nutrient that is required by most plants for production. Nitrogen fertilizer is commonly added to crops during the growing season to increase economical crop yield. From 2011 to 2015, the global demand for N application was projected to increase from approximately 95,000 tons to 103,000 tons (FAO, 2011). This increase could be attributed to the fact that global food production needs to be increased by at least 70% to feed an additional 2.3 billion people as projected in 2050, increasing the pressure on land and water resources (FAO, 2009; Delaney, 2013; Spiertz 2010). Also, the world population has increased by 78% and the amount of active N in the environment has increased by 120% since 1970 (Galloway et al., 2008). Research has shown wheat yields increased 2 to 3 fold with the addition of N-fertilizer (Rasmussen et al., 1998). For corn, the most important grain crop globally (Green et al., 2018), yields increased from 3 to 14 t ha with N-fertilizer application (Dobermann and Cassman, 2002). Other research suggests the use of N-fertilizers have nearly doubled grain crop yields (Lassaletta et al., 2014). Over 36% of the global corn is produced in the United States, with roughly 33% grown in the Midwest Corn Belt (Ort and Long, 2014; FAO, 2017).

1.1.2 Nitrogen Loss Processes

Unfortunately, 41 – 50% of the applied N-fertilizer since the 1950s has been estimated to have been lost to the environment through N loss processes (Ladha et al., 2016). Nitrate leaching pose a significant threat to water quality systems (Chiwa et al., 2012), significantly impacting environmental and human health (Cameron et al., 2013). Nitrate toxicity has been linked to

cancer and other serious health conditions if ingested through drinking water (Grizzetti et al., 2011). In aquatic systems, increased concentrations of NO_3^- can lead to anoxic conditions, impacting fish communities (Cameron et al., 2013). Ju and Zhou (2017) found that ammonia (NH_3) volatilization, nitrate (NO_3^-) leaching, and denitrification accounted for roughly 23, 18, and 2% of the applied N fertilizer, respectively. Similarly, the findings of Zhou et al. (2016) concluded that NH_3 volatilization and NO_3^- leaching were the main N loss pathways in a subtropical wheat-maize system, constituting 78 and 93% of hydrological and gaseous N-losses, respectively.

1.1.3 Problem of Greenhouse Gas Emissions

Carbon dioxide (CO_2), methane (CH_4) and nitrous oxide (N_2O) are main greenhouse gases (GHGs) that have significantly increased the radiative forcing of the Earth's atmosphere (Prather et al. 1994). This increase is partly attributed to the longevity of these main GHGs in the atmosphere, often taking decades break down (IPC, 2007). Human activity is also responsible for increasing GHG emissions through the burning of fossil fuels and changes in land usage (USEPA, 2018). Between 2000 and 2012, CO_2 emissions increased by 2.9% (Olivier et al., 2013). Since pre-industrial levels, CH_4 and N_2O concentrations have increased by approximately 150% and 20%, respectively (IPCC, 2007). Most of the N_2O emissions can be attributed to the increased usage of N-based fertilizers. In 2005, the global concentration of N_2O was 319 ppb (IPCC, 2007), and it is anticipated to increase by up to 60% by 2030 (FAO, 2003). In 2016, U.S. N_2O emissions were 13% higher than in 1990, with agriculture responsible for roughly 77% of total N_2O emissions. (USEPA, 2018). With a global warming potential (GWP) approximately 300 times greater than that of CO_2, and 12 times greater than that of CH_4 (Forster et al., 2007),

N_2O is involved in ozone destruction within the troposphere (IPCC, 2001). Thus, even small amounts of N_2O emissions from agricultural systems can have detrimental environmental impacts (Venterea et al., 2012).

As a result of increased GHG emissions through anthropogenic activity, scientists have been concerned as the Earth has continued to get warmer (IPCC, 2007). Global temperatures have already increased by roughly 0.4°C since 1980 (IPCC, 2001). By 2100, average global temperatures are expected to increase as high as 4.8°C (Hayhoe et al., 2017). Temperatures have risen in the Midwestern United states by more than 1.0°C between 1900 and 2010, with a majority of the warming occurring between 1980 and 2010. Due to some of the impacts GHG's have on the environment, the United States' Environmental Protection Agency (USEPA) has set goals for decreasing national (and global) GHG emissions as part of its strategy to adapt to climate change.

1.1.4 Nitrification, Denitrification, and Influential Factors

Nitrous oxide has a residence time of 118 years in the atmosphere (Prather and Hsu, 2010). Nitrous oxide in soil is produced primarily through the processes of autotrophic nitrification and heterotrophic denitrification (Braker and Conrad, 2011). Nitrification is the microbial facilitated enzymatic process in which ammonium (NH_4^+) (or ammonia (NH_3)) is oxidized to nitrate (NO_3^-). Denitrification is the microbial facilitated reduction of nitrate (NO_3^-) to dinitrogen (N_2), with other gases such as N_2O, and nitric oxide (NO), being formed as intermediates (Robertson and Groffman, 2007). Most enzymes involved in denitrification include a metal co-factor such as Mo, Fe, Cu, or Zn (Signor and Cerri, 2013). Nitrifier denitrification and

chemo-denitrification are two other process that can result in N_2O emissions (Venterea et al., 2012). Nitrifier denitrification is the pathway in which ammonia is oxidized to nitrite (NO_2^-), then reduced to NO, N_2O, and N_2 (Wrage et al., 2001). Chemo-denitrification occurs when NO_2^-, an intermediate in denitrification, reacts with organic compounds and forms N_2O and N_2 (Stevens and Laughlin, 1998). Further, indirect denitrification may occur when N compounds are transported to other environmental reservoirs (Venterea et al., 2012). In all, nitrification and denitrification are responsible for approximately 50% of the global human N_2O emissions (IPCC, 2007).

Nitrogen fertilizer rate is the best single variable estimator of soil N_2O emissions (Shcherbak et al., 2014). Bouman et al. (2002) observed a significant increase in N_2O emissions as N application rate increased. Fertilizer composition is another important factor that can influence N_2O emissions. The most common forms of N-based fertilizers include anhydrous ammonia, urea, and urea-ammonium nitrate solutions. Bouman et al. (2002) observed lower N_2O emissions for nitrate-based fertilizers compared to ammonium-based fertilizers, animal manure, and a combination of the two. As fertilizer rate increased, Liang and MacKenzie (1994) observed denitrification production increased linearly. At fertilization rates of ≤ 250 kg ha^{-1}, Wang et al. (2018) observed an exponential increase in soil denitrification rates. The application of potassium in addition to N fertilizer also increases N_2O emissions by 46-175% compared to N fertilizer application only (Li, 2020).

Along with N-fertilization application and rate, other field management practices, such as tilling, influence denitrification. Groffman (1985) compared nitrification and denitrification fluxes between no-tillage (NT) and conventional tillage (CT) agricultural systems. He reported

high nitrification and denitrification rates in the top 5 cm of the NT system, but higher rates at the 5 – 13 and 13 – 21cm depths of the CT system. Mkhabela et al. (2008) also observed higher N_2O rates in fields under NT compared to CT. They also reported lower $N_2O/(N_2O+N_2)$ in fields under NT, suggesting complete denitrification to N_2 was more prevalent under NT systems. On the contrary, Elmi et al. (2003) measured N_2O production under three different tillage systems (NT, CT, and reduced tillage) and observed similar N_2O emissions under each system.

Soil volumetric water content (VWC) is a significant factor influencing denitrification, as it is an indication of oxygen presence (Heinen, 2006). Spatial patterns of N_2O emissions have been observed to be associated with soil VWC (Poblador et al., 2017). A water-filled pore space (WFPS) between 60 – 70% provides ideal conditions for N_2O production to occur through nitrification(Bateman and Baggs 2005; Akiyama et al., 2013). There is an exponential relationship between denitrification rate and soil moisture between 20 and 40% gravimetric water content (Machefert and Dise, 2004). In sandy and loamy soils, Mekala and Nambi (2017) reported significant denitrification at > 90% VWC. Tan et al., (2016) also observed an overall increase in denitrification as a function of high VWC.

Temperature is another significant driver of denitrification. Grundmann et al. (1995) observed maximum soil nitrification occurred at temperatures between 20 and 25 °C. Nitrification rates tend to slow down when the soil temperature is around 10 °C (Sabey et al., 1956). Saturated, anoxic soils are ideal conditions for denitrification to occur (Linn and Doran, 1984). As soil temperature increases, denitrifier activity increases in a linear relationship, with the maximum activity occurring at 25 °C (Braker et al., 2010). Phillips et al. (2015) observed an increase in mean N_2O and N_2 fluxes between 19 and 35 °C. Other studies have observed

maximum denitrification for a system occurring at 40 °C, with N_2 production dominating above 40 °C (Lai et al., 2019). However, denitrification occurring between 0 and 35 °C is The Q_{10} value defines the sensitivity of a reaction rate for every 10 °C increase. For denitrification resulting in N_2O and N_2 production, the Q_{10} are 2.0 and 1.4, respectively (Stanford et al., 1975; Phillips et al., 2015). Yu et al. (2020) reports Q_{10} values ranging from 1.31 to 2.98 for N_2O, and from 1.69 to 3.83 for N_2, suggesting N_2 production rates are more sensitive to changes in temperature than N_2O between 15 and 35 °C.

Soil pH shapes soil microbial communities over a long period of time (Lauber et al., 2009; Zhalnina et al., 2015), and is considered a master variable for N_2O production in soils (Qu et al., 2014), significantly impacting denitrification production (Čuhel et al., 2010; Cheng et al., 2013). Early research suggest the optimum pH for denitrification is between 7.0 and 8.0 (Van Cleemput and Patrick, 1974). Simek et al. (2002) determined the soil pH at which short (30 – 90 min) and long (6 – 48 hr) term denitrification were likely to occur. They observed the optimum pH for short-term denitrification is near natural soil pH, and between 6.6 and 8.3 for long-term denitrification. This is supported by Parkin et al. (1985), who suggested prolonged exposure to low pH causes denitrifying communities to adapt to the low-pH environment. Simek et al. (2002) also observed predominantly N_2O at $pH < 7$ and predominantly N_2 at $pH > 8$.

Soil organic matter (including soil organic C) is an important factor for many microbial processes such as denitrification (Ullah and Faulkner, 2006), as it is necessary for microbial growth and development. Studies have substantiated the significant positive relationship between denitrification potential and soil organic matter (Groffman and Crawford, 2003; Gift et al., 2010). Results of Weier et al. (1993) and Rozas et al. (2001) indicate that C availability was the

most significant limiting factor, even at low NO_3^- concentrations. Denitrification rarely occurs deep within the soil profile, likely due to the low abundance of denitrifiers as a result of low organic C concentration (Chen et al., 2018). Barrett et al. (2016) found that either partial or complete denitrification is dependent on the carbon source. When their samples were treated with glucose-C, partial denitrification was dominant indicated by higher N_2O fluxes. Dissolved organic C resulted in complete denitrification to N_2.

1.1.5 Denitrification Mitigation Strategies

Polymer-coated fertilizers are enhanced efficiency fertilizers that release nutrients by diffusion through a semi-permeable polymer membrane. The release rate of the PCF's is dependent on the composition and thickness of the polymer (Akiyama et al., 2009). A significant advantage of PCF's includes the opportunity to synchronize N release with plant demand, leading to a decrease in environmental N loss (Shaviv, 2001). In a study conducted by Tian et al. (2015), they observed a 52% decrease in N_2O emissions with the use of polymer-coated urea (PCU). Other reported reduction were as low as 14%, and as high as 58% (Akiyama et al., 2009). On a Minnesota loamy sand, Hyatt et al. (2010) observed a significant reduction in N_2O emissions with the use of PCU compared to conventional fertilizers in fields grown under potatoes. In contrast, Akiyama et al. (2013) did not observe a decrease in N_2O emissions with PCU application.

Using urease and nitrification inhibitors (UIs and NIs) in combination with PCF's have the potential to substantially reduce environmental N loss (Lam et al., 2018). Urease inhibitors disrupt the enzyme urea amidohydrolase, which catalyzes the hydrolysis of urea into ammonia

and carbon dioxide. The activity of urease is responsible for a majority of N lost through NH_3 volatilization (Upadhyay, 2012) since urea accounts for >60% fertilizer sold worldwide (Prud'homme, 2016). The most common UI is Agrotain (N-(n-butyl) thiophosphoric triamide), also known as NBPT (Cantarella et al., 2018), and has been proven to reduce NH_3 volatilization after N application under temperate soils by 22 to 47% (Sing et al., 2013; Suter et al., 2013). The use of NBPT also decreased N_2O production by up to 62% (Sing et al., 2013; Lam et al., 2018). Nitrification inhibitors slow the microbial facilitated transformation of NH_4^+ to NO_3^{-1}, which decreases available substrate for denitrification (Zerulla et al., 2001). Commonly studied NIs include DMPP (3,4-dimethylpyrazol-phosphate), DCD (dicyandiamide), and nitrapyin (2-chloro-6-(trichloromethyl) pyridine) (Zerulla et al., 2001; Liu et al., 2013; Elmi et al., 2017; Calderon et al., 2005; Niu et al., 2018). Recent studies have shown N_2O emissions can potentially be reduced by 15 to 87% with the use of NIs compared to conventional fertilizers (Lam et al., 2018; Liu et al., 2013; Steusloff et al., 2019; Khalil et al., 2009). Utilizing a combination of both UIs and NIs may provide further significant reduction in denitrification emissions. In a study conducted by Pereira et al. (2013), they observed a 92% decrease in NO emissions and a 75% decrease in N_2O emissions relative to the UI alone.

1.1.6 Measuring Denitrifier Enzyme Activity in Soils Using Next Generation Sequencing Techniques.

A main goal of soil microbial research includes understanding what microorganisms are present and assessing their abundance and activity. (Zimmerman et al., 2014). Cultural laboratory methods have traditionally been used to determine the presence of specific microorganisms or groups of related microbes. However, it has been estimated that roughly 99%

of the soil microorganisms are unculturable (Davis et al., 2005; Epstein, 2013). Utilizing DNA sequencing methods allows for the study of those unculturable microorganisms. Currently, there are roughly 652 microorganisms that contain the genes for enzymes involved in denitrification (Graf et al., 2014). Figure 1.1 is an illustration of the denitrification pathways and genes associated with each step. Some genes have been observed in both denitrifying and non-denitrifying microorganisms, making the estimates for denitrification that much more difficult (Hendriks et al., 2000).

There are several sequencing methods for DNA that enable the quantification of specific genes present in a sample. In some cases, based on the sequence of the DNA primer, a specific organism or species can be identified. Reverse-transcriptase quantitative polymerase chain reaction (RT-qPCR) is considered the gold standard for gene expression analysis and quantification due to its accuracy, sensitivity, and rapid results (Derveaux et al., 2010). The RT-qPCR occurs in three steps. First, RNA is converted to cDNA. Next, the cDNA is amplified using the PCR. The last step is the quantification of amplification products in real time (Gibson et al., 1996). The only difference between real-time qPCR and RT-qPCR is the starting molecule. Real-time qPCR is DNA-based while RT-qPCR is RNA based. Other sequencing technology includes DNA microarray analysis, Roche/454 FLX pyrosequencing, Illumina sequencing, Sanger sequencing, and SOLiD sequencing (Mardis, 2008). The use of a microarray involves a microchip that contains arrays of DNA elements that can be related to a particular gene expression. Pyrosequencing utilizes DNA polymerase to add nucleotides and involves the release of pyrophosphate in the end, activating a luciferase enzyme that produces light. The production of light is related to the number of nucleotides that are added, and serves as the basis for

quantification (Mardis, 2008). Sanger sequencing has been widely utilized to analyze environmental and clinical samples (Iaconelli et al., 2017; Mancini et al., 2018; Trabaud et al., 2017; Tsiatis et al., 2010). This method also allows for the identification of specific sequences and can provide sequences up to 1000 base pairs long (Sanger et al., 1977; Zimmerman et al., 2014). Similar to pyrosequencing, SOLiD DNA library is created on beads, however, sequences are read twice, making it highly accurate (Hurd and Nelson, 2009). Nanostring sequencing is a relatively new technology that has been critical in clinical research (Norton et al., 2013; Saba et al., 2015; Scott et al., 2013) and to understand microbial N dynamics in agricultural soils (Cloutier et al., 2019). The nCounter system, developed by Nanostring Technologies, performs gene detection by assigning unique bar codes containing capture probes, and then fluorescence is quantified with a digital analyzer (Geiss et al., 2008; Cloutier et al., 2019). There are many advantages to utilizing the nCounter. First, it can analyze multiple DNA or mRNA targets without PCR. Second, the DNA and mRNA probes are highly specific, meaning only the target sequence will be detected. Lastly, it can detect molecules present in low abundance. Since the nCounter has a high specificity, major drawbacks with this method include its inability to detect unidentified genes (Cloutier et al., 2019).

Droplet digital polymerase chain reaction (ddPCR) uses Taq polymerase chemistry for genetic amplification (Taylor et al., 2017) and is conducted in four steps. After RNA isolation and the necessary primer, probe, and supermix are prepared, the samples are placed into a droplet generator that partitions the samples into roughly 20,000 droplets at the nL size. Next, the droplets are amplified through PCR using a thermocycler. Once amplification is complete, the sample is placed in a droplet reader that uses a two-color detection system to determine whether

the targeted sequence is present. Lastly, the ddPCR software determines the concentration in the sample by comparing the number of positive and negative reads (Bio-Rad Laboratories, Inc.). Droplet digital PCR follows Poisson statistics, with the equation,

$\lambda = -\ln(1-p)$, being used for endpoint calculations. Here, λ represents the average number of target sequences per replicate reaction and p is the fraction of positive end-point reactions (Hindson et al., 2011)

Droplet digital polymerase chain reaction provides researchers with a quick, robust, cheaper and accurate way of understanding and quantifying functional genes. It has been highly utilized in the medical field, including HIV quantification (Trypsteen et al., 2016) and quantification of donor DNA for transplant recipients (Beck et al., 2013). In addition, this method has also been used in environmental samples to quantify DNA and estimate the distribution of aquatic animals from a fish farm (Doi et al., 2015) and estimate the number of rotavirus present in water samples (Rački et al., 2014). The ddPCR mechanism has also been used to study soil microbiology. For instance, ddPCR was used to measure the relative abundance of various *Aspergillus* species in a vineyard soil (Palumbo et al., 2016). Dong et al. (2014) evaluated ddPCR to characterize plasmid reference material that was used for quantifying ammonia oxidizers and denitrifiers from a coarse loamy soil under cotton – spring maize rotation in China. Currently, there are not any studies that have applied ddPCR technology to study denitrification in soils, which makes this proposed study unique (see below). However, other quantification techniques, such as qPCR, have been used to quantify functional genes responsible for a range of processes in soils. These studies have included quantification of genes capable of degrading contaminants in soils, such as polycyclic aromatic hydrocarbons (Shahsavari et al.,

2016) and the herbicide atrazine (Thompson et al., 2010). In addition, qPCR has been applied to quantification of genes associated with nitrate-reducing bacteria (López-Gutiérrez et al., 2004) and the *nos*Z gene which codes for nitrous oxide reductase (Henry et al., 2006). Tomasek et al. (2017) analyzed sediment samples from an agricultural watershed for *nor*B, *nar*G, *nir*S, *nir*K, and *nos*Z and Smith et al. (2007) measured the abundance of nitrate and nitrite reductase genes in estuarine sediments using qPCR analysis.

Having been developed in 2011 (Hindson et al., 2011), there are many advantages to ddPCR. One advantage is during analysis, a standard curve does not need to be developed to determine sample concentration (Taylor et al., 2017). Avoiding the development of a curve will make results more comparable amongst researchers (Koepfli et al., 2016). In other types of real time qPCR, a standard curve is necessary to determine absolute quantification of gene copies. A second advantage is ddPCR is more accurate and precise than qPCR. Hindson et al. (2013) conducted a study in which they compared microRNA quantification by both ddPCR and qPCR. Their results showed ddPCR decreased variability amongst samples between 37 and 86%. Accuracy can also be attributed to the probe that is utilized in ddPCR. Thompson et al. (2010) conducted a study in which they estimated the abundance of atrazine chlorohydrolase gene, *atzA*, in soils using both a TaqMan probe chemistry and SYBR Green real-time qPCR chemistry. They observed that the TaqMan probe had the sensitivity to detect lower copy numbers in samples and provided more consistent, repeatable, and accurate results compared to the SYBR analysis. Furthermore, Hindson et al. (2013) also observed that ddPCR provided greater reproducibility of results across days compared to qPCR by a factor of roughly seven. Koepfli et al. (2016) also observed greater reproducibility in the results from ddPCR compared to qPCR when measuring

the abundance of *P. falciparum* and *P. vivax* in clinical patients. A third advantage is ddPCR is sensitive enough to obtain measurements from samples with low quantities of target sequence and low contamination. In a study conducted by Taylor et al. (2017), they directly compared results from ddPCR and qPCR analysis using purified synthetic DNA. It was observed that when samples contained low quantities of target sequence, both ddPCR and qPCR showed similar numbers of detection. However, when the samples contained certain contaminants that hindered the activity of Taq polymerase, the efficiency of qPCR decreased. Rački et al. (2014) also observed improved success when using ddPCR on environmental samples containing contaminants compared to qPCR. During this study, the acceptable number of droplets were obtained with every contaminant in their study except for the samples with humic acid, which was slightly below the acceptable criterion.

Even though ddPCR has many benefits, its major limitation is that it requires prior knowledge about the targeted gene or species must be known for primer development. It is also possible, but very unlikely, the wrong base pairs are integrated during the polymerization process (Garibyan and Avashia, 2013). In a study comparing two genes that code for nosZ, Orellana et al. (2014) observed that the two genes share 60.9% ± 8.2% nucleotide identity. Results from ddPCR analysis provides the opportunity to quantify gene expression for the denitrifying community and relate it to actual denitrification measurements that occur in the field. This is similar to that of N*é*meth (2012), in which they quantified specific genes involved in the N-cycle and compared them to the spring-thaw microbial N_2O flux in corn fields. Thus, denitrifying enzyme abundance can be related to soil conditions in the field, such as landscape position, soil moisture, soil temperature, and soil oxygen levels. Currently, there is a gap in the literature that

pertains to relating denitrifying gene quantity to the denitrifying community in soils in general, but more specifically, on poorly drained claypan soils.

1.2 Need for the Research

Claypan soils occupy roughly 4 million ha across the Midwest, including Missouri, Illinois, and Kansas (Anderson et al., 1990). Argillic horizons are the major contributor to the poor drainage of claypan soils, resulting in very low saturated hydraulic conductivity (K_{sat}) when they are wet. During significant rainfall events that saturate the claypan, a perched water table can develop above the claypan, causing lateral sub-surface flow known as interflow (Minshall and Jamison, 1965; Blanco-Canqui et al., 2002). The physical characteristics of claypan soils combined with a humid, temperate rainfall pattern creates optimal conditions for denitrification to occur as prolonged saturated conditions may persist throughout the landscape, not just in lower topographic areas.

Furthermore, previous research suggests that gaseous emissions of applied N fertilizer may be the major loss pathway for N in agricultural production systems, especially in poorly drained soils. On a silty clay loam in Venice, Italy, Gumiero et al. (2011) observed high denitrification rates from soil horizons saturated by a perched water table. Similarly, Burt et al. (2002) concluded denitrification rates increase as the water table becomes elevated in the profile, especially for longer periods of time. In a study conducted by Blevins et al. (1996), they applied ^{15}N-nitrate fertilizer in a northern Missouri field over two growing seasons. Using a mass balance approach, the study directly measured the ^{15}N in soil, water, and plants (corn). After the two growing seasons, roughly 38% of the N was unaccounted for and was no longer present in

the soil-water-plant system. Approximately 30% of the N was present in the saturated zone of the soil, 27.3% in the grain, and roughly 5% was present in the unsaturated zone of the soil. It is speculated that the unaccounted N was lost from the soil through denitrification. Furthermore, there are hotspots and hot moments that occur, in which soil N_2O emissions may be high in a particular area in the field for a short amount of time (Groffman et al., 2009). Obtaining a greater understanding about the denitrifying community could provide a better understanding of both the spatial and temporal variability of soil N_2O emissions. This research also aims to provide information on the relationship between denitrifier gene abundance and emissions of the different gas products of denitrification since this has not been definitively established (Butterbach-Bahl et al., 2013). To help establish this relationship, it important to recognize gene presence, gene abundance, and gene distribution within the environment as important factors (Smith and Osborn, 2009). The studies presented below represent an integrated approach to studying denitrification in claypan soils. The overarching goal of these studies will be to quantify the spatial and temporal variation in denitrification in two claypan fields with contrasting crop management.

1.3 Objectives and Hypothesis

Primary Research Objective

To estimate denitrification and investigate the spatial distribution of denitrification and denitrification gene abundance, on poorly drained claypan soils.

Specific Research Objectives

1. Relate abundance of *nos*Z to measured denitrification flux from soil cores collected across landscape transects.
2. Use the denitrification enzyme activity (DEA) for measuring spatial dependence and variation from grid samples collected from two fields and relate DEA N_2O flux to *nos*Z gene abundance and total denitrification flux of the soil cores.
3. Use the data from soil cores, DEA assays, and high resolution field sensor data (soil moisture, temperature, and oxygen), to develop field-scale denitrification estimates and determine its importance to the N budget.

Specific Research Hypotheses

1. Denitrification is a major loss pathway of N fertilizer in claypan soils compared.
2. Denitrification is influenced by soil properties that vary with landscape position, rather than management strategies.

1.4 Potential Significance of Research

Denitrification is a difficult process to study as it encompasses a wide array of environmental variables. This research will aid in the scientific understanding of the process of denitrification and the inter-relationships between soil properties, environmental variables, denitrifying genes and expression, and the denitrifying microbial community. With the wealth of data collected in association with this study and the statistical analyses, the development of field-scale maps for denitrification potential of the surface soils, and computation of seasonal and annual denitrification rates at the field-scale based on the sensor data will aid in our understanding of how important denitrification is to the N budget of agricultural systems. This

work supports algorithms for predicting denitrification at the field-scale, and thus, improve the ability of existing computer models to simulate N dynamics. Furthermore, this work will contribute to a better understanding of the contribution of agricultural production systems to soil N_2O emissions from soils and their impact on global climate change. From a management perspective, understanding the magnitude of denitrification and its potential relationship to landscape position, management, and season will lead to recommendations for crop and soil management practices that improve N fertilizer use efficiency and decrease greenhouse gas emissions.

1.5 Dissertation Organization

This dissertation is organized in a series of five chapters. Chapter 1 was the literature review that discussed the need to better understand denitrification, past and present problems with N_2O emissions, how environmental factors influence denitrification, how management strategies impact denitrification, and the molecular methods that are utilized to understand the soil microbial denitrifying community. Spatial variability of actual and potential N_2O emissions on Missouri claypan soils is discussed in chapter 2. Chapter 3 is a comparative analysis of three next-generation sequencing techniques measuring nosZ abundance in Missouri claypan soils. Chapter 4 models and estimates denitrification rates at the field scale on Missouri claypan soils. The close of the dissertation is chapter 5, which discusses the overall conclusions of this research.

1.6 References

Akiyama, H., X. Yan, and K. Yagi. 2009. Evaluation of effectiveness of enhanced-efficiency fertilizers as mitigation options for N2O and NO emissions from agricultural soils: meta-analysis: Mitigation options for N2O and NO emissions. Global Change Biology 16(6): 1837–1846. doi: 10.1111/j.1365-2486.2009.02031.x.

Akiyama, H., S. Morimoto, M. Hayatsu, A. Hayakawa, S. Sudo, et al. 2013. Nitrification, ammonia-oxidizing communities, and N2O and CH4 fluxes in an imperfectly drained agricultural field fertilized with coated urea with and without dicyandiamide. Biol Fertil Soils 49(2): 213–223. doi: 10.1007/s00374-012-0713-2.

Anderson, S.H., C.J. Gantzer, and J.R. Brown. 1990. Soil physical properties after 100 years of continuous cultivation. J. Soil and Water Conserv. 45: 117-121.

Barrett, M., M.I. Khalil, M.M.R. Jahangir, C. Lee, L.M. Cardenas, et al. 2016. Carbon amendment and soil depth affect the distribution and abundance of denitrifiers in agricultural soils. Environ Sci Pollut Res 23(8): 7899–7910. doi: 10.1007/s11356-015-6030-1.

Bateman, E.J., and E.M. Baggs. 2005. Contributions of nitrification and denitrification to N2O emissions from soils at different water-filled pore space. Biology and Fertility of Soils 41(6): 379–388. doi: 10.1007/s00374-005-0858-3.

Beck, J., S. Bierau, S. Balzer, R. Andag, P. Kanzow, J. Schmitz, J. Gaedcke, O. Moerer, J.E. Slotta, P. Walson, O. Kollmar, M. Oellerich, and E. Schutz. 2013. Digital Droplet PCR for Rapid Quantification of Donor DNA in the Circulation of Transplant Recipients as a Potential Universal Biomarker of Graft Injury. Clinical Chemistry 59(12): 1732–1741. doi: 10.1373/clinchem.2013.210328.

Blanco-Canqui, H., C.J. Gantzer, S.H. Anderson, E.E. Alberts, and F. Ghidey. 2002. Saturated Hydraulic Conductivity and Its Impact on Simulated Runoff for Claypan Soils. Soil Sci. Soc. Am. J. 66(5): 1596. doi: 10.2136/sssaj2002.1596.

Blevins, D.W., D.H. Wilkison, B.P. Kelly, and S.R. Silva. 1996. Movement of nitrate fertilizer to glacial till and runoff from a claypan soil. J. Environ. Qual. 25:584-593. doi: 10.2134/jeq1996.00472425002500030026x.

Bouwman, A.F., L.J.M. Boumans, and N.H. Batjes. 2002. Emissions of N 2 O and NO from fertilized fields: Summary of available measurement data: Summary of NO and N2O measurement data. Global Biogeochem. Cycles 16(4): 6-1-6–13. doi: 10.1029/2001GB001811.

Braker, G., J. Schwarz, and R. Conrad. 2010. Influence of temperature on the composition and activity of denitrifying soil communities: Temperature effects on soil denitrifier communities. FEMS Microbiology Ecology: no-no. doi: 10.1111/j.1574-6941.2010.00884.x.

Braker, G. and R. Conrad. 2011. Diversity, structure, and size of N_2O-producing microbial communities in soils-what matters for their functioning? Advances in Applied Microbiology. 75:33-70.

Burt, T.., G. Pinay, F.. Matheson, N.. Haycock, A. Butturini, J.. Clement, S. Danielescu, D.. Dowrick, M.. Hefting, A. Hillbricht-Ilkowska, and V. Maitre. 2002. Water table fluctuations in the riparian zone: comparative results from a pan-European experiment. Journal of Hydrology 265(1–4): 129–148. doi: 10.1016/S0022-1694(02)00102-6.

Butterbach-Bahl, K. E.M. Baggs, M. Dannenmann, R. Kiese, and S. Zechmeister-Boltenstern. 2013. Nitrous oxide emissions from soils: how well do we understand the processes and their controls? Philosophical Transactions of the Royal Society B. 368

Calderon, FJ. G.W. McCarty, and J.B. Reeves, III. 2005. Nitrapyrin delays denitrification on manured soils. Soil Sci. 170(5): 350-359. doi: 10.1097/01.ss.0000169905.94861.c7.

Cameron, K.C., H.J. Di, and J.L. Moir. 2013. Nitrogen losses from the soil/plant system: a review: Nitrogen losses. Ann Appl Biol 162(2): 145–173. doi: 10.1111/aab.12014.

Cantarella, H., R. Otto, J.R. Soares, and A.G. de B. Silva. 2018. Agronomic efficiency of NBPT as a urease inhibitor: A review. Journal of Advanced Research 13: 19–27. doi: 10.1016/j.jare.2018.05.008.

Chen, S., F. Wang, Y. Zhang, S. Qin, S. Wei, et al. 2018. Organic carbon availability limiting microbial denitrification in the deep vadose zone: Carbon limits denitrification in deep vadose zone. Environ Microbiol 20(3): 980–992. doi: 10.1111/1462-2920.14027.

Cheng, Y., J. Wang, B. Mary, J. Zhang, Z. Cai, et al. 2013. Soil pH has contrasting effects on gross and net nitrogen mineralizations in adjacent forest and grassland soils in central Alberta, Canada. Soil Biology and Biochemistry 57: 848–857. doi: 10.1016/j.soilbio.2012.08.021.

Chiwa, M., N. Onikura, J. Ide, and A. Kume. 2012. Impact of N-saturated upland forests on downstream N pollution in the Tatara river basin, Japan. Ecosystems 15(2): 230–241. doi: 10.1007/s10021-011-9505-z.

Cleemput, O.V., W.H. Patrick, and R.C. McIlhenny. 1976. Nitrite decomposition in flooded soil under different pH and redox potential conditions. Soil Sci. Soc. Am. J. 40(6): 55-60.

Cloutier, M.L., A. Bhowmik, T.H. Bell, and M.A. Bruns. 2019. Innovative technologies can improve understanding of microbial nitrogen dynamics in agricultural soils. Agric. environ. lett. 4(1): 1–6. doi: 10.2134/ael2019.08.0032.

Čuhel, J., M. Šimek, R.J. Laughlin, D. Bru, D. Chèneby, et al. 2010. Insights into the effect of soil pH on N_2O and N_2 emissions and denitrifier community size and activity. AEM 76(6): 1870–1878. doi: 10.1128/AEM.02484-09.

Davis. K.E.R., S.J. Joseph, and P.H. Janssen. 2005. Effects of growth medium, inoculum size, and incubation time on culturability and isolation of soil bacteria. Appl. Environ. Microbiol. 71:826-834.

Delaney, K.R. 2013. Children, hunger, and poverty. Journal of Child and Adolescent Psychiatric Nursing. 27(1): 45-47.

Derveaux, S., J. Vandesompele, and J. Hellemans. 2010. How to do successful gene expression analysis using real-time PCR. Methods 50(4): 227–230. doi: 10.1016/j.ymeth.2009.11.001.

Dobermann, A., and K.G. Cassman. 2002. Plant nutrient management for enhanced productivity in intensive grain production systems of the United States and Asia. In: Horst, W.J., Bürkert, A., Claassen, N., Flessa, H., Frommer, W.B., et al., editors, Progress in Plant Nutrition: Plenary Lectures of the XIV International Plant Nutrition Colloquium. Springer Netherlands, Dordrecht. p. 153–175

Doi, H., K. Uchii, T. Takahara, S. Matsuhashi, H. Yamanaka, and T. Minamoto. 2015. Use of droplet digital PCR for estimation of fish abundance and biomass in environmental DNA Surveys. PLOS ONE 10(3): e0122763. doi: 10.1371/journal.pone.0122763.

Dong, L., Y. Meng, J. Wang, and Y. Liu. 2014. Evaluation of droplet digital PCR for characterizing plasmid reference material used for quantifying ammonia oxidizers and denitrifiers. Anal Bioanal Chem 406(6): 1701–1712. doi: 10.1007/s00216-013-7546-1.

Drury, C.F., X. Yang, W.D. Reynolds, W. Calder, T.O. Oloya, et al. 2017. Combining urease and nitrification inhibitors with incorporation reduces ammonia and nitrous oxide emissions and increases Corn Yields. J. Environ. Qual. 46(5): 939–949. doi: 10.2134/jeq2017.03.0106.

Elmi, A.A., C. Madramootoo, C. Hamel, and A. Liu. 2003. Denitrification and nitrous oxide to nitrous oxide plus dinitrogen ratios in the soil profile under three tillage systems. Biology and Fertility of Soils 38(6): 340–348. doi: 10.1007/s00374-003-0663-9.

Epstein, SS. 2013. The phenomenon of microbial uncultivability. Curr. Opin. Microbial. 16:636-642.

Food and Agricultural Organization (FAO). 2009. Global agriculture towards 2050. Rome, Italy: FAO. Available at http://www.fao.org/fileadmin/templates/wsfs/docs/Issues_papers/HLEF2050_Global_Agriculture.pdf. (verified 6 October, 2020).

Food and Agricultural Organization (FAO). 2011. Current world fertilizer trends and outlook to 2015. Rome, Italy: FAO. Available at http://www.fao.org/3/a-av252e.pdf. (verified 6 October 2020).

Food and Agriculture Organization (FAO). 2017.. FAO Statistical Databases, http://faostat.fao.org (2017).

Forster, P., V. Ramaswamy, P. Artaxo, T. Berntsen, R. Betts, D.W. Fahey, J. Haywood, J. Lean, D.C. Lowe, G. Myhre, J. Nganga, R. Prinn, G. Raga, M. Schulz and R. Van Dorland, 2007: Changes in atmospheric constituents and in radiative Forcing. In: Climate Change 2007: The physical science basis. Contribution of Working Group I to the Fourth Assessment Report of the Intergovernmental Panel on Climate Change [Solomon, S., D. Qin, M. Manning, Z. Chen, M. Marquis, K.B. Averyt, M.Tignor and H.L. Miller (eds.)]. Cambridge University Press, Cambridge, United Kingdom and New York, NY, USA.

Freney, J.R., O.T. Denmead, and J.R. Simpson. 1979. Nitrous oxide emission from soils at low moisture contents. Soil Biol. Biochem. 11:167-173.

Galloway, J.N., A.R. Townsend, j.W. Erisman, M. Bekunda, Z. Cai, J.R. Freney, L.A. Martinelli, S.P. Seitzinger, and M.A. Sutton. 2008. Transformation of the nitrogen cycle: recent trends, questions, and potential solutions. Science. 320:889-892.

Garibyan, L., and N. Avashia. 2013. Polymerase Chain Reaction. Journal of Investigative Dermatology 133(3): 1–4. doi: 10.1038/jid.2013.1.

Geiss, G.K., R.E. Bumgarner, B. Birditt, T. Dahl, N. Dowidar, et al. 2008. Direct multiplexed measurement of gene expression with color-coded probe pairs. Nat Biotechnol 26(3): 317–325. doi: 10.1038/nbt1385.

Gibson, U.E., C.A. Heid, and P.M. Williams. 1996. A novel method for real time quantitative RT-PCR. Genome Research 6(10): 995–1001. doi: 10.1101/gr.6.10.995.

Gift, D.M., P.M. Groffman, S.S. Kaushal, and P.M. Mayer. 2010. Denitrification potential, root biomass, and organic matter in degraded and restored urban riparian zones. Restoration Ecology 18(1): 113–120. doi: 10.1111/j.1526-100X.2008.00438.x.

Graf, D.R.H., C.M. Jones, and S. Hallin. 2014. Intergenomic comparisons highlight modularity of the denitrification pathway and underpin the importance of community structure for n(2)o emissions. PLOS.

Green, T.R., H. Kipka, O. David, and G.S. McMaster. 2018. Where is the USA corn belt, and how is it changing? Science of The Total Environment 618: 1613–1618. doi: 10.1016/j.scitotenv.2017.09.325.

Grizzetti B., Bouraoui F., Billen G., van Grinsven H., Cardoso A.C., Thieu V., Garnier J., Curtis C., Howarth R., Johnes P. (2011) Nitrogen as a threat to European water quality. In The European Nitrogen Assessment: Sources, Effects and Policy Perspectives, pp. 379–404. Eds M.A. Sutton, C.M. Howard, J.W. Erisman, G. Billen, A. Bleeker, P. Grennfelt and H. van Grinsven. Cambridge, UK: Cambridge University Press.

Groffman, P.M. 1985. Nitrification and denitrification in conventional and no-tillage soils. Soil Sci. Soc. of Am. J. 49(2): 329–334. doi: 10.2136/sssaj1985.03615995004900020011x.

Groffman, P.M., K. Butterbach-Bahl, R.W. Fulweiler, A.J. Gold, J.L. Morse, E.K. Stander, C. Tague, C. Tonitto, and P. Vidon. 2009. Challenges to incorporating spatially and temporally eplicit phenomena (hotspots and hot moments) in dentrification models. Biogeochemistry. 93:49-77.

Groffman, P.M., and M.K. Crawford. 2003. Denitrification potential in urban riparian zones. J. Environ. Qual. 32(3): 1144–1149. doi: 10.2134/jeq2003.1144.

Grundmann, G.L. P. Renault, L. Rosso, and R. Bardin. 1995. Differential effects of soil water content and temperature on nitrification and aeration. Soil Sci. Soc. Am. J. doi:10.2136/sssaj1995.03615995005900050021x

Gumiero, B., B. Boz, P. Cornelio, and S. Casella. 2011. Shallow groundwater nitrogen and denitrification in a newly afforested, subirrigated riparian buffer: Denitrification in a riparian buffer. Journal of Applied Ecology 48(5): 1135–1144. doi: 10.1111/j.1365-2664.2011.02025.x.

Hayhoe, K., J. Edmonds, R.E. Kopp, A.N. LeGrande, B.M. Sanderson, M.F. Wehner, and D.J. Wuebbles, 2017: Climate models, scenarios, and projections. In: Climate Science Special Report: Fourth National Climate Assessment, Volume I [Wuebbles, D.J., D.W. Fahey, K.A. Hibbard, D.J. Dokken, B.C. Stewart, and T.K. Maycock (eds.)]. U.S. Global Change Research Program, Washington, DC, USA, pp. 133-160, doi: 10.7930/J0WH2N54.

Heinen, M. 2006. Simplified denitrification models: Overview and properties. Geoderma 133(3–4): 444–463. doi: 10.1016/j.geoderma.2005.06.010.

Hendriks, J., A. Oubrie, J. Castresana, A. Urbani, S. Gemeinhardt, and M. Sarasste. 2000. Nitric oxide reductases in bacteria. Biochemica Et Biophysica Acta-Bioenergetcs. 1459:266-273.

Henry, S., D. Bru, B. Stres, S. Hallet, and L. Philippot. 2006. Quantitative detection of the nosZ gene, encoding nitrous oxide reductase, and comparison of the abundances of 16S rRNA, narG, nirK, and nosZ genes in soils. Applied and Environmental Microbiology 72(8): 5181–5189. doi: 10.1128/AEM.00231-06.

Hindson, C.M., J.R. Chevillet, H.A. Briggs, E.N. Gallichotte, I.K. Ruf, B.J. Hindson, R.L. Vessella, and M. Tewari. 2013. Absolute quantification by droplet digital PCR versus analog real-time PCR. Nature Methods 10(10): 1003–1005. doi: 10.1038/nmeth.2633.

Hindson, B.J., K.D. Ness, D.A. Masquelier, P. Belgrader, N.J. Heredia, A.J. Makarewicz, I.J. Bright, M.Y. Lucero, A.L. Hiddessen, T.C. Legler, T.K. Kitano, M.R. Hodel, J.F. Petersen, P.W. Wyatt, E.R. Steenblock, P.H. Shah, L.J. Bousse, C.B. Troup, J.C. Mellen, D.K. Wittmann, N.G. Erndt, T.H. Cauley, R.T. Koehler, A.P. So, S. Dube, K.A. Rose, L. Montesclaros, S. Wang, D.P. Stumbo, S.P. Hodges, S. Romine, F.P. Milanovich, H.E. White, J.F. Regan, G.A. Karlin-Neumann, C.M. Hindson, S. Saxonov, and B.W. Colston. 2011. High-Throughput Droplet Digital PCR System for Absolute Quantitation of DNA Copy Number. Analytical Chemistry 83(22): 8604–8610. doi: 10.1021/ac202028g.

Hurd, P.J. and C.J. Nelson. 2009. Advantages of next-generation sequencing versus the microarray in epigenetic research. Briefings in Funct. Genomics. and Proteomics. 8(3):174-183

Hyatt, C.R., R.T. Venterea, C.J. Rosen, M. McNearney, M.L. Wilson, et al. 2010. Polymer-coated urea maintains potato yields and reduces nitrous oxide emissions in a Minnesota loamy sand. Soil Sci. Soc. Am. J. 74(2): 419–428. doi: 10.2136/sssaj2009.0126.

IPCC. 2007. Climate change 2007. The Scientific Basis. Contribution Working Group I to the Third Assessment Report of the Intergovernmnetal Panel on Climate Change. Cambridge Univ. Press, Cambridge.

IPCC. 2001. Climate Change 2001. Working Group II: Impacts, adaptation and vulnerability . Cambridge Univ. Press, Cambridge.

IPCC. 2007. Climate change 2007. Working Group I: The physical science basis. IPCC Fourth Assessment Report: Climate Change 2007. Cambridge Univ. Press, Cambridge.

Ju, X., and C. Zhou. 2017. Nitrogen cycling and environmental impacts in upland agricultural soils in North China: A review. Journal of Integrative Agriculture 16(12): 2848–2862. doi: 10.1016/S2095-3119(17)61743-X.

Khalil, M.I., R. Gutser, and U. Schmidhalter. 2009. Effects of urease and nitrification inhibitors added to urea on nitrous oxide emissions from a loess soil. J. Plant Nutr. Soil Sci. 172(5): 651–660. doi: 10.1002/jpln.200800197.

Koepfli, C., W. Nguitragool, N.E. Hofmann, L.J. Robinson, M. Ome-Kaius, J. Sattabongkot, I. Felger, and I. Mueller. 2016. Sensitive and accurate quantification of human malaria parasites using droplet digital PCR (ddPCR). Scientific Reports 6(1). doi: 10.1038/srep39183.

Ladha, J.K., A. Tirol-Padre, C.K. Reddy, K.G. Cassman, S. Verma, et al. 2016. Global nitrogen budgets in cereals: A 50-year assessment for maize, rice and wheat production systems. Sci Rep 6(1): 19355. doi: 10.1038/srep19355.

Lai, T.V., R. Farquharson, and M.D. Denton. 2019. High soil temperatures alter the rates of nitrification, denitrification and associated N_2O emissions. J Soils Sediments 19(5): 2176–2189. doi: 10.1007/s11368-018-02238-7.

Lam, S.K., H. Suter, M. Bai, C. Walker, R. Davies, et al. 2018. Using urease and nitrification inhibitors to decrease ammonia and nitrous oxide emissions and improve productivity in a subtropical pasture. Science of The Total Environment 644: 1531–1535. doi: 10.1016/j.scitotenv.2018.07.092.

Lassaletta, L., G. Billen, B. Grizzetti, J. Anglade, and J. Garnier. 2014. 50 year trends in nitrogen use efficiency of world cropping systems: the relationship between yield and nitrogen input to cropland. Environ. Res. Lett. 9(10): 105011. doi: 10.1088/1748-9326/9/10/105011.

Lauber, C.L., M. Hamady, R. Knight, and N. Fierer. 2009. Pyrosequencing-based assessment of soil pH as a predictor of soil bacterial community structure at the continental scale. AEM 75(15): 5111–5120. doi: 10.1128/AEM.00335-09.

Li, Z. 2020. N2O emissions and product ratios of nitrification and denitrification are altered by K fertilizer in acidic agricultural soils. Environmental Pollution: 8.

Liang, B.C., and A.F. MacKenzie. 1994. Changes of soil nitrate-nitrogen and denitrification as affected by nitrogen fertilizer on two Quebec soils. J. environ. qual. 23(3): 521–525. doi: 10.2134/jeq1994.00472425002300030017x.

Linn, D.M., and J.W. Doran. 1984. Effect of water-filled pore space on carbon dioxide and nitrous oxide production in tilled and non-tilled soils. Soil Sci. Soc. Am. J. 48:1267-1272.

Liu, C., K. Wang, and X. Zheng. 2013. Effects of nitrification inhibitors (DCD and DMPP) on nitrous oxide emission, crop yield and nitrogen uptake in a wheat-maize cropping system. Biogeosciences Discuss. 10(1): 711–737. doi: 10.5194/bgd-10-711-2013.

López-Gutiérrez, J.C., S. Henry, S. Hallet, F. Martin-Laurent, G. Catroux, and L. Philippot. 2004. Quantification of a novel group of nitrate-reducing bacteria in the environment by real-time PCR. Journal of Microbiological Methods 57(3): 399–407. doi: 10.1016/j.mimet.2004.02.009.

Machefert, S.E., and N.B. Dise. 2004. Hydrological controls on denitrification in riparian ecosystems. Hydrol. Earth Syst. Sci. 8(4): 686–694. doi: 10.5194/hess-8-686-2004.

Mardis, E.R. 2008. Next-generation DNA sequencing methods. Annu. Rev. Genomics Hum. Get. 9:387-402.

Mekala, C., and I.M. Nambi. 2017. Understanding the hydrologic control of N cycle: Effect of water filled pore space on heterotrophic nitrification, denitrification and dissimilatory nitrate reduction to ammonium mechanisms in unsaturated soils. Journal of Contaminant Hydrology 202: 11–22. doi: 10.1016/j.jconhyd.2017.04.005.

Minshall, N.E., and V.C. Jamison. 1965. Interflow in claypan soils. Water Resour. Res. 1:381-390. https://doi.org/10.1029/WR001i003p00381.

Mkhabela, M.S., A. Madani, R. Gordon, D. Burton, D. Cudmore, et al. 2008. Gaseous and leaching nitrogen losses from no-tillage and conventional tillage systems following surface application of cattle manure. Soil and Tillage Research 98(2): 187–199. doi: 10.1016/j.still.2007.12.005.

N*é*meth, D.D. 2012. Nitrous oxide emissions and abundance of N-cycling microorganisms in corn-based biofuel cropping systems. Thesis.

Niu, Y., J. Luo, D. Liu, C. Müller, M. Zaman, et al. 2018. Effect of biochar and nitrapyrin on nitrous oxide and nitric oxide emissions from a sandy loam soil cropped to maize. Biol Fertil Soils 54(5): 645–658. doi: 10.1007/s00374-018-1289-2.

Norton, N., Z. Sun, Y.W. Asmann, D.J. Serie, B.M. Necela, et al. 2013. Gene expression, single nucleotide variant and fusion transcript discovery in archival material from breast tumors (S.S. Dadras, editor). PLoS ONE 8(11): e81925. doi: 10.1371/journal.pone.0081925.

Olivier, J.G.J., G. Janssens-Maenhout, M. Muntean, and J.A.H.W. Peters. 2013. Trends in global CO2 emissions: 2013 report.

Orellana, L.H., L.M. Rodriguez-R, S. Higgins, J.C. Chee-Sanford, R.A. Sanford, K.M. Ritalahti, F.E. Loffler, and K.T. Konstantinidis. 2014. Detecting nitrous oxide reductase (nosZ) genes in soil metagenomes: Method development and implications for the nitrogen Cycle. mBio 5(3): e01193-14-e01193-14. doi: 10.1128/mBio.01193-14.

Ort, D.R., and S.P. Long. 2014. Limits on yields in the corn belt. Science 344(6183): 484–485. doi: 10.1126/science.1253884.

Palumbo, J.D., T.L. O'Keeffe, and M.W. Fidelibus. 2016. Characterization of Aspergillus section Nigri species populations in vineyard soil using droplet digital PCR. Letters in Applied Microbiology 63(6): 458–465. doi: 10.1111/lam.12667.

Parkin, T.B., A.J. Sexstone, and J.M. Tiedje. 1985. Adaptation of denitrifying populations to low soil pH. Appl. Env. Micro. 49(5): 1053-1056.

Pereira, J., A.S. Barneze, T.H. Misselbrook, J. Coutinho, N. Moreira, et al. 2013. Effects of a urease inhibitor and aluminium chloride alone or combined with a nitrification inhibitor on gaseous N emissions following soil application of cattle urine. Biosystems Engineering 115(4): 396–407. doi: 10.1016/j.biosystemseng.2013.05.002.

Phillips, R., A. McMillan, T. Palmada, J. Dando, and D. Giltrap. 2015. Temperature effects on N 2 O and N 2 denitrification end-products for a New Zealand pasture soil. New Zealand Journal of Agricultural Research 58(1): 89–95. doi: 10.1080/00288233.2014.969380.

Poblador, S., A. Lupon, S. Sabaté, and F. Sabater. 2017. Soil water content drives spatiotemporal patterns of CO2 and N2O emissions from a Mediterranean riparian forest soil. Biogeosciences 14(18): 4195–4208. doi: 10.5194/bg-14-4195-2017.

Prather,M. et al., in Climate Change 1994, J. T. Houghton et al., Eds. (Cambridge Univ. Press, New York, 1995), pp. 73–126

Prather, M. J., and J. Hsu. 2010. Coupling of nitrous oxide and methane by global atmospheric chemistry. Science, 330(6006), 925-954.

Prud'homme, M. 2016. Global fertilizer supply and trade. IFA strategic forum. Dubai, UAE.

Qu, Z., J. Wang, T. Almoy, and L.R. Bakken. 2014. Excessive use of nitrogen in Chinese agriculture results in high $N_2O/(N_2O+N_2)$ product ratio of denitrification, primarily due to acidification of the soils. Global Change Biology (20):165-1698. doi: 10.111/gcb.12461

Rački, N., D. Morisset, I. Gutierrez-Aguirre, and M. Ravnikar. 2014. One-step RT-droplet digital PCR: a breakthrough in the quantification of waterborne RNA viruses. Anal Bioanal Chem 406(3): 661–667. doi: 10.1007/s00216-013-7476-y.

Rački, N., T. Dreo, I. Gutierrez-Aguirre, A. Blejec, and M. Ravnikar. 2014. Reverse transcriptase droplet digital PCR shows high resilience to PCR inhibitors from plant, soil and water samples. Plant Methods 10(1). doi: 10.1186/s13007-014-0042-6.

Rasmussen, P.E. 1998. Long-term agroecosystem experiments: Assessing agricultural sustainability and global change. Science 282(5390): 893–896. doi: 10.1126/science.282.5390.893.

Robertson, GP. and P. Groffman. 2007. Nitrogen transformations. In: Paul EA (ed) Soil microbiology, ecology, and biochemistry. 3rd edn. Academic/Eslevier, New York. Pp. 341-364.

Rozas, H.R.S., H.E. Echeverría, and L.I. Picone. 2001. Denitrification in maize under no-tillage: effect of nitrogen rate and application time. Soil Sci. Soc. Am. J. 65(4): 1314–1323. doi: 10.2136/sssaj2001.6541314x.

Saba, N.F., M. Wilson, G. Doho, J. DaSilva, R. Benjamin Isett, et al. 2015. Mutation and transcriptional profiling of formalin-fixed paraffin embedded specimens as companion methods to immunohistochemistry for determining therapeutic targets in oropharyngeal squamous cell carcinoma (OPSCC): A pilot of proof of principle. Head and Neck Pathol 9(2): 223–235. doi: 10.1007/s12105-014-0566-0.

Sabey, B.R., W.V. Bartholomew, R. Shaw, and J. Pesek. 1956. Influence of temperature on nitrification in Soils. Soil Sci. Soc. Am. J. 20(3): 357. doi: 10.2136/sssaj1956.03615995002000030016x.

Sanger F., S. Nicklen, and A.R. Coulson. 1977. DNA sequencing with chain-terminating inhibitors. P. Natl. Acad. Sci. USA. 74:5463-5467.

Scott, D.W., F.C. Chan, F. Hong, S. Rogic, K.L. Tan, et al. 2013. Gene expression–based model using formalin-fixed paraffin-embedded biopsies predicts overall survival in advanced-stage classical hodgkin lymphoma. JCO 31(6): 692–700. doi: 10.1200/JCO.2012.43.4589.

Shahsavari, E., A. Aburto-Medina, M. Taha, and A.S. Ball. 2016. A quantitative PCR approach for quantification of functional genes involved in the degradation of polycyclic aromatic hydrocarbons in contaminated soils. MethodsX 3: 205–211. doi: 10.1016/j.mex.2016.02.005.

Shaviv, A. 2001. Advances in controlled-release fertilizers. Adv. in Agronomy. Elsevier. p. 1–49

Shcherbak, I., N. Millar, and G.P. Robertson. 2014. Global metaanalysis of the nonlinear response of soil nitrous oxide (N2O) emissions to fertilizer nitrogen. Proceedings of the National Academy of Sciences 111(25): 9199–9204. doi: 10.1073/pnas.1322434111.

Signor, D., and C.E.P. Cerri. 2013. Nitrous oxide emissions in agricultural soils: a review. Pesqui. Agropecu. Trop. 43(3): 322–338. doi: 10.1590/S1983-40632013000300014.

Simek, M., L. Jisova, and D.W. Hopkins. 2002. What is the so-called optimum pH for denitrification in soil? Soil Bio. And Biochem. 34: 1227-1234.

Singh, J., A. Kunhikrishnan, N.S. Bolan, and S. Saggar. 2013. Impact of urease inhibitor on ammonia and nitrous oxide emissions from temperate pasture soil cores receiving urea fertilizer and cattle urine. Science of The Total Environment 465: 56–63. doi: 10.1016/j.scitotenv.2013.02.018.

Smith, C.J., and A.M. Osborn. 2009. Advantages and limitations of quantitative PCR (Q-PCR)-based approaches in microbial ecology: Application of Q-PCR in microbial ecology. FEMS Microbiology Ecology 67(1): 6–20. doi: 10.1111/j.1574-6941.2008.00629.x.

Smith, C.J., D.B. Nedwell, L.F. Dong, and A.M. Osborn. 2007. Diversity and abundance of nitrate reductase genes (narG and napA), nitrite reductase genes (nirS and nrfA), and their transcripts in estuarine sediments. Applied and Environmental Microbiology 73(11): 3612–3622. doi: 10.1128/AEM.02894-06.

Smith, P., D. Martino, Z. Cai, D. Gwary, H. Janzen, P. Kumar, B. McCarl, S. Ogle, F. O'Mara, C. Rice, B. Scholes, and O. Sirotenko. 2007. Agriculture climate change mitigation. In: B. Metz, O Davidon, P. Bosch, R. Dave, and L. Meyer, editors, Contribution of working group III to the fourth assessment report of the Intergovernmental Panel on Climate Change. Cambridge Univ. Press, New York.

Spiertz, J.H.J. 2010. Nitrogen, sustainable agriculture and food security. A review. Agron. Sustain. Dev. 30(1): 43–55. doi: 10.1051/agro:2008064.

Stanford, G., S. Dzienia, and R.A. Vander Pol. 1975. Effect of Temperature on Denitrification Rate in Soils. Soil Sci. Soc. Am J. 39(5): 867–870. doi: 10.2136/sssaj1975.03615995003900050024x.

Steusloff, T.W., K.A. Nelson, P.P. Motavalli, and G. Singh. 2019. Urea nitrapyrin placement effects on soil nitrous oxide emissions in claypan soil. J. environ. qual. 48(5): 1444–1453. doi: 10.2134/jeq2019.01.0031.

Stevens, R.J., and R.J. Laughlin. 1998. Measurement of nitrous oxide and di-nitrogen emissions from agricultural soils. Nut. Cyc. in Agroeco. 52: 131-139.

Suter, H., H. Sultana, D. Turner, R. Davies, C. Walker, et al. 2013. Influence of urea fertiliser formulation, urease inhibitor and season on ammonia loss from ryegrass. Nutr Cycl Agroecosyst 95(2): 175–185. doi: 10.1007/s10705-013-9556-y.

Tan, X., D. Shao, and W. Gu. 2018. Effects of temperature and soil moisture on gross nitrification and denitrification rates of a Chinese lowland paddy field soil. Paddy Water Environ 16(4): 687–698. doi: 10.1007/s10333-018-0660-0.

Taylor, S.C., G. Laperriere, and H. Germain. 2017. Droplet Digital PCR versus qPCR for gene expression analysis with low abundant targets: from variable nonsense to publication quality data. Scientific Reports 7(1). doi: 10.1038/s41598-017-02217-x.

Thompson, B. M., Lin, C. H., Hsieh, H. Y., Kremer, R. J., Lerch, R. N., and Garrett, H. E. 2010. Evaluation of PCR-based quantification techniques to estimate the abundance of atrazine chlorohydrolase gene atzA in rhizosphere soils. J. Environ. Qual. 39:1999-2005.

Tian, Z., J.J. Wang, S. Liu, Z. Zhang, S.K. Dodla, et al. 2015. Application effects of coated urea and urease and nitrification inhibitors on ammonia and greenhouse gas emissions from a subtropical cotton field of the Mississippi delta region. Science of The Total Environment 533: 329–338. doi: 10.1016/j.scitotenv.2015.06.147Trypsteen, W., M. Kiselinova, L. Vandekerckhove, and W. De Spiegelaere. 2016. Diagnostic utility of droplet digital PCR for HIV reservoir quantification. J Virus Erad 2(3): 162–169.

Tomasek, A., J.L. Kozarek, M. Hondzo, N. Lurndahl, M.J. Sadowsky, et al. 2017. Environmental drivers of denitrification rates and denitrifying gene abundances in channels and riparian areas: DRIVERS OF DENITRIFICATION. Water Resour. Res. 53(8): 6523–6538. doi: 10.1002/2016WR019566.

Ullah, S., and S.P. Faulkner. 2006. Use of cotton gin trash to enhance denitrification in restored forested wetlands. Forest Ecology and Management 237(1–3): 557–563. doi: 10.1016/j.foreco.2006.09.075.

United States Environmental Protection Agency (USEPA) 2018. Inventory of U.S. greenhouse gas emissions and sinks 1990-2016. Available at https://www.epa.gov/sites/production/files/2018-01/documents/2018_complete_report.pdf (verified 1 September 2018)

Upadhyay, L.S.B. 2012. Urease inhibitors: A review. Indian J. Biotech. 11: 381-388.

Venterea, R.T., A.D. Halvorson, N. Kitchen, M.A. Liebig, M.A. Cavigelli, et al. 2012. Challenges and opportunities for mitigating nitrous oxide emissions from fertilized cropping systems. Frontiers in Ecology and the Environment 10(10): 562–570. doi: 10.1890/120062.

Wang, J., D.R. Chadwick, Y. Cheng, and X. Yan. 2018. Global analysis of agricultural soil denitrification in response to fertilizer nitrogen. Science of The Total Environment 616–617: 908–917. doi: 10.1016/j.scitotenv.2017.10.229.

Weier, K.L., J.W. Doran, J.F. Power, and D.T. Walters. 1993. Denitrification and the dinitrogen/nitrous oxide ratio as affected by soil water, available carbon, and nitrate. Soil Sci. Soc. of Amer. J. 57(1): 66–72. doi: 10.2136/sssaj1993.03615995005700010013x.

Wrage, N., G.L. Velthof, M.L. van Beusichem, and O. Oenema. 2001. Role of nitrifier denitrification in the production of nitrous oxide. Soil Bio. 33(12-13): 1723-1732. https://doi.org/10.1016/S0038-0717(01)00096-7.

Yu,H., Y. Fang, and R. Kang. 2020. Response of N2O and N2 emissions in forest soils to temperature change across China. EGU General Assembly Conference Abstracts.

Zerulla, W., T. Barth, J. Dressel, K. Erhardt, K. Horchler von Locquenghien, et al. 2001. 3,4-Dimethylpyrazole phosphate (DMPP) - a new nitrification inhibitor for agriculture and horticulture. Biology and Fertility of Soils 34(2): 79–84. doi: 10.1007/s003740100380.

Zhalnina, K., R. Dias, P.D. de Quadros, A. Davis-Richardson, F.A.O. Camargo, et al. 2015. Soil pH Determines Microbial Diversity and Composition in the Park Grass Experiment. Microb Ecol 69(2): 395–406. doi: 10.1007/s00248-014-0530-2.

Zhou, M., B. Zhu, N. Brüggemann, M. Dannenmann, Y. Wang, et al. 2016. Sustaining crop productivity while reducing environmental nitrogen losses in the subtropical wheat-maize cropping systems: A comprehensive case study of nitrogen cycling and balance. Agriculture, Ecosystems & Environment 231: 1–14. doi: 10.1016/j.agee.2016.06.022.

Zimmerman, N. J. Izard, C. Klatt, J. Zhou, and E. Aronson. 2014. The unseen world: environmental microbial sequencing and identification methods for ecologists. Front. Ecol. Environ. 12(4): 224-231.

CHAPTER 2

SPATIAL VARIABILITY OF ACTUAL AND POTENTIAL DENITRIFICATION EMISSIONS ON MISSOURI CLAYPAN SOILS

2.1 Abstract

Denitrification in agricultural soils is responsible for a majority of anthropogenic nitrous oxide (N_2O) production and N_2O has a global warming potential approximately 300 times that of carbon dioxide. The objective of this research was to assess the spatial dependence of soil N_2O flux from claypan soils. Surface soil samples (0-10 cm) were collected on a 90-m grid from two central Missouri claypan fields that were representing different typical agricultural management systems. Potential denitrification rates were measured using the denitrification enzyme activity (DEA) protocol and actual denitrification rates of N_2O and N_2 were measured with the N-free atmospheric recirculation method (N-FARM). Potential denitrification rates were not significantly different between fields, but they were greater in the toeslope position ($p < 0.05$) compared to the back-slope and summit positions. Actual denitrification was dominated by N_2 rather than N_2O emissions in both fields, and fluxes of both gases were not significantly affected by landscape position. Actual N_2, N_2O, and total denitrification ($N_2 + N_2O$) fluxes were not different between fields. Actual denitrification fluxes showed a similar landscape pattern to that of denitrification potential, with the backslope having lower emissions than the summit and toeslope. Although the high smectitic clay content of upland soils provides environmental conditions suitable for denitrification, these results indicated that potential denitrification rates were higher in the toeslope position due to accumulation of soil C from long-term sediment deposition. Thus, the increased rates of complete denitrification (NO_3^- to N_2) in the backslope potentially resulted from greater soil loss at this landscape position, leading to shallow claypan

depth and extended saturated conditions near the surface. Therefore, long-term erosion patterns rather than current or recent crop management systems controlled observed spatial patterns of denitrification on these claypan fields.

2.2 Introduction

Denitrification is the soil microbial facilitated reduction of nitrate to a series of gases including nitrous oxide (N_2O), a potent greenhouse gas (GHG), and di-nitrogen (N_2) (Knowles, 1982), and is the least well quantified process in the soil nitrogen (N) cycle (Parkin et al., 1984). Nitrous oxide is a potent greenhouse gas with a global warming potential (GWP) greater than that of methane (CH_4) and carbon dioxide (CO_2) (Forster et al., 2007), and is predominantly produced from agricultural systems (Oenema et al., 2001). Staying in the atmosphere for ~118 years before decomposition, N_2O is also a tropospheric ozone depleting gas (Prather and Hsu, 2010; IPCC, 2001). Globally, there has been an interest in significantly reducing GHG emissions. In 2015, the Paris Agreement was drafted by the United Nations to bring international attention to the significance of global warming and climate change. This agreement aims to limit the rate at which the global average temperature increase compared to pre-industrial levels (UNFCCC, 2015). Since N_2O has such a higher GWP than CH_4 and CO_2, there is great interest in developing and implementing agricultural practices that reduce cumulative N_2O emissions (Millar et al., 2010). Denitrification is also a major factor contributing to lower nitrogen use efficiency (NUE) (Cassman et al., 1998). Thus, decreasing N_2O production from agricultural systems may potentially increase NUE, improving crop production and sustainability, while decreasing GHG emissions associated with crop production.

The Central Claypan Areas (Major Land Resource Area 113) cover roughly four million hectares in the Midwest United States, mainly in northeastern Missouri and south-central Illinois

(Anderson et al., 1990; Lerch et al., 2008). Claypan soils are characterized by a smectitic argillic horizon (B_t) in which the clay content increases 100% compared to the horizon directly above it (Myers et al., 2007). The claypan is the key hydrologic feature of the soils, resulting in both high runoff under wet conditions and development of preferential flow paths due to extensive vertical soil cracking when dry. Saturated hydraulic conductivity of these soils is very low (<10 mm/h) (Nash et al., 2012; Blanco-Canqui et al., 2002; Mudgal et al., 2010), and under saturated conditions, a perched water table forms at the top of the claypan. As a result, they are considered poorly drained and crop management is especially difficult on these soils as prolonged wet conditions make field operations challenging in spring (Hsiao et al., 2018). Further, the drainage characteristics of claypan soils combined with their widespread occurrence in upland landscape positions creates potentially ideal conditions for denitrification to occur throughout claypan watersheds, not just in lower landscape positions.

Denitrification production is impacted by several factors including tillage practices and nitrogen (N)-based fertilizer type, placement, and rate (Millar et al., 2010), soil pH (Čuhel and Šimek, 2011), soil water content and water-filled pore space (WFPS) (Dobbie and Smith, 2001), the presence of denitrifying microbial communities, nitrate concentration, and the amount and quality of organic carbon (Sirivedhin and Gray, 2006; Florinsky et al., 2004). Landscape topography patterns are drivers of these soil properties that influence denitrification patterns (Pennock et al., 1992). On a Canadian soil, Corre et al. (1996) observed significantly higher denitrification rates in the footslope compared to the backslope. Similary, Chintala et al. (2015) observed greater denitrification potential in the footslope compared to the summit; however, actual N_2O and total denitrification rates were lower in the footslope. Florinksy et al. (2004) reported no relationship between N_2O flux and landscape position.

The nitrogen-free atmospheric recirculation method (N-FARM) has been utilized to better understand denitrification (Burgin et al., 2010; Burgin and Groffman, 2012; Morse et al., 2015; Morse et al., 2015). Described first by Parkin et al. (1984), this method involves continuously circulating a gas to fill the soil micropores. It has been adapted by others (Swerts et al., 1995; Butterbach-Bahl et al., 2002; Burgin et al., 2010). Burgin et al. (2010) used the N-FARM to better understand how soil O_2 levels regulate denitrification. They observed greater denitrification rates at 0% O_2 compared to 20% O_2 levels in both the control and within the treatment in which nitrate NO_3^- was added. Denitrification potential was also measured and provided similar results in regards to O_2 concentration. However, average denitrification potential rates were greater than actual denitrification rates by at least 10-fold. Morse et al. (2015) used a similar setup to measure soil-atmosphere N_2O and CO_2 fluxes during snowmelt in a northern hardwood forest. They observed that denitrification was significantly influenced by elevation and season, with more denitrification occurring during snowmelt. In another study conducted by Morse et al. (2015), the used the N-FARM to measure soil denitrification flux in forest soils.

The DEA assay was developed to determine denitrification potential of a soil under non-limiting conditions (Groffman et al., 1999). Use of the DEA with grid soil sampling allows for interpretation of spatial patterns in denitrification across fields to better understand landscape scale factors controlling denitrification. When coupled with actual denitrification rates, there is a major opportunity to better understand the factors that regulate denitrification. Further, the impact landscape position has on soil properties that influence denitrification has not been extensively studied, in particularly on claypan soils. Stanley (1998) identified and isolated facultative anaerobes on these soils that suggest these soils have a high denitrification potential.

Thus, the objectives of this study were to: 1) use the DEA assay for measuring spatial variation in denitrification in two claypan fields under different management practices; 2) measure actual N_2O and N_2 flux of intact soil cores from the same two fields using N-FARM; 3) establish a relationship between potential and actual denitrification rates for the fields; and 4) assess the effect of landscape position on potential and actual denitrification rates.

2.3 Materials and Methods

2.3.1 Site Location

This study was conducted in two fields within the Goodwater Creek Experimental Watershed (GCEW) which is a core part of the Central Mississippi River Basin long-term agroecosystem research (LTAR) network located in northeastern Missouri (Figure 2.1 A). One field, Field 1 (39°13'46.92" N , -92°7'0.84" W), is an 'aspirational' system implemented in 2016 and is under no-till (NT), corn-soybean-wheat (C-S-W) rotation management system with a variable N rate application designed to be more sustainable than typical production systems of the region. A cover crop is planted following wheat and the field effectively has 100% residue cover following corn and soybean. The other field, Field 3 (39°13'55.56" N, -92°9'0.36" W), is designated as 'business as usual' and is representative of typical row crop production systems in the region with disc tillage and corn-soybean-soybean (C-S-S) rotation management system. Management information during the years of this study are listed in Table 2.1. The common soils series include Putnam or Adco silt loam in the summit position, Mexico silt loam in the shoulder position, and Leonard silt loam in the side-slope position, all classified as fine, smectitic, mesic Vertic Albaqualfs. The common soil series in the toeslope position is Moniteau silt loam (fine-silty, mixed, superactive, mesic Typic Endoaqualfs) (Soil Survey, 2019).

2.3.2 Soil Sampling and Characterization

Six sets of intact soil cores were obtained within each field along two landscape transects, covering a catena sequence from summit to toeslope positions (Figure 2.2 A and B). Soil cores were collected in May and November 2016 and March and November 2017. In addition, a set of cores were collected in Field 3 in April 2018 and in Field 1 in September 2018. Six cores were collected per transect in duplicate for a total of 24 cores per field. Cores were collected to depths of 60-80 cm such that at least one claypan horizon was included. Each core was collected in a 5 cm diameter plastic liner, which was capped at each end, and immediately placed in coolers, with or without ice depending on the sample date. The soil cores were then refrigerated until analyses were performed. At each sample time, one set of intact cores was used for actual denitrification measurements by the N-FARM (see below) and the other for basic characterization of soil chemical and physical properties.

Grid sampling was conducted in each field to obtain soils for the DEA assay. Surface soils were collected to a 10 cm depth on a 90 m grid within each field, for a total of ~45 samples per field (Figure 2.2 A and B). In Field 1, additional soil samples were obtained near the edge of the field next to the drainage way to represent riparian conditions. In Field 3, additional samples were acquired from the riparian area to the west of the field and along the northern boundary of the field. At each sample location, 5-10 sub-samples were collected using a hand-held soil probe (1.27 cm diameter) within ~0.3 m circumference of the grid location and composited. All samples were passed through a sieve with 2 mm openings. The samples were analyzed by the University of Missouri Soil and Plant Testing Laboratory using standard soil testing procedures (Nathan et al., 2006) for concentrations of nitrate-N, ammonium-N, organic matter, and other characteristics (Table 2.2). Total organic carbon (TOC) was calculated by dividing organic

matter content by 1.72. Grid samples were obtained from Field 3 on April 12, 2018 and from Field 1 on July 23, 2018. In addition, soil samples were obtained in the fall of 2015 from the two fields using the same 90 m grid to a depth of 60 cm in 15 cm intervals. These samples were analyzed for soil biomass C (BC) and biomass N (BN) concentrations using potassium sulfate (K_2SO_4) extraction and chloroform fumigation (Brookes et al., 1985), and the data for the 0-15 cm depth were used in this study.

2.3.3 Landscape Delineation

Soil samples were designated in the summit, backslope, and toeslope landscape positions (Figure 2.2 A&B). In order to objectively separate soil samples by landscape position, the light detection and ranging (LiDAR) data for Boone County was used (https://data-msdis.opendata.arcgis.com/). For Field 1, a combination of soil mapping units, aerial imagery showing the drainage channel in the center of the field, observed depth to claypan in soil cores, and the 1.5 m LiDAR data was used to determine the boundaries for each landscape position. For Field 3, the boundaries were determined based solely on the 1.5 m LiDAR data.

2.3.4 Denitrification Potential

The DEA assay was used to measure potential denitrification of the grid soil samples from both fields (Groffman et al. 1999). The DEA media consisted of 0.72 g KNO_3, 0.5 g glucose, 0.125 g chloramphenicol, and DI water brought to 1L, and was added to two reps of 5 g of sieved soil samples in a 125 Erlenmeyer flask. The gas from the flask was evacuated for three minutes and flushed for one minute with N_2, with this cycle occurring three times. The incubation process followed the evacuation with addition of 5 mL of acetylene to each flask to prevent N_2O from being reduced to N_2 during the incubation or analysis. Lastly, the flask were placed on a shaker table at 125 rpm and two 10 mL gas samples were extracted from each flask

at t_1=30 minutes and t_2=90 minutes. The gas samples were analyzed for N_2O concentration with a gas chromatograph (GC) (Shimadzu, Kyoto, Japan) equipped with a headspace autosampler and an electron capture detector (ECD).

2.3.5 Actual Denitrification Measurements

Total denitrification flux of intact soil cores (N_2 plus N_2O), hereafter referred to as actual denitrification, was measured using N-FARM, in which He and O_2 are continuously circulated to fill the soil macropores and exclude atmospheric N_2 (Parkin et al., 1984). The soil cores were encased in stainless steel tubes connected to a gas-tight flow injection system built from Swagelok connections (Swagelok Co., Solon, OH), which is connected to a GC (Shimadzu, Kyoto, Japan) containing a He chamber that uses a thermal conductivity detector (TCD) to measure N_2, and an electron capture detector (ECD) to measure N_2O. The different gas treatments included a mixture of He and O_2, with O_2 concentrations of 0 and 20%. The soil cores were injected with incubation gasses, with gas removal by a vacuum every 90 seconds for roughly 14 hours. During this timeframe, N_2 was being evacuate from the cores, allowing N_2 production to be measured from the soil cores, instead of atmospheric N_2. Next, the system was set to an incubation state, allowing gaseous products to produce and accumulate in the stainless steel tubes. After flushing was complete and denitrification products produced in the tubes, gas samples were taken over a 4-6 hour period, at three time intervals, t_0 (0 min), t_1 (2-3 hours after t_0), and t_2 (2-3 hours after t_1) (Burgin et al., 2010).

2.3.6 Statistical Analysis

The Mann Whitney U test was performed to determine whether there were differences in potential and actual flux rates between fields. One-way analysis of variance with Tukey's multiple comparison test were used to determine landscape effects on denitrification potential,

actual N_2O and N_2 flux, and soil concentrations of BC, BN, TOC, NO_3-N, and NH_4-N. Pearson correlation tests were performed to determine possible relationships between potential and actual flux and soil concentrations of BC, BN, TOC, NO_3-N, and NH_4-N. Multiple linear regression models were developed to predict potential and actual denitrification based on landscape position and soil concentrations of BC, BN, TOC, NO_3-N, and NH_4-N. Significance level for all analyses was $\alpha = 0.10$, unless noted otherwise. All analyses were conducted using SAS 9.4 (SAS Institute Inc., Cary, NC, USA).

2.4 Results

2.4.1 Management, Landscape Position, and Denitrification Potential

Average denitrification potential for Fields 1 and 3 were both 1.11 kg N $ha^{-1}day^{-1}$ (Figure 2.3). While mean denitrification potential was not significantly different between fields, N_2O flux variability was approximately 39% higher in Field 3 compared to Field 1. Since potential denitrification rates were not significantly different between fields, N_2O fluxes were pooled to assess landscape effects. Denitrification potential fluxes were very similar at the summit (0.92 kg N $ha^{-1}day^{-1}$) and backslope (0.95 kg N $ha^{-1}day^{-1}$) and significantly greater in the toeslope (1.63 kg N $ha^{-1}day^{-1}$) than the upper landscape positions (Figure 2.4).

Using the 90-m grid samples, estimated spatial distribution of potential N_2O flux for Fields 1 and 3 were generated, along with hot spot and cold spot analysis (Figures 2.5). Soil samples from the edge of Field 1 were omitted from these analysis due to the large distance from the main field samples. Estimates of potential N_2O flux for Field 1 ranged from approximately 0.082 to 2.611 kg N ha^{-1} day^{-1} and from 0.003 to 4.692 kg N ha^{-1} day^{-1} for Field 3. Denitrification potential was higher in the toeslope landscape position for both fields. However, in Field 1, hot and cold spots were more spatially varied than Field 3 with significant hotspots identified in the

summit ($p < 0.10$), backslope ($p < 0.05$), and toeslope ($p < 0.01$), and significant cold spots identified in the summit ($p < 0.10$) and backslope ($p < 0.05$) positions. In Field 3, there were no significant cold spots identified, and the two hotspots identified in the toeslope position were both located in the southeast corner of the field (Fig. 2.5B).

2.4.2 Soil Characteristics and Landscape Position

Microbial biomass C measurements for the summit, backslope, and toeslope positions were 66.0, 47.2, and 94.0 mg L^{-1}, respectively (Table 2.3). Average BC concentration in the toeslope was significantly greater than average BC concentration in the backslope ($p < 0.10$), but it was not significantly different from the summit, despite the toeslope having~35% greater BC. Biomass N measurements were similar across all landscape positions, and there were no significantly differences in BN across landscape ($p > 0.10$). Nitrate-N concentrations for the summit, backslope, and toeslope landscape positions were 21.7, 17.4, and 30.3 g ha^{-1}, respectively. Average NO_3-N concentration in the toeslope was significantly higher than the other two landscape positions. Similarly, NH_4-N concentrations were highest in the toeslope (3.07 g ha^{-1}) and were significantly greater than the backslope, but not the summit position ($p < 0.10$). Total organic carbon was also highest in the topeslope, and it was significantly greater than TOC concentrations of the summit and backslope which were similarly low and not significantly different (Table 2.3).

2.4.3 Relationship of Soil Properties to Denitrification Potential

Figure 2.6 A and B illustrate co-kriged estimates of denitrification potential in relation with NO_3^-, NH_4^+, and TOC as co-variables. In Field 1, estimates ranged from 0.0026 to 0.0824 kg N ha^{-1} day^{-1}, with the higher denitrification potential estimates in the toeslope. Estimates for Field 3 ranged from approximately 0.0034 to 4.6921 kg N ha^{-1} day^{-1} (Figure 2.6A). Similarly,

estimates in Field 3 were higher in the toeslope. However, there were also high estimates of denitrification potential present in other landscape positions. While the kriged and co-kriged denitrification potential estimates were very similar in Field 3, co-kriged estimates for Field 1 appear to mute the landscape effects compared to the kriged estimates. As a result, the range of co-kriged estimates for Field 1 were much lower than the kriged data (Figure 2.5A; Figure 2.6A). The co-kriged maps for both fields more closely align with landscape position and the spatial distribution of soil series than the kriged maps (Figure 2.1 B&C; Figure 2.5 A&B). The co-kriged parameters were strongly landscape dependent and as a result, influenced the DEA estimates to reflect landscape and soil series differences to a greater extent than the kriged data. Thus, the co-kriged estimates appear to be more useful than the kriged estimates. This is supported by the significant correlation that existed between BN, NO_3-N, TOC, and denitrification potential.

2.4.4 Actual Denitrification

Figure 2.7 illustrates actual denitrification rates for Fields 1 and 3 partitioned by N_2O and N_2 fluxes, showing that N_2 flux accounted for >85% of the total denitrification ($N_2/(N_2O + N_2)$). Total denitrification (N_2O+N_2) rates were not significantly different between fields nor were the individual N_2 and N_2O rates, despite the fact that Field 3 had nearly twice the rates of Field 1. As a result, total denitrification rates were pooled across fields to assess the effects of landscape position (Figure 2.8). Actual N_2 flux rates for the summit, backslope, and toeslope landscape positions were 0.178, 0.120, and 0.367 kg N $ha^{-1}day^{-1}$, respectively. Figure 2.8 also illustrates that total denitrification emissions measured by N-FARM for Fields 1 and 3 were significantly lower than denitrification potential overall and at every landscape position (p = 0.05).

2.4.5 Variables for Predicting Potential and Actual Denitrification

Regression analyses showed the models containing the variables landscape, BC, BN, NO_3-N , NH_4-N , and TOC were useful for predicting denitrification potential ($p = 0.0003$), but not for actual N_2O, N_2, or $N_2O + N_2$ rates ($p > 0.10$) (Table 2.3). Landscape, NO_3-N , and TOC were significant variables in the model for denitrification potential. In addition, denitrification potential was significantly correlated to BN, NO_3-N, and TOC, but not to actual N_2O or N_2 rates (Table 2.4). Actual N_2 and N_2O rates were only significantly correlated to each other ($p < 0.10$) and not to any of the soil parameters.

2.5 Discussion

2.5.1 Management Impact on Actual and Potential Denitrification

Results from this study suggest management was not a significant factor in regards to denitrification potential in the two fields (Figure 2.3). These results were opposite to those of Pareja-Sánchez et al. (2020), who found that denitrification potential was impacted by tillage, N application timing, and type of N fertilizer applied. Management impacts on denitrification potential were also reported by Groffman et al. (1993), in which they observed higher denitrification potential in unburned sites compared to disturbed sites that were burned, grazed, or cultivated. A major difference between those studies and this one was the soils and climate. Pareja-Sánchez et al. (2020) conducted their study in Spain under semiarid conditions, and Groffman et al. (1993) conducted their research on Mollisols in Central Kansas, while this study was performed on Alfisols in the southern Corn Belt.

Although actual denitrification was not significantly different between the two fields, total denitrification was approximately two times greater in Field 3 than Field 1 and much more variable (Figure 2.7). Thus, management may have impacted the magnitude and variability of

actual denitrification. These results are similar to that of Fiorini et al. (2020), in which they observed a 40-55% decrease when combining an NT and cover crop management practice compared to a conventional tillage management practice. Conversely, in the comparison of NT and conventional tillage, Liu et al. (2006) and MacKenzie et al. (1997) observed an increase in soil N_2O production under NT management systems. These studies suggested that greater WFPS was maintained under NT management, resulting in increased N_2O production (Bateman and Baggs, 2005; Dobbie and Smith, 2001; Linn and Doran, 1984; Ruser et al., 2006). Our results are also opposite of Wang and Zou (2020), who observed an increase in N_2O emissions under no-till compared to total denitrification. Even in our 'aspirational' system under no-till, a significant majority of total denitrification emissions were N_2. Nash et al. (2012) also observed an increase in N_2O emissions in fields under no-till/surface broadcasted N treatment compared to strip-till/deep banded N placement on a Missouri claypan soil. However, the magnitude at which tillage practices impact soil N_2O emissions remains highly variable (Gregorich et al., 2008).

A possible explanation for the increase in total denitrification for Field 3 would be due to a higher NO_3^- concentration compared to Field 1 (Table 2.2). Nitrate concentrations in Field 3 were approximately 2.3 % lower in the summit, but 31.5, and 51.8% greater than Field 1 in the backslope and toeslope landscape positions, respectively. Senbayram et al. (2011) observed much higher $N_2O/(N_2O+N_2)$ when NO_3^- concentrations were high. The lower concentration of free NO_3^- in Field 1 could be due to the lower rates of N fertilizer applied, the type of fertilizer applied (Table 2.1), and/or crops in Field 1 may have a higher NUE than those in Field 3. MacKenzie et al. (1997) suggested the increase in N_2O emissions they observed from corn plots compared with soybean and alfalfa was likely due to the increase in NO_3^- fertilization of those plots. Pareja-Sánchez et al. (2020) observed a significant increase in N_2O emissions at 400 kg N

ha^{-1}, a high fertilizer rate application when combined with NT under Mediterranean climate conditions.

2.5.2 Actual and Estimated Denitrification, Denitrification Potential, and Landscape Position

Since denitrification potential was not statistically significantly different between fields, N_2O flux data were combined across fields to assess landscape position effects. The greater denitrification potential in the toeslope position (Figure 2.4) was related to the soil characteristics as the toeslope soils had the highest concentrations of BC, BN, NO_3-N, NH_4-N, and TOC compared to the summit and backslope landscape positions (Table 2.3). Further, denitrification potential was significantly correlated to BN, NO_3-N, and TOC levels in soils (Table 2.4); thus, the greater concentrations of these parameters in the toeslope position were key factors driving denitrification potential. This also supported our hypothesis that landscape position drives soil characteristics and qualities that promote denitrification. Furthermore, Baffaut et al. (2013) assessed sediment transportation and soil erosion from these fields. They calculated in their model for Fields 1 and 3, the average suspended sediment deposits are 4,361 and 1,465 kg ha^{-1} $year^{-1}$, respectively. As a result, sediment deposition in the toeslope position has led to a more favorable soil environment for denitrification to occur compared to the higher slope position (Geyer et al., 1992). Our results were also similar to those of Shrewsbury et al. (2016), who also observed higher DEA in the lower foot/toeslope compared to higher landscape positions. As in our study, Li et al. (2018) reported topography explained the greatest amount of variation for denitrification potential.

Actual denitrification rates were not significantly different across landscape position, but they showed a similar landscape pattern to that of denitrification potential (Figure 2.8). This result was opposite to that of Groffman et al. (1993) in which they observed greater

denitrification in the summit on a prairie soil likely due to loess deposition (Jantz et al. 1975). Similarly, soils in this study have a clay loess parent material. However, hotspot and hot moments can be difficult to capture because they can occur at small, medium, and large field scales (Groffman et al., 2009). Our results were similar to those observed in Ambus (1998) who reported denitrification rates in the lower landscape position that were 10 to 100 times higher than those in higher landscape positions. The greater actual N_2 and N_2O fluxes observed in the toeslope were likely related to greater long-term topsoil addition at this position from upper landscape positions. Overall, N_2 flux dominated denitrification in both Fields, with N_2O emission accounting for only 6.5% of the total denitrification. These results were similar to that of Burgin and Groffman (2012), in which N_2 production was generally 5-10 times greater than N_2O production from soil samples analyzed with the N-FARM, and demonstrate that complete denitrification of NO_3^- to N_2 commonly occurs in these poorly drained claypan soils (Bergsma et al., 2002).

2.6 Conclusion

Potential and actual denitrification flux were found to be strongly landscape position dependent while crop management had no significant effect on potential or actual denitrification rates between study fields. Denitrification was significantly greater at the toeslope compared to upper landscape positions due to greater soil concentrations of organic C and organic and inorganic N. Long-term sediment deposition, that has buried the claypan to depths of >60cm, has created a soil environment that promotes growth and activity of denitrifying bacteria. In both fields, potential denitrification was spatially dependent and a majority of both fields had fluxes <1.5 kg N ha^{-1} day^{-1}. The spatial pattern of potential denitrification also indicated that long-term erosion rather than current management controlled denitrification in these fields. Actual

denitrification was not significantly affected by landscape position, indicating that upper landscape positions can be important to gaseous N loss from these claypan fields. In addition, actual denitrification was dominated by loss as N_2 (>85% of total flux) rather than N_2O. Thus, denitrification in claypan soils, regardless of crop management, resulted in low GHG emissions..

2.7 Acknowledgements

I would like to express my appreciation to the USDA-ARS for their financial contribution and continued support of this study. I would also like to thank my dissertation advisors, Dr. Robert Lerch and Dr. Peter Motavalli, for supporting me and providing input every step of the way during this study. My other committee members, Dr. Kristen Veum, and Dr. Peter Scharf, have also provided unique input to make this study successful. Dr. Peter Groffman and his team of researchers have been extremely helpful throughout this process by analyzing samples with the N-FARM and answering all of my questions related to analysis. Lastly, I would like to thank Edward Winchester for his help with sample collection throughout this study.

2.8 References

Ambus, P. 1998. Nitrous oxide production by denitrification and nitrification in temperate forest, grassland and agricultural soils. Euro. J. of Soil Sc. 49:495-502.

Anderson, S.H., and R. Brown. 1990. Soil physical properties after I00 years of continuous cultivation. Journal of Soil and Water Conservation: 6.

Baffaut, C., F. Ghidey, K.A. Sudduth, R.N. Lerch, and E. John Sadler. 2013. Long-term suspended sediment transport in the Goodwater Creek Experimental Watershed and Salt River Basin, Missouri, USA: Data and Analysis Note. Water Resour. Res. 49(11): 7827–7830. doi: 10.1002/wrcr.20511.

Bateman, E.J., and E.M. Baggs. 2005. Contributions of nitrification and denitrification to N_2O emissions from soils at different water-filled pore space. Biol Fertil Soils 41(6): 379–388. doi: 10.1007/s00374-005-0858-3.

Bergsma, T.T., G.P. Robertson, and N.E. Ostrom. 2002. Influence of soil moisture and land use history on denitrification end-products. J. Environ. Qual. 31(3): 711–717. doi: 10.2134/jeq2002.7110.

Burgin, A.J., and P.M. Groffman. 2012. Soil O_2 controls denitrification rates and N_2O yield in a riparian wetland. J. Geophys. Res. 117(G1). doi: 10.1029/2011JG001799.

Burgin, A.J., P.M. Groffman, and D.N. Lewis. 2010. Factors regulating denitrification in a riparian wetland. Soil Sci. Soc. Am. J. 74(5): 1826–1833. doi: 10.2136/sssaj2009.0463.

Chintala, R., R.K. Owen, T.E. Schumacher, K.A. Spokas, L.M. McDonald, et al. 2015. Denitrification kinetics in biomass- and biochar-amended soils of different landscape positions. Environ Sci Pollut Res 22(7): 5152–5163. doi: 10.1007/s11356-014-3762-2.

Corre, M.D., C. van Kessel, and D.J. Pennock. 1996. Landscape and seasonal patterns of nitrous oxide emissions in a semiarid region. Soil Sci. Soc. of Am. J. 60(6): 1806–1815. doi: 10.2136/sssaj1996.03615995006000060028x.

Čuhel, J., and M. Šimek. 2011. Proximal and distal control by pH of denitrification rate in a pasture soil. Agriculture, Ecosystems & Environment 141(1–2): 230–233. doi: 10.1016/j.agee.2011.02.016.

Dobbie, K.E., and K.A. Smith. 2001. The effects of temperature, water-filled pore space and land use on N2O emissions from an imperfectly drained gleysol. Eur J Soil Science 52(4): 667–673. doi: 10.1046/j.1365-2389.2001.00395.x.

Fiorini, A., S.C. Maris, D. Abalos, S. Amaducci, and V. Tabaglio. 2020. Combining no-till with rye (Secale cereale L.) cover crop mitigates nitrous oxide emissions without decreasing yield. Soil and Tillage Research 196: 104442. doi: 10.1016/j.still.2019.104442.

Florinsky, I.V., S. McMahon, and D.L. Burton. 2004a. Topographic control of soil microbial activity: a case study of denitrifiers. Geoderma 119(1–2): 33–53. doi: 10.1016/S0016-7061(03)00224-6.

Florinsky, I.V., S. McMahon, and D.L. Burton. 2004b. Topographic control of soil microbial activity: a case study of denitrifiers. Geoderma 119(1–2): 33–53. doi: 10.1016/S0016-7061(03)00224-6.

Gregorich, E.G., P. Rochette, P. St-Georges, U.F. McKim, and C. Chan. 2008. Tillage effects on N_2O emission from soils under corn and soybeans in Eastern Canada. Can. J. Soil. Sci. 88(2): 153–161. doi: 10.4141/CJSS06041.

Hsiao, C.-J., G.F. Sassenrath, L.H. Zeglin, G.M. Hettiarachchi, and C.W. Rice. 2018. Vertical changes of soil microbial properties in claypan soils. Soil Biology and Biochemistry 121: 154–164. doi: 10.1016/j.soilbio.2018.03.012.

Iaconelli, M., B. Valdazo-González, M. Equestre, A.R. Ciccaglione, C. Marcantonio, et al. 2017. Molecular characterization of human adenoviruses in urban wastewaters using next generation and Sanger sequencing. Water Research 121: 240–247. doi: 10.1016/j.watres.2017.05.039.

Knowles, R. 1982. Denitrification. Microbiological Reviews. 46(1): 43-70.

Lerch, R.N., N.R. Kitchen, R.J. Kremer, W.W. Donald, E.E. Alberts, et al. 2005. Development of a conservation-oriented precision agriculture system: Water and soil quality assessment. : 11.

Linn, D.M., and J.W. Doran. 1984. Effect of water-filled pore space on carbon dioxide and nitrous oxide production in tilled and nontilled Soils. Soil Sci Soc. Am. J. 48(6): 1267–1272. doi: 10.2136/sssaj1984.03615995004800060013x.

Liu, X.J., A.R. Mosier, A.D. Halvorson, and F.S. Zhang. 2006. The impact of nitrogen placement and tillage on NO, N_2O, CH_4 and CO_2 fluxes from a clay loam soil. Plant Soil 280(1–2): 177–188. doi: 10.1007/s11104-005-2950-8.

MacKenzie, A.F., M.X. Fan, and F. Cadrin. 1997. Nitrous oxide emission as affected by tillage, corn-soybean-alfalfa rotations and nitrogen fertilization. Can. J. Soil. Sci. 77(2): 145–152. doi: 10.4141/S96-104.

Mancini, P. G.B. Ferraro, M. Iaconelli, E. Suffredini, B. Valdazo-Gonzalez, S. Della Libera, M. Divizia, and G. La Rosa. 2019. Molecular characterization of human Sapovirus in

untreated sewage in Italy by amplicon-based sanger and next-generation sequencing. J. Appl. Microbiol., 126(1):324-331. doi: 10.1111/jam.14129

Millar, N., G.P. Robertson, P.R. Grace, R.J. Gehl, and J.P. Hoben. 2010. Nitrogen fertilizer management for nitrous oxide (N2O) mitigation in intensive corn (Maize) production: an emissions reduction protocol for US Midwest agriculture. Mitig Adapt Strateg Glob Change 15(2): 185–204. doi: 10.1007/s11027-010-9212-7.

Morse, J.L., J. Durán, F. Beall, E.M. Enanga, I.F. Creed, et al. 2015a. Soil denitrification fluxes from three northeastern North American forests across a range of nitrogen deposition. Oecologia 177(1): 17–27. doi: 10.1007/s00442-014-3117-1.

Morse, J.L., J. Durán, and P.M. Groffman. 2015b. Soil denitrification fluxes in a northern hardwood forest: The importance of snowmelt and implications for ecosystem N budgets. Ecosystems 18(3): 520–532. doi: 10.1007/s10021-015-9844-2.

Mudgal, A., S.H. Anderson, C. Baffaut, N.R. Kitchen, and E.J. Sadler. 2010. Effects of long-term soil and crop management on soil hydraulic properties for claypan soils. Journal of Soil and Water Conservation 65(6): 393–403. doi: 10.2489/jswc.65.6.393.

Myers, D.B., N.R. Kitchen, K.A. Sudduth, R.E. Sharp, and R.J. Miles. 2007. Soybean root distribution related to claypan soil properties and apparent soil electrical conductivity. Crop Sci. 47(4): 1498–1509. doi: 10.2135/cropsci2006.07.0460.

Nash, P.R., P.P. Motavalli, and K.A. Nelson. 2012. Nitrous oxide emissions from claypan soils due to nitrogen fertilizer source and tillage/fertilizer placement practices. Soil Sci. Soc. Am. J. 76(3): 983–993. doi: 10.2136/sssaj2011.0296.

Oenema, O., G. Velthof, and P. Kuikman. Technical and policy aspects of strategies to decrease greenhouse gas emissions from agriculture. : 15.

Pareja-Sánchez, E., C. Cantero-Martínez, J. Álvaro-Fuentes, and D. Plaza-Bonilla. 2020. Impact of tillage and N fertilization rate on soil N_2O emissions in irrigated maize in a Mediterranean agroecosystem. Agriculture, Ecosystems & Environment 287: 106687. doi: 10.1016/j.agee.2019.106687.

Parkin, T.B., H.F. Kaspar, A.J. Sexstone, and J.M. Tiedje. 1984. A gas-flow soil core method to measure field denitrification rates. Soil Biology and Biochemistry 16(4): 323–330. doi: 10.1016/0038-0717(84)90026-9.

Pennock, D.J., C. van Kessel, R.E. Farrell, and R.A. Sutherland. 1992. Landscape-scale variations in denitrification. Soil Sci. Soc. Am. J. 56(3): 770–776. doi: 10.2136/sssaj1992.03615995005600030016x.

Rogelj, J., M. den Elzen, N. Höhne, T. Fransen, H. Fekete, et al. 2016. Paris agreement climate proposals need a boost to keep warming well below 2 °C. Nature 534(7609): 631–639. doi: 10.1038/nature18307.

Ruser, R., H. Flessa, R. Russow, G. Schmidt, F. Buegger, et al. 2006. Emission of N_2O, N_2 and CO_2 from soil fertilized with nitrate: effect of compaction, soil moisture and rewetting. Soil Biology and Biochemistry 38(2): 263–274. doi: 10.1016/j.soilbio.2005.05.005.

Sadler, E.J., R.N. Lerch, N.R. Kitchen, S.H. Anderson, C. Baffaut, et al. 2015. Long-term agroecosystem research in the Central Mississippi River Basin: Introduction, establishment, and overview. J. Environ. Qual. 44(1): 3–12. doi: 10.2134/jeq2014.11.0481.

Senbayram, M., R. Chen, A. Budai, L. Bakken, and K. Dittert. 2012. N_2O emission and the $N_2O/(N_2O+N_2)$ product ratio of denitrification as controlled by available carbon substrates and nitrate concentrations. Agriculture, Ecosystems & Environment 147: 4–12. doi: 10.1016/j.agee.2011.06.022.

Shrewsbury, L.H., J.L. Smith, D.R. Huggins, L. Carpenter-Boggs, and C.L. Reardon. 2016. Denitrifier abundance has a greater influence on denitrification rates at larger landscape scales but is a lesser driver than environmental variables. Soil Biology and Biochemistry 103: 221–231. doi: 10.1016/j.soilbio.2016.08.016.

Signor, D., and C.E.P. Cerri. 2013. Nitrous oxide emissions in agricultural soils: a review. Pesqui. Agropecu. Trop. 43(3): 322–338. doi: 10.1590/S1983-40632013000300014.

Sirivedhin, T., and K.A. Gray. 2006. Factors affecting denitrification rates in experimental wetlands: Field and laboratory studies. Ecological Engineering 26(2): 167–181. doi: 10.1016/j.ecoleng.2005.09.001.

Soil Survey Staff, Natural Resources Conservation Service, United States Department of Agriculture. 2019. Web soil survey. Available online at the following link: http://websoilsurvey.sc.egov.usda.gov/. Accessed [07/16/2020].

Stanley, Lynn. 1998. A characterization of bacterial populations from two sites. Dissertation. UMI Microform 9924929.

Trabaud, M., V. Icard, C. Ramiere, J. Tardy, C. Scholtes, and P. Andre. 2017. Comparison of HIV-1 drug-resistance genotyping by ultra-deep sequencing and sanger sequencing using clinical sapmles. J. Med. Vir., 89(11):1912-1919. doi: 10.1002/jmv.24872.

Tsiatis, A.C., A. Norris-Kirby, R.G. Rich, M.J. Hafez, C.D. Gocke, et al. 2010. Comparison of sanger sequencing, pyrosequencing, and melting curve analysis for the detection of KRAS mutations. The Journal of Molecular Diagnostics 12(4): 425–432. doi: 10.2353/jmoldx.2010.090188.

United Nations Framework Convention on Climate Change (UNFCCC). 2015. Paris Agreement.

Wang, J., and J. Zou. 2020. No-till increases soil denitrification via its positive effects on the activity and abundance of the denitrifying community. Soil Biology and Biochemistry 142: 107706. doi: 10.1016/j.soilbio.2020.107706.

2.9 Tables and Figures

Table 2.1: Crop management information for Fields 1 and 3.

Field	Year	Crop	Management Activity	N Fertilizer Form and Rate	Date
1	2016	Corn	Planting		15-May
			N fertilizer application	Urea, 122 kg N ha^{-1}	03-June
	2017	Soybean/Wheat	Planting		17-May
			N fertilizer application	Urea, 33.6 kg N ha^{-1}	18-Oct
			Wheat planting		20-Oct
	2018	Wheat	N fertilizer application	Urea, 67.2 kg N ha^{-1}	21-Mar
			N fertilizer application	32% Liquid N, 60.0 kg N ha^{-1}	30-Apr
			Cover crop mixture planted		09-Aug
	2019	Corn	Planting		16-May
			N Fertilizer Application	Urea, 112 kg N ha^{-1}	03-June
3	2016	Soybean	Pre-plant tillage		21-Mar
			Planting		22-May
			N fertilizer application	Anhydrous NH_3, 202 kg N ha^{-1}	21-Nov
	2017	Corn	N and P fertilizer application	$NH_4H_2PO_4$ (MAP), 21.3 kg N and 100 kg P ha^{-1}	14-Feb
			Pre-plant tillage		19-Apr
			Planting		19-Apr
			Post-harvest tillage		02-Nov
	2018	Soybean	Pre-plant tillage		27-Apr
			Planting		12-May

Table 2.2: Selected mean (± standard deviation) initial soil properties for Fields 1 and Field 3 by landscape position.

	Landscape Position		
Soil property	Summit	Backslope	Toeslope
Field 1			
pH (0.01 M $CaCl_2$)	6.3 ± 0.4	6.1 ± 0.3	5.7 ± 0.8
Neut. acidity ($cmol_c\ kg^{-1}$)	0.9 ± 0.8	1.3 ± 0.7	2.9 ± 2.5
Organic matter ($g\ kg^{-1}$)	26.9 ± 2.9	28.3 ± 3.0	35.6 ± 8.1
Total Organic Carbon ($g\ kg^{-1}$)	15.7 ± 1.7	16.5 ± 1.8	20.7 ± 4.7
Bray I P ($kg\ ha^{-1}$)	59.1 ± 43.4	35.2 ± 17.1	45.2 ± 17.7
Exc. Ca ($kg\ ha^{-1}$)	3697 ± 642	3760 ± 421	3990 ± 1611
Exch. Mg ($kg\ ha^{-1}$)	298 ± 78	345 ± 109	406 ± 105
Exch. K ($kg\ ha^{-1}$)	154 ± 62	144 ± 21	228 ± 144
CEC ($cmol_c\ kg^{-1}$)	10.5 ± 1.5	11.1 ± 1.4	13.6 ± 3.4
NO_3^--N ($g\ ha^{-1}$)	21.8 ± 8.8	14.2 ± 7.9	22.9 ± 11.3
NH_4^+- N ($g\ ha^{-1}$)	2.5 ± 0.4	2.3 ± 0.2	3.7 ± 2.5
Field 3			
pH (0.01 M $CaCl_2$)	5.7 ± 0.5	5.7 ± 0.4	5.7 ± 0.4
Neut. acidity ($cmol_c\ kg^{-1}$)	2.8 ± 2.2	2.8 ± 1.1	2.6 ± 1.0
Organic matter ($g\ kg^{-1}$)	27.9 ± 3.3	28.5 ± 3.4	31.8 ± 4.2
Total Organic Carbon ($g\ kg^{-1}$)	16.2 ± 1.9	16.6 ± 2.0	18.5 ± 2.5
P Bray I ($kg\ ha^{-1}$)	80.4 ± 39.1	65.0 ± 18.0	95.0 ± 38.5
Exch. Ca ($kg\ ha^{-1}$)	4321 ± 800	4531 ± 846	4404 ± 806
Exch. Mg ($kg\ ha^{-1}$)	521 ± 214	550 ± 128	469 ± 80
Exch. K ($kg\ ha^{-1}$)	320 ± 142	260 ± 89.7	257 ± 62
CEC ($cmol_c\ kg^{-1}$)	14.8 ± 4.1	15.2 ± 2.6	14.5 ± 2.2
NO_3^--N ($g\ ha^{-1}$)	21.3 ± 12.6	19.5 ± 7.6	38.9 ± 16.7
NH_4^+- N ($g\ ha^{-1}$)	2.0 ± 0.9	1.9 ± 0.5	1.8 ± 0.7

Table 2.3. Additional soil properties across fields by landscape position.

	Landscape Position		
Soil Property	Summit	Backslope	Toeslope
BC† (mg L^{-1})	66.0^{ab‡}	47.2^{a}	94.0^{b}
BN (mg L^{-1})	5.02^{a}	4.78^{a}	6.69^{a}
NO_3-N (g ha^{-1})	21.7^{a}	17.4^{a}	30.3^{b}
NH_4-N (g ha^{-1})	2.38^{ab}	2.05^{a}	2.81^{b}
TOC (g kg^{-1})	1.58^{a}	1.65^{a}	1.97^{b}

†BC = Biomass C; BN = Biomass N; NO_3^- = Nitrate; NH_4^+ = Ammonia; TOC = Total Organic Carbon.

‡For each soil property (within rows), means followed by a different letter were significantly different based one-way ANOVA ($\alpha = 0.10$) and $Tukey_{(0.10)}$ multiple comparison test.

Table 2.4. Pearson correlation coefficient matrix for DEA, and actual N_2O and N_2 emissions.

Variable	DEA	N_2O	N_2
DEA	--	0.170	0.159
N_2O	0.170	--	0.669*
N_2	0.159	0.669*	--
BC	-0.034	0.015	0.178
BN	0.655*	0.132	0.133
NO_3-N	0.639*	0.234	0.172
NH_4-N	-0.044	0.046	0.001
TOC	0.648*	0.135	0.072

* Indicates statistical significance at the $P \leq 0.10$ significance level.

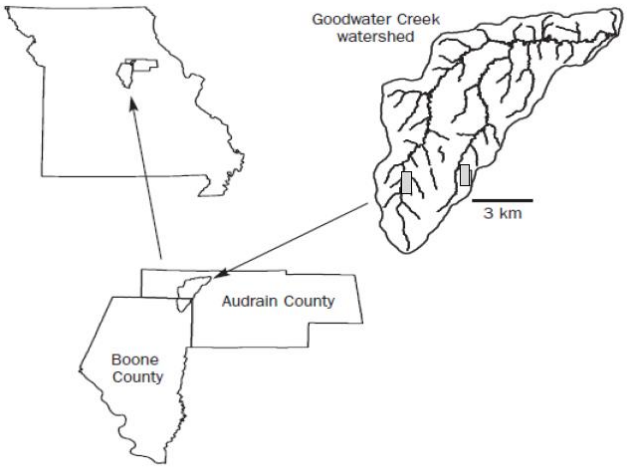

Figure 2.1: Location of study (Lerch et al., 2005; Sadler et al., 2015) in the Goodwater Creek watershed near Centralia, MO.

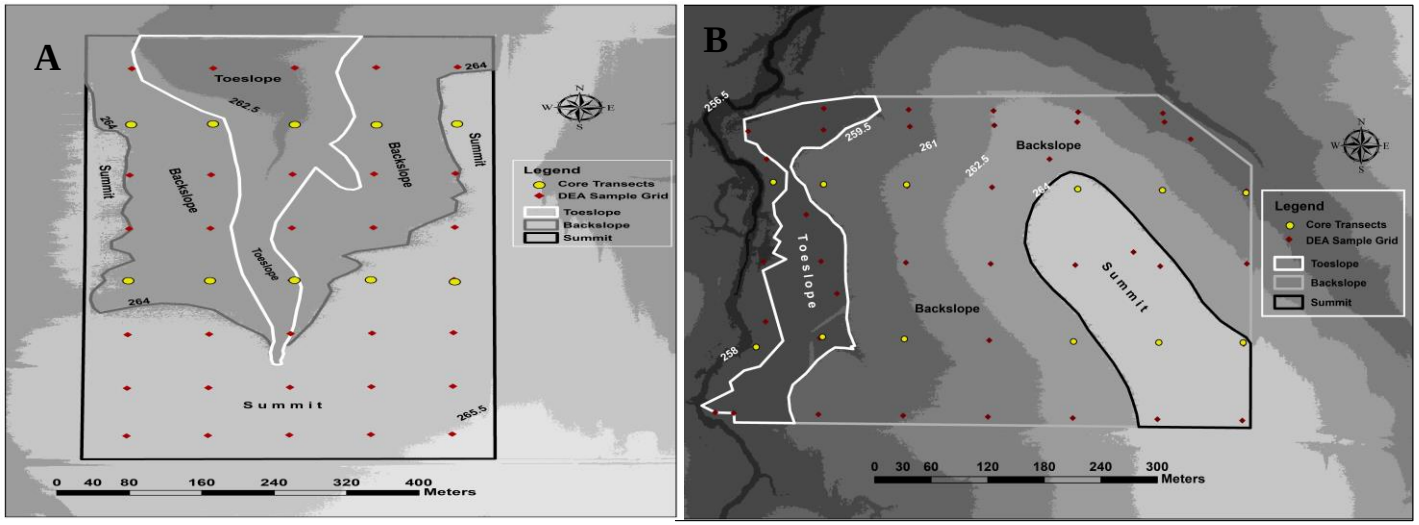

Figure 2.2: Core transect and 90 m grid sampling locations in identified landscape positions for Field 1(A) and Field 3 (B).

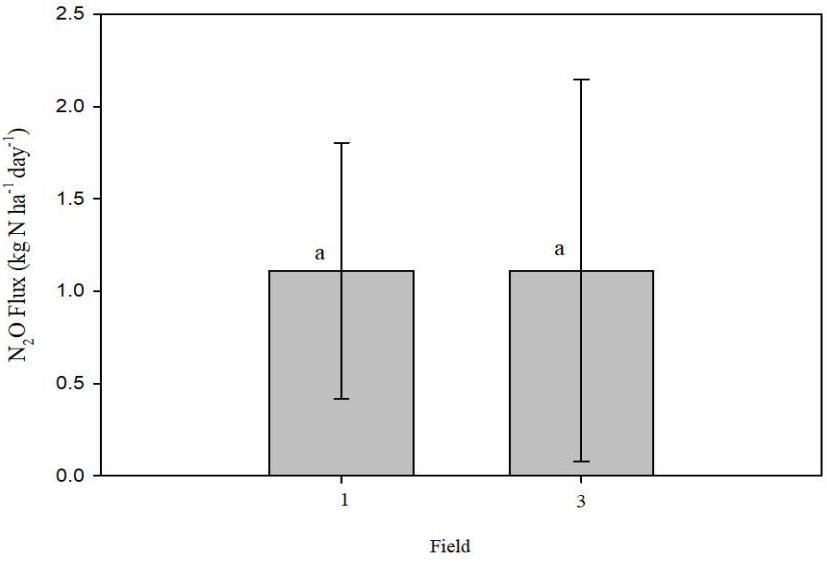

Figure 2.3: Potential N_2O flux rates between two fields under different management practices. Vertical bars represent standard deviation. Same letters denote no significant differences observed at α=0.05.

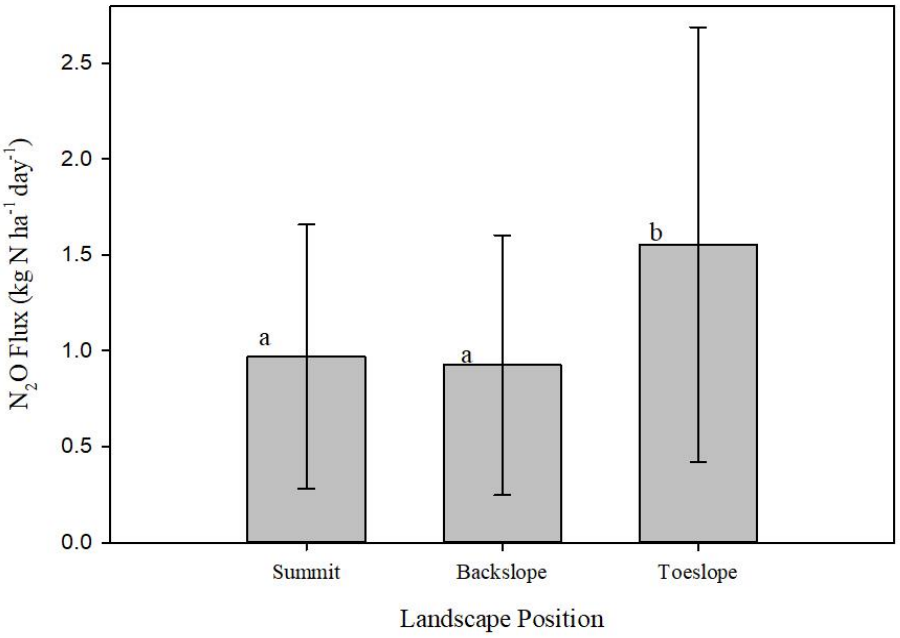

Figure 2.4: Denitrification potential by landscape position. Vertical bars represent standard deviation. Different letters denote significant differences observed at α=0.05 .

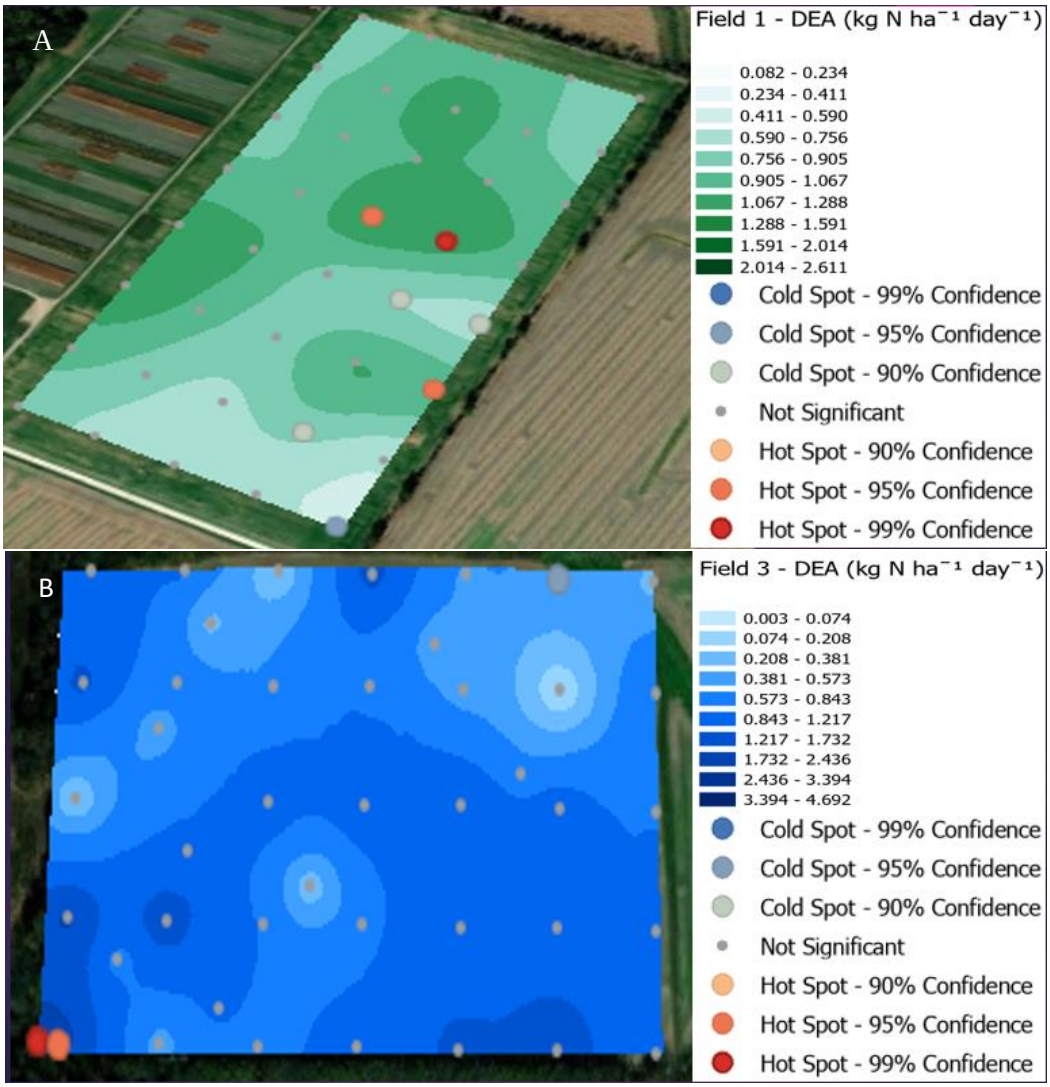

Figure 2.5: Kriged estimates of denitrification potential for Field 1 (A) and Field 3 (B).

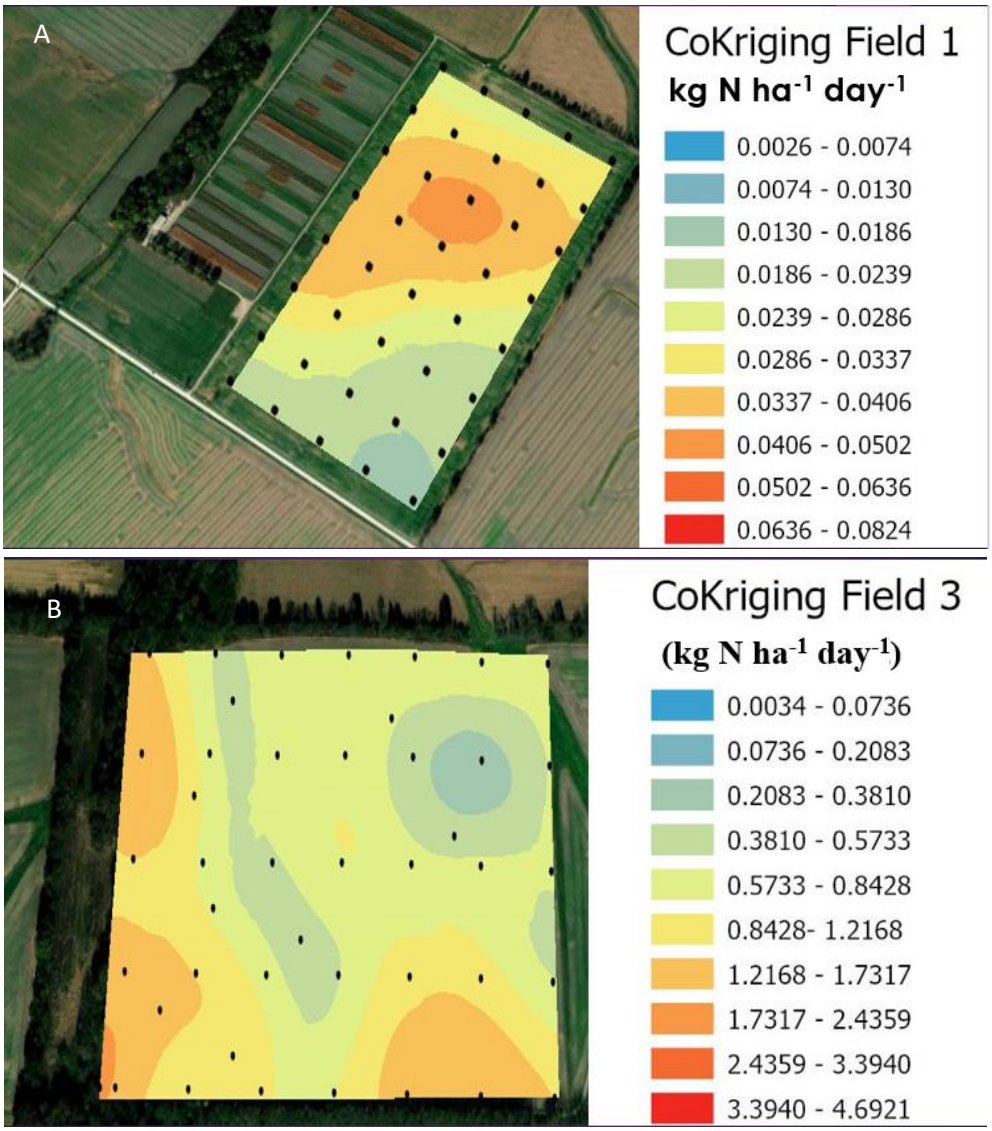

Figure 2.6: Co-kriged estimates of denitrification potential for Field 1 (A) and Field 3 (B) with NO_3^-, NH_4^+, and TOC as co-variables.

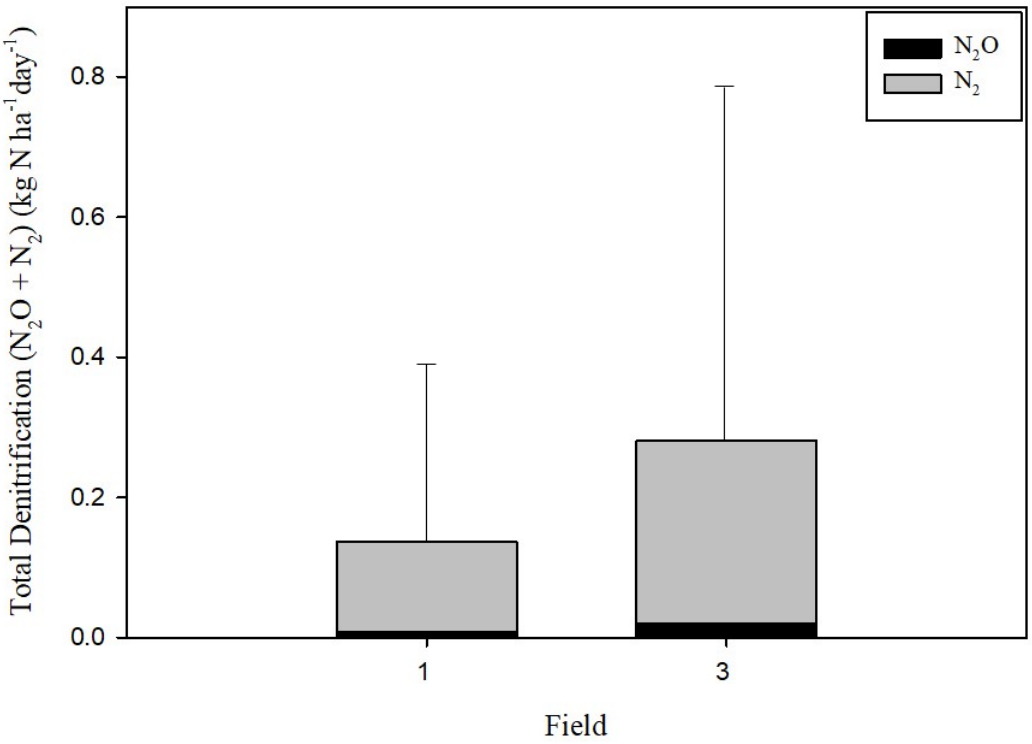

Figure 2.7: Actual denitrification for Fields 1 and 3 partitioned by N_2O and N_2 fluxes. Vertical bars represent standard deviation.

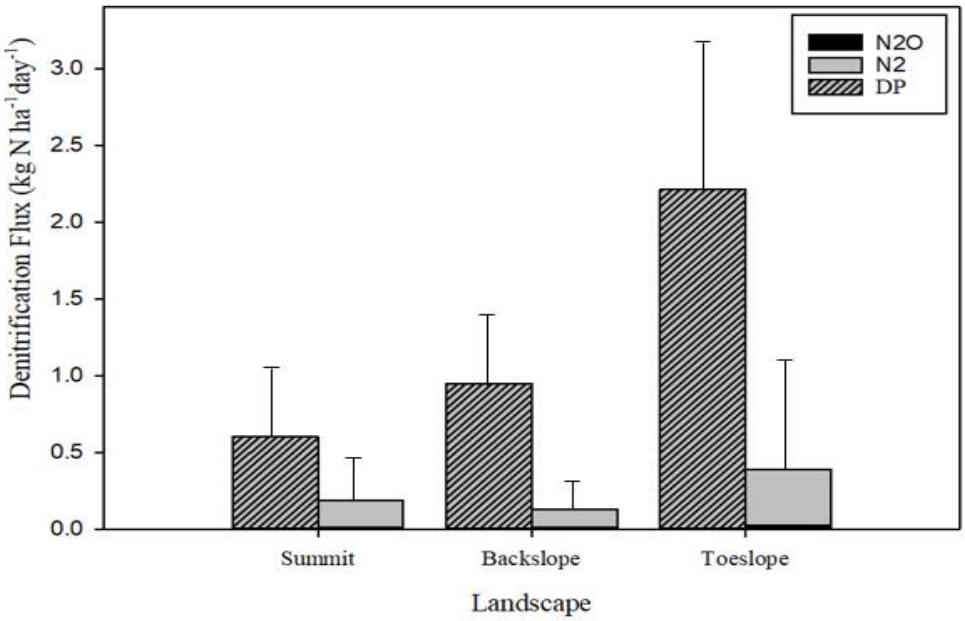

Figure 2.8: Denitrification Potential, Actual N_2O and Actual N_2 by landscape position. Vertical bars represent standard deviation.

CHAPTER 3

COMPARATIVE ANALYSIS OF THREE NEXT-GENERATION SEQUENCING TECHNIQUES TO MEASURE *NOSZ* ABUNDANCE ON MISSOURI CLAYPAN SOILS

3.1 Abstract

Quantitative next-generation sequencing techniques have been critical in gaining a better understanding of microbial ecosystems. The objectives of this research were to: 1) understand how depth influences RNA concentration and *nos*Z abundance; and 2) compare and evaluate multiple RNA-based sequencing methods for quantifying *nos*Z abundance in Missouri claypan soils. Research sites consisted of two claypan soil fields in Central Missouri. Triplicate soil cores were collected from two landscape transects across both fields. One set of cores was analyzed for extractable soil RNA, and *nos*Z gene abundance using real-time quantitative polymerase chain reaction (RT-qPCR), droplet digital polymerase chain reaction (ddPCR), and nanostring sequencing (NS) at two depths (0-15 cm and 15-30 cm). Another set of cores were analyzed for N_2 using a gas flow soil core incubation system. There were significant differences in soil RNA quantities between the two depths, with an average of 54.5 mg kg^{-1} at 0-15 cm and 14.2 mg kg^{-1} at 15-30 cm. The low soil RNA concentrations in the subsoil prevented quantification of the *nos*Z gene, and suggested low overall microbial activity below 15 cm depth. Total *nos*Z estimates for RT-qPCR, ddPCR, and NS for these two fields were 180, 386, and 17.3 copies g^{-1}, respectively. The ddPCR method resulted in significantly greater gene copy estimates than those of RT-qPCR and NS ($p < 0.10$). There were no statistical differences in *nos*Z abundance between RT-qPCR and NS, and both methods showed minimal variability of *nos*Z abundance compared to ddPCR. Abundance of *nos*Z by landscape position showed different patterns for each method,

and none of the methods successfully captured the spatial variation of N_2 emissions or other soil properties.

3.2 Introduction

3.2.1 Next-Generation Gene Sequencing Technologies

Understanding the soil microbial community is necessary to understand soil function. Prior to DNA sequencing technology, researchers had to rely on culture-based methods, such as plating, to understand soil microbiology (Elsas and Boersma, 2011). This practice began in the late 1800s as Louis Pasteur discovered with yeast cells that bacteria can be isolated and grown. However, to successfully isolate bacteria, information about the microorganism's reproduction and growth conditions must be known (Monod, 1949). This can serve as a limitation because medium are selective and only certain microbiota are culturable (Elsas and Boersma, 2011).

Real-time quantitative polymerase chain reaction (RT-qPCR) has become the most popular next-generation sequencing due to its sensitivity and capability to provide rapid and robust results (Meyer, 2010). This diagnostic tool is powerful and has been used in studies to quantify sequences in DNA and RNA in soils and other environmental samples (Schriewer et al., 2011). A major limitation, however, has been the sensitivity of the method for soils (Fortunato et al., 2018), as phenolic compounds and humic substances decrease the efficiency of PCR due to the inhibition of fluorescence (Wilson, 1997; Audemard et al., 2004; Sidstedt et al., 2020). Droplet digital polymerase chain reaction (ddPCR) became commercially available in 2011 and provided a new way to perform sequencing with the added benefit of avoiding the development of a standard curve during analysis. By protocol, after droplets are developed containing the target sequence, the reader determines whether the sample is positive for the target. This allows for a more precise analysis and reproducible results compared to RT-qPCR, especially for

samples that are prone to inhibition through contamination (Hindson et al., 2011; Racki et al., 2014; Taylor et al., 2017). This also allows for the quantification of extremely low-concentration targets (Racki et al., 2014; Verhaegan et al., 2016).

Nanostring technology was developed in the early 2000s and became commercially available in 2008. Since then, it has been utilized in multiple clinical applications (Xu et al., 2016; Curini et al., 2019; Hay et al., 2020) and on RNA from plant materials (Othman et al., 2018). At the time of this publication, and prior to data presented here, NS has not been applied to soils. Similar to RT-qPCR and ddPCR, NS uses fluorescent technology to quantify specific target sequences from isolated RNA. In contrast, NS uses fluorescent barcodes to bind to the nucleic acids instead of fluorescent probes (Reis et al., 2011). Strengths of this technology include its ability to read target sequences up to 800 base pairs long, which allows for high specificity, and up to twelve samples can be analyzed for multiple genes concurrently (Reis et al., 2011), which can be an effective and economical way to quantify multiple genes associated with a known biological pathway, such as denitrification.

3.2.2 Genetic Material, Denitrification, Depth, and Landscape Position

Studies of the microbiome in surface soils and subsoils have provided a better understanding of soil functionality (Bandick and Dick, 1999; Taylor et al., 2001; Kramer et al., 2013). While it was observed that most microbial biomass C is found near the soil surface (Fang and Moncrieff, 2005), over 50% of global soil organic carbon (SOC) is below a depth of 30 cm (Jobbagy and Jackson, 2000). Soil nutrients that support microbial biomass and enzymes decrease with depth (Eilers et al., 2012; Stone et al., 2014). Landscape position is also major factor influencing genetic material. On claypan soils (from Field 3; see below), Stanley (1998) observed denitrification in 57% of isolates from summit samples compared to 100% of isolates

from the toeslope. Furthermore, facultative anaerobes were evenly distributed in surface and sub-surface horizons in the toeslope while they were only present below 160 cm in the summit.

3.2.3 Research Needs and Objective

Previous research has compared multiple next-generation sequencing techniques, including RT-qPCR and ddPCR; however, this is the first study comparing RT-qPCR, ddPCR, and NS for soils. Each of these three next-generation technologies mentioned have the potential to provide much needed information on the denitrifying microbial community. Denitrification is the microbial facilitated conversion of nitrate (NO_3^-) to dinitrogen (N_2) under anoxic conditions, producing other gases as intermediates in the process. The enzyme nitrous oxide reductase is responsible for facilitating the final transformation of N_2O to N_2, and the gene which codes for it is designated, *nos*Z (Zumft, 1997). In the Midwest, poorly drained claypan soils provide suitable conditions over the entire landscape for denitrification to occur due to the potential of water ponding for a significant period of time combined with a warm and humid climate (Nash et al., 2015). The objectives of this research were to understand how depth influences RNA concentration, and compare and evaluate multiple RNA-based sequencing methods for quantifying the *nos*Z gene abundance in Missouri claypan soils.

3.3 Materials and Methods

3.3.1 Site Location

This study was conducted in two fields at the Goodwater Creek Experimental Watershed (GCEW) in the Central Mississippi River Basin member of the long-term agroecosystem research (LTAR) network located in northeastern Missouri (Field 1 - 39°13’46.92” N , -92°7’0.84” W, Field 3 - 39°13’55.56” N, -92°9’0.36” W) (Fig. 3.1). These are claypan soils formed from a clay loess parent material with smectitic minerology, and the characteristics of

these soils has been described in detail by Lerch et al. (2008) and Sadler et al., (2015). Management information for these fields is given in Chapter 2 (Table 2.1). Studies in these fields have been on-going since 1991, and the crop management history is well documented. In addition, Kitchen et al. (1997) further described the land management history of these fields from 1930 to 1990, reporting significant application or disposal of manure on Field 3.

3.3.2 Soil Sampling

Two sets of intact soil cores were obtained within each field along two landscape transects (Figure 3.2 A and B) for Field 1 in September 2018, and for Field 3 in April 2018, using a hydrologic soil probe in 5 cm plastic liner. Six cores were collected per transect in Field 1 and 7 cores were collected from Field 3. Cores were collected to depths of 60-80 cm such that at least one claypan horizon was included. Out of the cores collected, one was analyzed using the N-free atmospheric recirculation method (N-FARM) as described in Chapter 2, section 2.3.4.

3.3.3. Soil RNA Extraction and cDNA generation

Soil RNA extraction was conducted using the RNeasy PowerSoil Total RNA kit (Qiagen, Germantown, MD) and protocol on up to 2 g of field moist soil. For RNA extraction, soils were separated in to two depths, 0-15 cm, and 15-30 cm. Total RNA was converted to cDNA using the SuperScip IV VILO Master Mix (Thermo Fisher Scientific, Waltham, MA) protocol and was stored at -80 °C until RT-qPCR, ddPCR, and NS. Soil RNA extraction and all gene sequencing analyses described below were performed by MOgene (St. Louis, MO; https://www.mogene.com/).

3.3.4. RT-qPCR Analysis

Real-time qPCR was conducted by using a 7900HT Fast Real-Time PCR System (Applied Biosystem, Foster City, CA) to determine transcript abundances of *nos*Z. The

information for primers and probes used in the analysis are listed in Table 3.2. Primers for *nos*Z1F and *nos*Z1R were those identified in Henry et al. (2006) as potentially universal primers for the *nos*Z gene and probes were designed by Mo-Gene using a tool on the Integrated DNA Technologies website (https://www.idtdna.com). Real-time qPCR for *nos*Z gene abundance was performed using 10 μL TaqMan Fast Advanced Master Mix (2X), 1 μL of TaqMan Assay (20X), 7 μL of Nuclease-Free Water, and 2 μL of the sample cDNA. Polymerase activation occurred at 95 °C for 10 minutes. Cycling conditions included 40 cycles in which denaturing occurred at 95°C for 1 s, and annealing/extending at 60°C for 20 s.

3.3.5. ddPCR Analysis

Droplet digital PCR was also performed on the cDNA from the soil samples using a Bio-Rad QX200 Droplet Digital PCR system (Hercules, CA). Primers and probes for this analysis are the same as those listed for the RT-qPCR analysis. Sample preparation included adding 22 μL ddPCR supermix (developed by Bio-Rad) along with 5 μL of cDNA and 6 μL of water were added to each well. Each sample was analyzed in triplicate. Next, droplets were generated using a manual QX200 droplet generator, followed by PCR amplification using a Bio-Rad C1000 Cycler (Hercules, California). Cycling conditions are listed on Table 3.3. Next, data acquisition occurred using QX One software. Positive and negative droplets were measured using QunataSoft Analysis Pro Software (Bio-Rad, v1.0.596).

3.3.6. Nanostring Sequencing Analysis

Nanostring sequencing was performed using the nanostring nCounter SPRINT Profiler (Nanostring Technologies, Inc., Seattle, WA) following their nCounter Elements TagSets technology protocol. The probes were developed by Nanostring Technologies, Inc. (Seattle, WA, USA) and are listed along with the target sequence information for this analysis in Table 3.4. The

*nos*Z target sequence was from *Pseudomonas aeruginosa* (Accession PA3392.2) and the acp (Acyl Carrier Protein-P) gene was used for quality control to ensure that the correct target gene within the target organisms were analyzed. A total of 100 ng of RNA from each sample was used for analysis. Starting with 65 µL of reagent that TagSet tube, a master mix was developed by first adding 130 µL of hybridization buffer and 13 µL of the 30X Probe A. Next, the tube was mixed and briefly spun down at less than 1,000 rpm before adding 13 µL of 30X Probe B and performing the same mixing procedure. Next, 17 µL of master mix and 100 ng of sample RNA was added to a tube, then nuclease-free water was added to each tube to bring the volume of each reaction to 30 µL. The hybridization temperature was 67 °C and took between 16-21 hours. After hybridization was complete, the temperature was changed to 4 °C, The tubes were then mix and spun down at <1,000 rpm, incubated for approximately 16 hours, then analyzed with the nCounter.

3.3.7 Statistical Analysis

Statistical analysis for this study was conducted using the SAS v9.4 statistical program (SAS Institute, Inc., Cary, NC, USA). An analysis of variance (ANOVA) was conducted using PROC GLM to determine whether there were significant differences in total RNA concentration between each field, and a 2-way ANOVA was performed on RNA concentration with depth and landscape as factors to determine their significance and to investigate possible significant interactions. An ANOVA was also conducted to determine whether *nos*Z gene abundance, expressed on a dry soil basis, was significantly different between fields. The Mann Whitney U test was used to compare *nos*Z gene abundance for each molecular method between fields. Tukey's honest significant difference (HSD) was used to separate mean RNA concentration by

field, landscape position, and depth, and to separate mean *nos*Z gene abundance by field and landscape position for each sequencing method.

3.4 Results

3.4.1 RNA Concentration in claypan soils

Soil RNA concentrations were significantly greater in Field 1 compared to Field 3 at both depths and averaged over depth (Table 3.5). At the 0-15 cm depth, average RNA concentrations were 71.3 mg kg^{-1} for Field 1, and 40.1 mg kg^{-1} for Field 3. Lower in the soil profile at the 15-30 cm, average RNA concentrations were significantly lower in both fields, measuring 21.3 and 8.14 mg kg^{-1}, respectively. Results from an ANOVA indicated that depth was a significant predictor of RNA concentration ($p < 0.10$). Soil RNA concentrations by landscape position in Field 1 were were 35.3, 56.3, and 47.3 mg kg^{-1} for summit, backslope, and toeslope positions, respectively (Table 3.6). In Field 3, average RNA concentrations were 11.5 mg kg^{-1} in the summit, 29.1 mg kg^{-1} in the backslope, and 29.7 mg kg^{-1} in the toeslope. Average RNA concentrations in the summit of Field 1 were significantly greater at both depths than in Field 3, but RNA concentrations were not significantly different between fields at the backslope and toeslope positions. There were no significant landscape-depth interactions detected. However, there was a significant landscape effect detected at the 15-30 cm depth ($p < 0.10$), but not at the 0-15 cm depth.

*3.4.2 Using RT-qPCR, ddPCR, and nanostring technology to measure nos*Z *abundance*

Abundance of *nos*Z gene in surface soils showed no significant differences between fields for any of the methods, and further method comparisons were based on pooled data (Table 3.7). Results showed significant differences between methods in *nos*Z gene abundance, with average abundance in the order: ddPCR > RT-qPCR > NS (Figure 3.4). Average abundance of

*nos*Z measured with NS was 17.3 copies g^{-1}, with an extremely low variability in gene abundance, ranging from 8.77 to 54.9 copies g^{-1}. Analysis by ddPCR produced the highest quantity of *nos*Z gene abundance with an average of 386 copies g^{-1}, but the method also had the highest variability (Fig. 3.4). Gene abundance of *nos*Z by RT-qPCR were intermediate compared to the other methods, with an avergae of 180 copies g^{-1}.

Abundance of *nos*Z by landscape position for each method showed that RT-qPCR and NS methods varied much less than ddPCR (Figure 3.5). For RT-qPCR analysis, average *nos*Z gene abundances in the summit, backslope, and toeslope landscape positions were 146, 195, and 198 copies g^{-1}. Abundance of *nos*Z by RT-qPCR was significantly greater in the toeslope position compared to the summit ($p < 0.10$), while *nos*Z copies in the backslope and toeslope were similar. For NS, *nos*Z abundances were not significantly different by landscape position, and this method showed minimal variation in gene abundance across landscape position, ranging from 14.9 copies g^{-1} at the toeslope to 19.8 copies g^{-1} at the summit. For NS method, higher variability was observed in the summit compared to the other two landscape positions. Abundances of *nos*Z for samples analyzed with ddPCR for the summit, backslope, and toeslope were 333, 458, and 313 copies g^{-1}. Variability from this analysis was highest in the backslope, at least almost two times more than variability in the other two positions. The results from Tukey's HSD conclude there were no significant differences in *nos*Z abundance by landscape position for ddPCR and NS. However, abundance of *nos*Z measured by RT-qPCR was significantly higher in backslope and toeslope positions when compared to the summit. There were no significant landscape-method interactions detected.

3.5 Discussion

3.5.1. RNA Concentration by Depth and Landscape Position

In this study, there was a significant decrease in RNA concentration at the 15-30 cm depth compared to the 0-15 cm depth. In the summit and backslope positions of these fields, the 15-30 cm soil depth corresponds to the top of the claypan. The argillic horizons in the summit and backslope showed much greater decreases in RNA from 0-15 cm to 15-30 cm than in the toeslope (Table 3.6). Our results were similar to Taylor et al. (2002), in which they observed a decrease in biological activity decreased with depth. Although we did not measure biological activity directly, RNA concentration is an indicator as the relative instability of RNA suggest its presence is due to active gene transcription. A major difference in their study is they sampled a larger interval, ranging from 0 – 30 cm for the surface soil, to a deep sand layer 3.9 – 4.2 m deep on two agricultural fields under clay and sandy soils. Similarly, Griffiths et al. (2003) observed differences in bacterial community due to soil depth. They also observed the time sampling occurred influenced the bacterial community, with samples near the surface having greater genetic variation compared to the deeper samples most likely due to higher moisture content as a result of increased mineralizable C (Curtin et al., 2012). Specifically on claypan soils, Hsiao et al. (2018) observed a sharp decrease in both SOC and N with depth. Beyond 30 cm, both SOC and N fell below 1%, meaning there was no accumulation of biomaterials beyond the claypan layer. In our fields, the claypan layer can be present at a depth of 20 cm or less.

Despite the absence of significant landscape-depth interactions, the decrease in RNA concentration at the 0-15 cm depth to 15-30 cm depth was greatest in the backslope for Field 1 (~84% decrease), and in the summit for Field 3 (~93% decrease) (Table 3.6). The smallest decrease for Field 1 was 64%, observed in the summit, and was 47% for Field 3, observed in the

toeslope. Our results are similar to that of Stanley (1998), who observed small decreases in colony forming units in isolates from toeslope samples to approximately the 180cm depth, and larger decreases from samples in the summit and backslope. Further, RNA concentrations at the 0-15 and 15-30 cm depths were highest in the backslope and toeslope, respectively. Although no significant landscape effect was detected for RNA concentration at the 0-15 cm depth, the higher RNA concentration in the backslope position is an indication of RNA accumulation. Soil properties listed in Chapter 2 (Table 2.2; Table 2.3) indicate most soil properties are higher in the toeslope position. This discrepancy between RNA concentration and other soil properties should be further investigated.

3.5.2 Next-Generation Sequencing, nosZ Abundance, N_2 Flux, and other Soil Characteristics

Abundances of *nos*Z copies were extremely different between the three different next-generation sequencing techniques. An exhaustive literature review suggests prior to this study, *nos*Z has only been measured through PCR, RT-qPCR, and ddPCR analyses (Siciliano et al., 2007; Zhang et al., 2015; Zhang et al., 2013; Yang et al., 2018; Wang et al., 2012; Dong et al., 2014). Zmienko et al. (2015) observed extremely low variability when utilizing RT-qPCR to profile their reference genes for leaf senescence. In the direct comparison of RT-qPCR and ddPCR, Taylor et al. (2017) observed similar results for identical samples with low levels of contamination. When investigating the accuracy using RT-qPCR to measure *nos*Z abundance for a variety of denitrifiers, Sicilian et al. (2007) observed that RT-qPCR was accurate in measuring *nos*Z when templates consisted of up to six denitrifiers. Since the true or expected *nos*Z abundances were not known, the accuracy of the methods presented here cannot be assessed. However, their utility can be assessed by correlation of gene abundance to measured denitrification flux and soil properties in relation to landscape position (Ch. 2).

Results presented here showed that RT-qPCR and NS data were less variable than ddPCR (Table 3.7), but they all poorly corresponded to actual N_2 flux measured by N-FARM (see Ch. 2) and soil properties (Table 3.8). Only concentrations of NH_4^+-N significantly correlated with NS *nos*Z gene abundance measurements. Further, *nos*Z abundances measured by NS were 10- to 20-fold lower than the other methods and almost invariant across the landscape (Fig. 3.5). Compared to the other methods, ddPCR measurements of *nos*Z were the most variable and had a dissimilar pattern to observed differences in N_2 flux and denitrification potential across landscape position. The sequencing technologies used in this study did not successfully capture the landscape dependence of microbial denitrification as illustrated in Chapter 2. Contrarily, Dong et al. (2014) compared results from a plasmid containing *nos*Z to data generated through analysis of the same plasmid through liquid chromatography-isotope dilution mass spectrometry, which provided independent quantification. They found ddPCR to be a reliable technique for measuring *nos*Z. In our study, there was no apparent relationship between RT-qPCR, ddPCR, and NS measurements of *nos*Z with N_2 flux by landscape position. While NS produced drastically different results for *nos*Z gene abundance, it may be a useful tool when sequencing multiple *nos*Z gene targets across the denitrifying community.

3.6 Conclusion

The concentrations of extractable RNA were significantly greater in the top 15 cm of the soil profile, indicating the majority of active microorganisms, including denitrifiers, exist in the surface soil above the claypan. Extractable RNA at 0-15 cm depth was nearly four times greater than that at 15-30 cm, demonstrating the abrupt decrease in apparent microbial activity between the silt loam Ap horizon and the claypan Bt horizon. Comparison of three gene sequencing methods showed significant differences in *nos*Z abundance between methods, with ddPCR

resulting in the highest average *nos*Z abundances, but also the greatest variability. While ddPCR, RT-qPCR and NS have proven to be useful in clinical and other research applications, these methods gave results that poorly reflected denitrification. The lack of variability across landscape position for ddPCR, RT-qPCR and NS and absence of significant landscape-method interaction, also makes them of limited usefulness for assessing denitrification in soils. The sequencing methods in this study were not sufficient in capturing the spatial variation of denitrification and other soil properties. It is possible that the use of other *nos*Z primers with these technologies could provide a more promising relationship between *nos*Z abundance and denitrification measurements, and should be investigated.

3.7 Acknowledgements

I would like to express appreciation and gratitude to the USDA-ARS for their financial contribution and continued support of this study. I would also like to thank Sanjiv Bhave and his team at MO-Gene, and Cheryl Tan and her team at Nanostring Technologies, Inc. for the analysis of our soil samples.

3.8 References

Bandick, A.K., and R.P. Dick. 1999. Field management effects on soil enzyme activities. Soil Bio and Biochem. 31: 1471-1479.

Curtin, D., M.H. Beare, and G. Hernandez-Ramirez. 2012. Temperature and moisture effects on microbial biomass and soil organic matter mineralization. Soil Sci. Soc.Am. J. 76(6): 2055–2067. doi: 10.2136/sssaj2012.0011.

Dong, L., Y. Meng, J. Wang, and Y. Liu. 2014. Evaluation of droplet digital PCR for characterizing plasmid reference material used for quantifying ammonia oxidizers and denitrifiers. Anal Bioanal Chem 406(6): 1701–1712. doi: 10.1007/s00216-013-7546-1.

Eilers, K.G., S. Debenport, S. Anderson, and N. Fierer. 2012. Digging deeper to find unique microbial communities: The strong effect of depth on the structure of bacterial and archaeal communities in soil. Soil Biology and Biochemistry 50: 58–65. doi: 10.1016/j.soilbio.2012.03.011.

Elsas, J.D., and F.G.H. Boersma. 2011. A review of molecular methods to study the microbiota of soil and the mycosphere. European Journal of Soil Biology 47(2): 77–87. doi: 10.1016/j.ejsobi.2010.11.010.

Fang, C., and J.B. Moncrieff. 2005. The variation of soil microbial respiration with depth in relation to soil carbon composition. Plant Soil 268(1): 243–253. doi: 10.1007/s11104-004-0278-4.

Fortunato, G., I. Vaz-Moreira, C. Becerra-Castro, O.C. Nunes, and C.M. Manaia. 2018. A rationale for the high limits of quantification of antibiotic resistance genes in soil. Environmental Pollution 243: 1696–1703. doi: 10.1016/j.envpol.2018.09.128.

Griffiths, R.I., A.S. Whiteley, A.G. O'Donnell, and M.J. Bailey. 2003. Influence of depth and sampling time on bacterial community structure in an upland grassland soil. FEMS Microbiology Ecology 43(1): 35–43. doi: 10.1111/j.1574-6941.2003.tb01043.x.

Henry, S., D. Bru, B. Stres, S. Hallet, and L. Philippot. 2006. Quantitative detection of the nosZ gene, encoding nitrous oxide reductase, and comparison of the abundances of 16S rRNA, narG, nirK, and nosZ Genes in Soils. AEM 72(8): 5181–5189. doi: 10.1128/AEM.00231-06.

Hindson, B.J., K.D. Ness, D.A. Masquelier, P. Belgrader, N.J. Heredia, et al. 2011. High-throughput droplet digital PCR system for absolute quantitation of DNA copy number. Anal. Chem. 83(22): 8604–8610. doi: 10.1021/ac202028g.

Hsiao, C.-J., G.F. Sassenrath, L.H. Zeglin, G.M. Hettiarachchi, and C.W. Rice. 2018. Vertical changes of soil microbial properties in claypan soils. Soil Biology and Biochemistry 121: 154–164. doi: 10.1016/j.soilbio.2018.03.012.

Jobbágy, E.G., and R.B. Jackson. 2000. The vertical distribution of soil organic carbon and its relation to climate and vegetation. Ecological Applications 10(2): 423–436. doi: 10.1890/1051-0761(2000)010[0423:TVDOSO]2.0.CO;2.

Kramer, S., S. Marhan, H. Haslwimmer, L. Ruess, and E. Kandeler. 2013. Temporal variation in surface and subsoil abundance and function of the soil microbial community in an arable soil. Soil Biology and Biochemistry 61: 76–85. doi: 10.1016/j.soilbio.2013.02.006.

Luo, J., R.W. Tillman, R.E. White, and P.R. Ball. 1998. Variation in denitrification activity with soil depth under pasture. Soil Biology and Biochemistry 30(7): 897–903. doi: 10.1016/S0038-0717(97)00206-X.

Monod, J. 1949. The growth of bacterial cultures. Annual Review of Microbiology 3(1): 371–394. doi: 10.1146/annurev.mi.03.100149.002103.

Nash, P., P. Motavalli, K. Nelson, and R. Kremer. 2015. Ammonia and nitrous oxide gas loss with subsurface drainage and polymer-coated urea fertilizer in a poorly drained soil. Journal of Soil and Water Conservation 70(4): 267–275. doi: 10.2489/jswc.70.4.267.

Othman, N.Q. 2018. Validation of differential gene expression of transcriptome assembly via nanostring® technologies analysis platform. JOPR. doi: 10.21894/jopr.2018.0009.

Rački, N., T. Dreo, I. Gutierrez-Aguirre, A. Blejec, and M. Ravnikar. 2014. Reverse transcriptase droplet digital PCR shows high resilience to PCR inhibitors from plant, soil and water samples. Plant Methods 10(1): 42. doi: 10.1186/s13007-014-0042-6.

Reis, P.P., L. Waldron, R.S. Goswami, W. Xu, Y. Xuan, et al. 2011. mRNA transcript quantification in archival samples using multiplexed, color-coded probes. BMC Biotechnol 11: 46. doi: 10.1186/1472-6750-11-46.

Schriewer, A., A. Wehlmann, and S. Wuertz. 2011. Improving qPCR efficiency in environmental samples by selective removal of humic acids with DAX-8. Journal of Microbiological Methods 85(1): 16–21. doi: 10.1016/j.mimet.2010.12.027.

Siciliano, S.D., W. Ma, and S. Powell. Evaluation of quantitative polymerase chain reaction to assess nosZ gene prevalence in mixed microbial communities. Can. J. Micro. 53: 636-642.

Sidstedt, M., P. Rådström, and J. Hedman. 2020. PCR inhibition in qPCR, dPCR and MPS—mechanisms and solutions. Anal Bioanal Chem 412(9): 2009–2023. doi: 10.1007/s00216-020-02490-2.

Stanley, Lynn. 1998. A characterization of bacterial populations from two sites. Dissertation. UMI Microform 9924929.

Stone, M.M., J.L. DeForest, and A.F. Plante. 2014. Changes in extracellular enzyme activity and microbial community structure with soil depth at the Luquillo Critical Zone Observatory. Soil Biology and Biochemistry 75: 237–247. doi: 10.1016/j.soilbio.2014.04.017.

Taylor, S.C., G. Laperriere, and H. Germain. 2017. Droplet digital PCR versus qPCR for gene expression analysis with low abundant targets: from variable nonsense to publication quality data. Sci Rep 7(1): 2409. doi: 10.1038/s41598-017-02217-x.

Taylor, J.P., B. Wilson, M.S. Mills, and R.G. Burns. 2002. Comparison of microbial numbers and enzymatic activities in surface soils and subsoils using various techniques. Soil Biology and Biochemistry 34(3): 387–401. doi: 10.1016/S0038-0717(01)00199-7.

Verhaegen, B., K. De Reu, L. De Zutter, K. Verstraete, M. Heyndrickx, et al. 2016. Comparison of droplet digital PCR and qPCR for the quantification of shiga toxin-producing Escherichia coli in bovine feces. Toxins 8(5): 157. doi: 10.3390/toxins8050157.

Wang, C., G. Zhu, Y. Wang, S. Wang, and C. Yin. 2013. Nitrous oxide reductase gene (nosZ) and N_2O reduction along the littoral gradient of a eutrophic freshwater lake. Journal of Environmental Sciences 25(1): 44–52. doi: 10.1016/S1001-0742(12)60005-9.

Xu, W., N.V. Solis, S.G. Filler, and A.P. Mitchell. 2016. Pathogen gene expression profiling during infection using a nanoString nCounter platform. Methods Mol Biol 1361: 57–65. doi: 10.1007/978-1-4939-3079-1_3.

Yang, Y.-D., Y.-G. Hu, Z.-M. Wang, and Z.-H. Zeng. 2018. Variations of the nirS-, nirK-, and nosZ-denitrifying bacterial communities in a northern Chinese soil as affected by different long-term irrigation regimes. Environ Sci Pollut Res 25(14): 14057–14067. doi: 10.1007/s11356-018-1548-7.

Zhang, X., L. He, F. Zhang, W. Sun, and Z. Li. 2013. The Different potential of sponge bacterial symbionts in N_2 release indicated by the phylogenetic diversity and abundance analyses of denitrification Genes, nirK and nosZ. PLOS ONE 8(6): e65142. doi: 10.1371/journal.pone.0065142.

Zhang, L., G. Zeng, J. Zhang, Y. Chen, M. Yu, et al. 2015. Response of denitrifying genes coding for nitrite (nirK or nirS) and nitrous oxide (nosZ) reductases to different physico-chemical parameters during agricultural waste composting. Appl Microbiol Biotechnol 99(9): 4059–4070. doi: 10.1007/s00253-014-6293-3.

Zmienko, A., A. Samelak-Czajka, M. Goralski, E. Sobieszczuk-Nowicka, P. Kozlowski, et al. 2015. Selection of reference genes for qPCR- and ddPCR-based analyses of gene

expression in senescing barley leaves (Z.-H. Chen, editor). PLoS ONE 10(2): e0118226. doi: 10.1371/journal.pone.0118226.

Zumft, W.G. 1997. Cell biology and molecular basis of denitrification. Microbiology and molecular biology reviews : MMBR 61(4): 533–616. doi: 10.1128/.61.4.533-616.1997.

3.9 Tables and Figures

Table 3.1: Selected mean (± standard deviation) initial soil properties for the Field 1 and Field 3.

Field 1	
pH (0.01 M $CaCl_2$)	6.1 ± 0.6
Neut. acidity ($cmol_c\ kg^{-1}$)	1.6 ± 1.7
Organic matter ($g\ kg^{-1}$)	29.9 ± 6.2
Bray I P ($kg\ ha^{-1}$)	47.6 ± 31.6
Exc. Ca ($kg\ ha^{-1}$)	3802 ± 972
Exch. Mg ($kg\ ha^{-1}$)	344 ± 105
Exch. K ($kg\ ha^{-1}$)	172 ± 93
CEC ($cmol_c\ kg^{-1}$)	11.6 ± 2.5
NO_3^--N ($g\ ha^{-1}$)	0.02 ± .001
NH_4^+- N ($g\ ha^{-1}$)	0.003 ± 0.001
Field 3	
pH (0.01 M $CaCl_2$)	5.7 ± 0.4
Neut. acidity ($cmol_c\ kg^{-1}$)	2.7 ± 1.3
Organic matter ($g\ kg^{-1}$)	29.3 ± 3.9
P Bray I ($kg\ ha^{-1}$)	76.0 ± 31
Exch. Ca ($kg\ ha^{-1}$)	4458.59 ± 812
Exch. Mg ($kg\ ha^{-1}$)	522.7 ± 138.1
Exch. K ($kg\ ha^{-1}$)	270.1 ± 95.6
CEC ($cmol_c\ kg^{-1}$)	14.9 ± 2.8
NO_3^--N ($g\ ha^{-1}$)	0.03 ± 0.01
NH_4^+- N ($g\ ha^{-1}$)	0.002 ± 0.001

Table 3.2. Primer and probe information for RT-qPCR and ddPCR

Primer and Probe Information		
Primer	**Sequence**	**Reference**
nosZ1F	WCSYTGTTCMTCGACAGCCAG	Henry et al., 2006
nosZ1R	ATGTCGATCARCTGVKCRTTYTC	
Probe		
6-FAM/ZEN/IBFQ	CTG GAT CCT GTT CTG GGT ATT C	--
	AGT TCG TTG CCG GTG AG	
	/56-FAM/TG ACC ATC C/Zen/T CGG CTA CCT/3IABkFQ/	
HEX/ZEN/IBFQ	GCC TAT ACC ACG CTG TTC AT	--
	GAG TTT CTG GCG GAT GTA GTC	
	/5HEX/AG CCA GTT G/ZEN/GTGA AGT GGA ACC T/3IABkFQ	

Table 3.3: Cycling conditions for ddPCR

Cycling Step	Temperature (°C)	Time	Number of Cycles
Hold (QX ONE ddPCR System only)	25	3 min	1
Enzyme activation	95	10 min	1
Denaturation	94	30 sec	40
Annealing/extension	60	1 min	40
Enzyme deactivation	98	10 min	1
Hold	4	Infinite	1
	25	1 min	1

Table 3.4: Primer and probe sequences for nanostring analysis.

Target	Sequence
nosZ	CACGCTGTTCATCGACAGCCAGTTGGTGAAGTGGAACCTGGCCGACGCGGTGCGCGCCTACAA GGGCGAGAAGGTCGACTACATCCGCCAGAAACTCGAC
Acp	TGGCTCTGGAAGAGGAATTCGAGACCGAAATCCCTGACGAGAAAGCTGAAAAGATCACCACC GTTCAGGAAGCCATCGACTACATCGTTGCTCACCAGCA
Probe A	CCGCGTCGGCCAGGTTCCACTTCACCAACTGGCTGTCGATGAACAGCGTGCGAACCTAACTCC TCGCTACATTCCTATTGTTTTC
Probe B	CGAAAGCCATGACCTCCGATCACTCTCGAGTTTCTGGCGGATGTAGTCGACCTTCTCGCCCTTG TAGGCGCGCA

Table 3.5: RNA concentration for Fields 1 and 3 at the 0-15 cm and 15-30 cm depths.

	RNA Concentration	
Depth	**Field 1**	**Field 3**
cm	(mg kg^{-1})	
0-15	71.3 a† A‡	40.1 a B
15-30	21.3 b A	8.14 b B
Average	46.3 A	24.1 B

†Soil depth means within a landscape position (each column) followed by different lower case letters were significantly different at $\alpha = 0.05$.

‡Soil depth means between fields (each row) followed by different upper case letters were significantly different at $\alpha = 0.05$.

Table 3.6: RNA concentration for Fields 1 and 3 by soil depth and landscape position.

Landscape Position	Depth	RNA Concentration	
		Field 1	Field 3
	(cm)	(mg kg^{-1})	
Summit	0-15	51.9 a A	21.4 a B
	15-30	18.6 b A	1.51b B
Backslope	0-15	96.9 a A	49.9 a A
	15-30	15.8 b A	8.32 b A
Toeslope	0-15	65.1 a A	38.7 a A
	15-30	29.5 b A	20.7 a A

Table 3.7: NosZ gene abundance (± standard deviation) measured by qPCR, ddPCR, and NS.

Method	***nosZ* Abundance**	
	Field 1	**Field 3**
	copies g^{-1}	
RT-qPCR	175 ± 56.5 ab A	185 ± 54.0 ab A
ddPCR	529 ± 769 a A	264 ± 348 a A
NS	14.4 ± 4.37 b A	19.8 ± 10.6 b A

Table 3.8: Correlations ($p < 0.10$) between nosZ gene abundance measurements from RT-qPCR, ddPCR, and NS, with other variables as described in Ch. 2. Bold numbers indicate significance.

Method/Variable	**RNA**	**DP**	**N_2**	**BC**	**BN**	**NO_3^--N**	**NH_4^+-N**	**TOC**
RT-qPCR	0.284	0.071	0.073	0.198	0.143	0.161	-0.011	0.130
ddPCR	0.321	0.075	0.031	-0.033	-0.139	0.222	0.108	-0.008
NS	-0.251	-0.123	0.153	-0.145	-0.045	-0.204	**0.462**	0.036

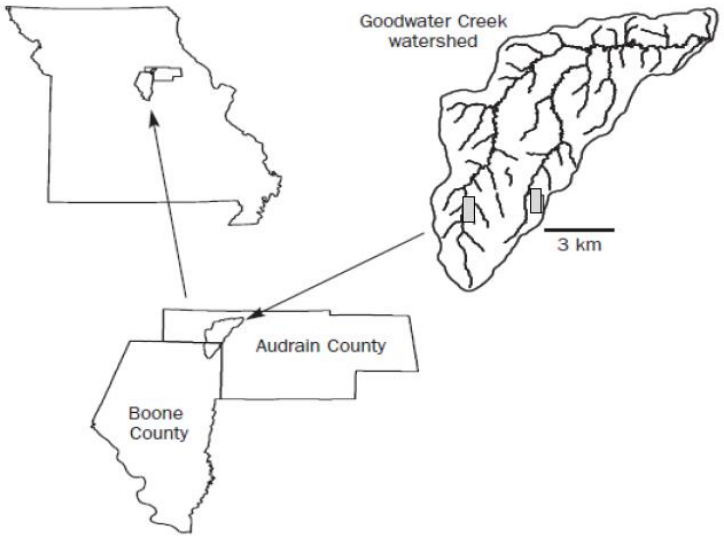

Figure 3.1: Location of study (Lerch et al., 2005; Sadler et al., 2015) in the Goodwater Creek watershed near Centralia, MO.

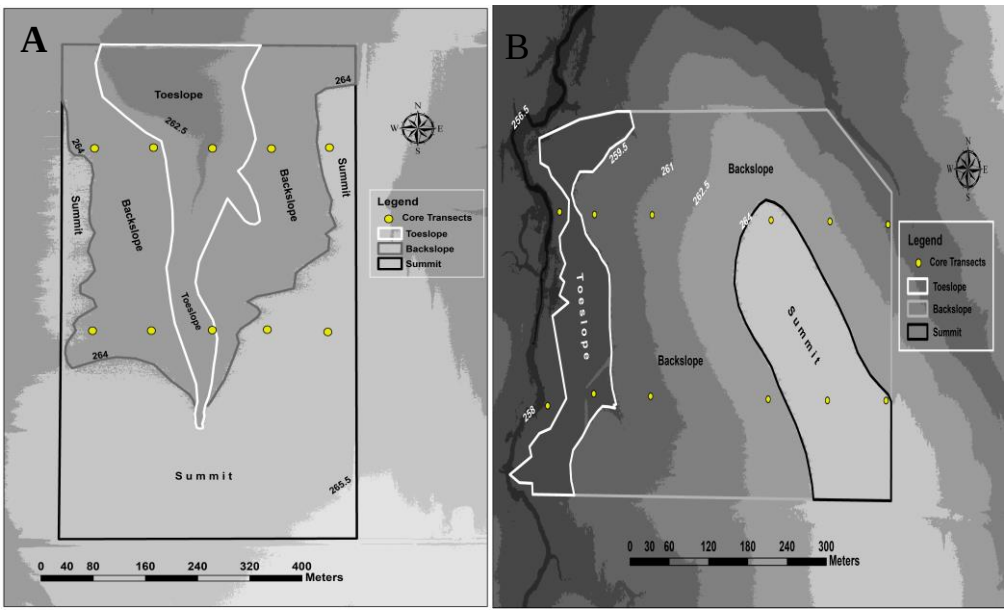

Figure 3.2 A&B: Core transect sampling locations for Field 1 (A) and Field 3 (B) with landscape position delineations.

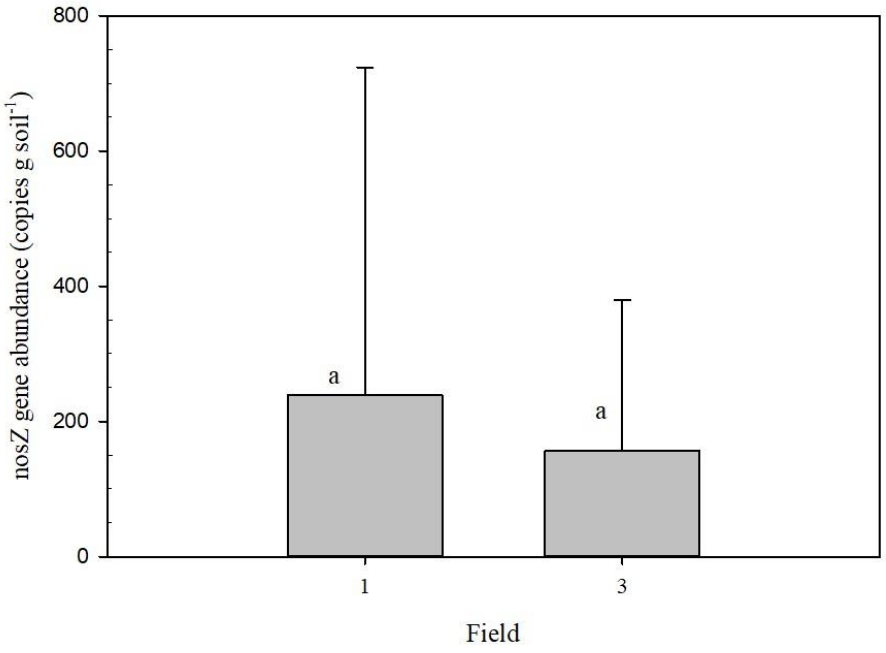

Figure 3.3: Total *nos*Z gene abundance measured with qPCR, ddPCR, and NS for Fields 1 and 3.

Vertical bars represent standard deviation. Same letters denote stati

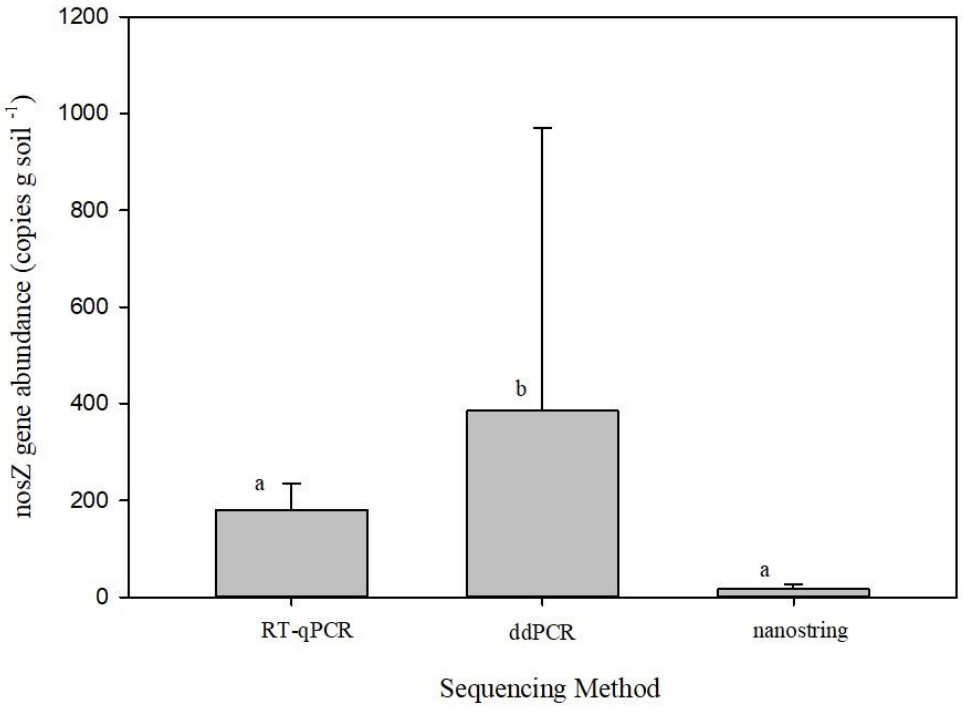

Figure 3.4: Total *nos*Z abundance by next-generation sequencing method.

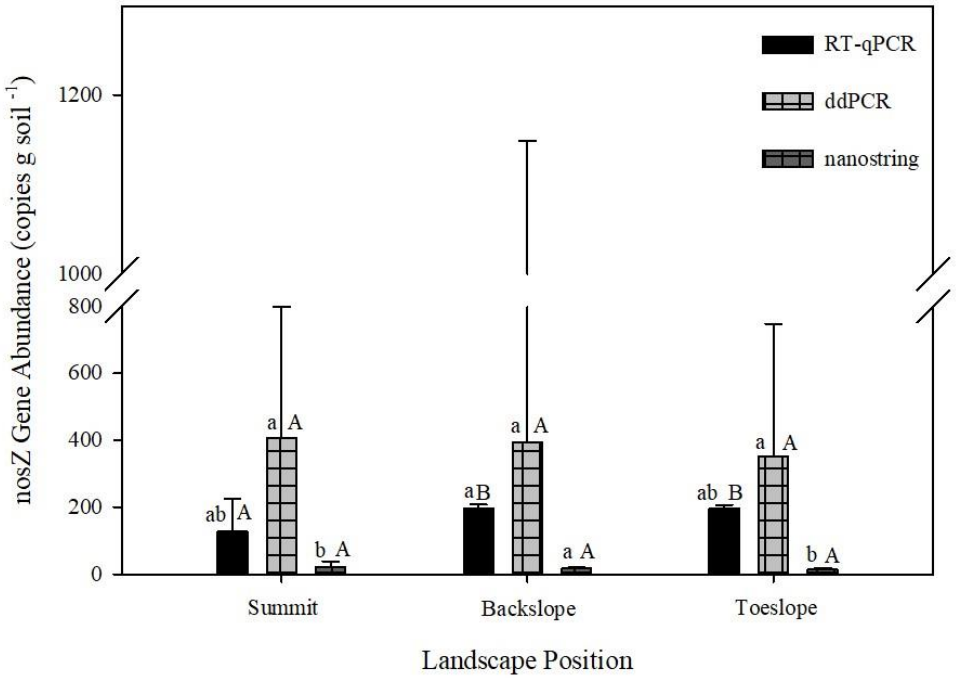

Figure 3.5: NosZ abundance by landscape position for RT-qPCR, ddPCR, and NS.

†Lower case letters denote comparison of mean *nosZ* abundance within a landscape position between methods at $\alpha = 0.05$.

‡Upper case letters denote comparison of mean *nosZ* abundance between landscape position for a particular method at $\alpha = 0.05$.

CHAPTER 4

FIELD-SCALE ESTIMATION OF DENITRIFICATION

4.1 Abstract

Denitrification is potentially a major loss pathway of fertilizer N used for crop production. The objective of this study was to develop a simple model to field-scale estimation of N_2O and N_2 fluxes based on measurements from the Nitrogen-Free Atmospheric Method (NFARM) and daily soil moisture and temperature data to estimate yearly denitrification fluxes. Intact soil cores were collected from two row crop fields in the Central Claypan Area of northeastern Missouri and used to measure N_2O and N_2 fluxes using NFARM. Soil temperature, O_2, and volumetric water content (VWC) were measured at 10 cm depth at three landscape positions in each field and these data used to establish a relationship between VWC and soil O_2 content. Denitrification was assumed to occur at and above VWC corresponding to soil O_2 of $\leq$5% and at temperatures $\geq$15^{o}C, with fluxes adjusted assuming a Q_{10} value of 2. Denitrification estimates were calculated for years in which corn or wheat were produced, due to N fertilizer application. Daily fluxes of N_2O ranged from 0.020 to 0.034 kg N $ha^{-1}d^{-1}$ and N_2 estimates were as high as 0.84 kg N $ha^{-1}d^{-1}$. Yearly denitrification estimates ranged from 0.54 to 9.26 kg N ha^{-1}. Denitrification accounted for at most 7.6% of total applied N. This study provides the first field-scale estimation of denitrification based on direct flux measurements and field-based soil environmental parameters. Results demonstrated the importance of denitrification can serve as a major loss pathway for fertilizer N in claypan fields and indicate the need for management practices that reduce gaseous N loss.

4.2 Introduction

Denitrification, the microbial facilitated reduction of nitrate (NO_3^-) to nitrous oxide (N_2O) and dinitrogen (N_2), serves as a significant loss to nitrogen (N) fertilizer applied in agricultural fields (Friedl et al., 2016). While important to the N-cycle, N_2O production detrimentally impacts the environment (Bouman et al., 2013). Nitrous oxide has a global warming potential 265-298 times that of carbon dioxide (CO_2), and 10-15 times that of methane (CH_4) (USEPA, 2020), and is responsible for the destruction of ozone (Crutzen, 1974; Portmann et al., 2012; Ramanathan et al., 1985, Ravishankara et al., 2009). Agricultural practices are responsible for a majority of anthropogenic N_2O emissions (USEPA, 2018) and are higher than natural ecosystems and non-intensive agroecosystems (Seitzinger et al., 2006).

Since the 1950s, there has been an increase in N-fertilizer usage by at least 10 Tg N y^{-1} (Ruddy et al., 2006). Higher N application rates has led to an in an increase in soil N_2O emissions (Nan et al., 2015; Wang et al., 2018). Extensive research has been conducted to estimate how denitrification is factored into the overall N-budget of agricultural systems. David et al. (2006) suggested that denitrification accounted for at least 80% of the un-accounted N in their mass balance. A recent study observed denitrification accounting for 37% of total N inputs (Castaldelli et al., 2020). Despite extensive research, there are still challenges to better understand overall denitrification contribution to the N-budget of agricultural systems (Almarez et al., 2020).

As an important component of the overall N-cycle, denitrification remains the most poorly assessed N transformation process (Del Grosso et al., 2020). To better understand it's importance, several models have been developed, with many based off denitrification potential (Heinen, 2005). Models vary from simple empirical equations to complex simulation models

(Gross et al., 2020). DAYCENT is a popular biogeochemical model used to simulate denitrification at the plot and landscape scales (Del Grosso et al., 2005; Parton et al., 1998). It incorporates all aspects of the CENTURY model but uses a daily time step instead of monthly (Del Grosso et al., 2005). Other process-based denitrification simulation models include the DeNitrification-DeComposition (DNDC) model (Li and Aber, 2000) and Agricultural Systems Modelling and Simulation (APSIM) (Thorburn et al., 2010). These models are quite complex and have a restraint of incorporating nitrification, plant N uptake, soil water, and nutrient movement as parameters to simulate N_2O emissions at large spatial scales (Del Grosso et al., 2020).

Despite much success, there are challenges faced by denitrification models. Hot spots and hot moments are characterized by small areas and brief periods where denitrification rates are high and account for a high percentage of total denitrification (McClain et al., 2003). The complex regulation of factors affecting distribution of O_2 and NO_3^- across the landscape causes hot spots and hot moments, which are not predicted by existing denitrification models, especially at the larger scale (Groffman et al., 2009). However, when informed by field observations, process-based models are powerful tools to investigate denitrification measurements in agricultural systems (Necpalova et al., 2015). Del Grosso et al. (2019) compared observed N_2O rates to modelled rates using DAYCENT. They observed similarities in actual and modelled N_2O emissions. However, their results also suggest that the model can be improved using soil pH as a parameter. The findings of Well et al. (2019) determined denitrification is underestimated if only surface flux measurements are used. They suggest using subsurface denitrification flux measurements to develop a corrective factor to successfully calculate total denitrification. Another way to improve denitrification models is to incorporate more biochemical factors and other associated processes in existing models (Del Grosso et al., 2020).

The nitrogen-free atmospheric recirculation method (NFARM) has been utilized to make measurements of total denitrification ($N_2O + N_2$) in the absence of atmospheric N_2 (Burgin et al., 2010; Burgin and Groffman, 2012; Morse et al., 2015; Morse et al., 2015). The objective of this study was to use NFARM measurements of total denitrification as the basis for estimating denitrification at the field-scale for two different Missouri fields under claypan soils. The model combines the NFARM fluxes with soil volumetric water content (VWC) and soil temperature as the main drivers for calculating denitrification. Field-scale estimations were made for years in which corn or wheat crops were grown and NFARM flux data for cores collected following N fertilizer application in both fields were used. This study provides the first field-scale estimation of denitrification based on actual denitrification measurements and field-based soil environmental parameters.

4.3 Materials and Methods

4.3.1 Site Location

This study included two fields at the Goodwater Creek Experimental Watershed (GCEW) in the Central Mississippi River Basin member of the long-term agroecosystem research (LTAR) network located in northeastern Missouri (Field 1 - 39°13’46.92” N , -92°7’0.84” W, Field 3 - 39°13’55.56” N, -92°9’0.36” W) (Fig. 4.1). These soils and management history for the years 2016, 2017, 2018, and 2019 were described in Chapters 2 and 3. Denitrification estimates were made for years in which wheat and corn were grown and N fertilizer applied to the fields. Field 1 was under corn in 2016 and 2019 and wheat in 2017-18 while Field 3 was under corn in 2017. Although total denitrification was not significantly different across landscape position, average fluxes were 2-3 times greater in the toeslope compared to upper landscape positions. Thus, the

landscape areas were determined for each field using LiDAR at 1.5-m intervals (Figure 4.2 A&B; Table 4.1).

4.3.2 Sensor Calibration

A network of soil sensors were installed across Fields 1 and 3 to record soil O_2, temperature, and moisture data at 5-minute intervals and capture the landscape-scale spatial and temporal variations in these parameters. Each field network included three nodes with four pairs of Apogee diffusion-head O_2 sensors (SO-110; Apogee Instruments, Inc., Logan, UT; Burgin et al., 2010) and volumetric water content (VWC) and temperature were measured using Decagon 5TM frequency domain reflectometry (FDR) sensors (Decagon Devices, Pullman, WA; Varble & Chavez, 2010). Two pairs of each sensor type were deployed in the A (or Ap) horizon (10 cm depth), and placed at various landscape positions, from summit to toeslope. Each node was equipped with a CR1000 data logger (Campbell Scientific, Inc., Logan, UT) and data was transferred via an existing telemetry system for automated daily downloading. Sensors were deployed for varying periods of time from 2016 to 2018, and data from four rainfall events were chosen.

The FDR sensors showed a low bias in the VWC data due to the high clay content of the soils and were corrected using time domain reflectometry (TDR) sensors (Seyfried et al., 2005). Both FDR and TDR sensors were deployed side-by-side at 10-cm depth to obtain data needed for the correction. The FDR sensors were corrected for multiple rainfall events that resulted in <5% soil O_2. To do this, the percent difference was calculated using the equation $(\frac{(\theta TDR - \theta FDR)}{\theta TDR}) * 100$. Three regions of distinct differences were identified to determine the volumetric water contents at which each correction would occur. Two were at 5 and 15 %, and the third consisted of a linear relationship between the two (Appendix A and Appendix B).

4.3.3. Flux Rates and Environmental Parameters

Flux rates for N_2O and N_2 in this model were obtained by the NFARM method as described in Chapter 2. Out of the 6 sets of cores that were analyzed for each field, only fluxes from those cores collected following recent N application were used: Field 1 – May 2016 and Nov 2017; and Field 3 – November 2017. In the absence of N fertilizer, fluxes were shown to be very low and did not represent denitrification under corn and wheat production. Flux rates were separated by landscape position for each field and are listed in Table 4.2.

The two critical environmental parameters controlling denitrification are soil O_2 and temperature. In the model presented, denitrification was assumed to occur at soil 0_2 $\leq$5% based on the findings of Burgin and Groffman (2012), and flux rates were adjusted for temperature, assuming a Q_{10} of 2. Soil O_2 data are not widely available as are VWC data (e.g., Soil Climate Analysis Network (SCAN) (https://www.wcc.nrcs.usda.gov/scan/); therefore, VWC was used to estimate soil O_2. By graphing soil VWC vs. soil O_2, the average VWC at which soil O_2 was $\leq$5% was 0.415 (+/- 0.020). Next, the lower limit of soil VWC was chosen as the criterion at which denitrification could occur, and hourly VWC data available at the Field 1 location (https://wcc.sc.egov.usda.gov/nwcc/site?sitenum=2195) were used to determine when VWC met the criteria.

Previous research suggests the Q_{10} value for denitrification, the rate of change that occurs when the temperature is increased by 10 °C, is approximately 2 in the 15 – 35°C range (Stanford et al., 1975; Phillips et al., 2015). This translates to denitrification rates doubling for every 10 °C increase in temperature. Others have calculated Q_{10} values of 1.6 in the 7 – 20°C range, and 2.8 in the 20 – 30°C range (Fischer and Whalen, 2005). Yu et al. (2020) observed Q_{10} values ranging from 1.31 to 2.98 for N_2O, and from 1.69 to 3.83 for N_2. In this study, the NFARM measured

denitrification at 20°C. As a result, we used the reported Q_{10} value of 2 as a basis to determine and apply rates from 15°C to 30°C. This was justified as the optimal reaction temperatures for denitrification is between 15 and 35°C (Liao et al., 2018). Mancino et al. (1988) observed significant denitrification at 30°C and above. For each landscape position, the denitrification rate applied at 30 °C was two times the measured rate from the NFARM. The rate at 15 °C was the measured rate from the NFARM divided by sqrt(2), which was solved for using the Q_{10} equation. Using the rates at the three temperatures, an equation following an exponential relationship was determined between rate and temperature (R^2=1) at each landscape within each field to calculate and apply the necessary rate in the model. Rate equations and conditions used to develop the model are listed in Table 4.3 and Table 4.4.

As shown in Table 2.1, Field 1 was under corn and wheat in 2016 and 2017, respectively. Corn was also planted in 2019, however, after the N was applied and corn planted, the stand was poor due to wet field conditions. The field remained wet too long to re-plant corn, so soybean was planted instead in June 2019. Since N fertilization had occurred, this year was still included in the estimates for denitrification. Field 3 was under corn only in 2017. Calculations for the calendar year were dependent on the date and frequency of N-fertilization and crop year. In both 2016 and 2019, Field 1 was under corn and fertilized once, so the calendar year was from January 1 to December 31 for each of those years. Wheat planting and N-fertilization occurred in October of 2017 for Field 1. As a result, the annual time frame for denitrification flux was from October 18, 2017 to October 17, 2018. Nitrogen fertilizer was also applied in March and April of 2018, so they were included in the total N inputs for that calendar year. Field 3 was grown under corn in 2017. Prior to planting, N fertilizer was applied in November of 2016 and in February 2017; thus, the calendar year started on Nov 22, 2016 and ended on November 21, 2017.

The daily soil VWC and temperature averages at the 10 cm depth from the SCAN site were sorted to identify when soil conditions met our criterion for denitrification. Next, daily flux rates were calculated using the following equation:

$$A_{xS}*R_{xS} + A_{xB}*R_{xB} + A_{xT}*R_{xT}$$

Here, A_x represents the area percentage (%) for Field x at each landscape position, and R_x is the applied flux rate (g N $ha^{-1}day^{-1}$) for Field x at each landscape position calculated using the associated rate equations listed in Table 4.3. Cumulative N_2O and N_2 emissions were then estimated by aggregating daily rates within each calendar year.

4.4 Results and Discussion

4.4.1 Yearly Estimates of N_2O and N_2

For Field 1, total denitrification estimates for the three years were 9.26, 0.54, and 8.01 kg N ha^{-1}, respectively (Figure 4.3A). In 2016, denitrification estimates accounted for roughly 7.6% of the total applied N. A total of 0.37 kg N ha^{-1} y^{-1} was estimated as N_2O, and 8.9 kg N ha^{-1} y^{-1} was estimated as N_2. When grown under wheat, < 1% of the total N application was accounted for through denitrification estimates. Percentage of total N application estimated as N_2O and N_2 in 2019 was lower than in 2016, representing 7.2%. Overall, average N_2O and N_2 emissions were 0.32 and 7.69 kg N ha^{-1}, respectively. Denitrification estimates for Field 3 grown under corn in 2017 were 3.96 kg N ha^{-1} (Figure 4.3B), and were lower than estimates in Field 1 when grown under corn. However, denitrification for Field 3 accounted for roughly 1.8% of 223 kg N ha^{-1} applied. Flux estimates of N_2O and N_2 were 0.15 and 3.8 kg N ha^{-1} y^{-1}, respectively.

4.4.2 Daily Estimates of N_2O and N_2, and Hot Moments/Hot Spots

Conditions for significant denitrification varied among years, but significant events occurred from May to September, with the greatest number of events occurring in 2019. This is

supported by the most precipitation occurring in 2019 (Table 4.5). Fluxes of N_2O production ranged from 0.023 to 0.034 kg N $ha^{-1}d^{-1}$. Dinitrogen fluxes ranged from 0.56 to 0.82 kg N $ha^{-1}d^{-1}$. The highest total denitrification estimate was on August 4, 2016 and the lowest flux estimates occurred both on September 11, and September 12. Despite a total precipitation of 770 mm in 2017-2018 (Table 4.5), suitable denitrification conditions occurred only once throughout the calendar year. On October 10, 2018, estimated N_2O and N_2 fluxes were 0.021 and 0.52 kg N ha^{-1} y^{-1}, respectively (Figure 4.3A). This is an indication that there are precipitation events that occur and do not induce conditions suitable for denitrification. In 2017, N_2O and N_2 estimates for Field 3 ranged from 0.020 to 0.033 kg N ha^{-1} d^{-1} and 0.50 to 0.84 kg N ha^{-1} d^{-1}, respectively (Figure 4.5). Despite widely varying conditions between years, when denitrification events occurred the total fluxes were generally between 0.40 to 0.80 kg N ha^{-1} d^{-1}. Thus, differences in annual losses mainly reflect the number of denitrification events each year. The irregular nature of the events was consistent with the notion of hot moments in which the conditions for denitrification occur sporadically. In terms of hot spots, based on the fluxes and temperature rate equations (Table 4.2 and 4.3), the summit position was the hot spot in Field 1, accounting for 83% of the annual flux while Field 3 had a nearly equal distribution of fluxes by landscape position.

4.4.3 Model Assumptions

While the model presented was capable of estimating denitrification fluxes on an event-basis at the field-scale, several simplifying assumptions exist within it. First, this model assumes that N_2O and N_2 fluxes have the same temperature dependence. Rate equations for both were developed based on the Q_{10} value of 2. A second assumption was that once the VWC threshold was reached, temperature drove the denitrification reactions. Denitrification typically increases as a both soil VWC and temperature increase (Philippot et al., 2007). However, O_2 concentration

is the one of the most important factors in denitrification regulation (Firestone et al., 1979; Tiedje, 1988; Burgin et al., 2010). Further, some studies have observed an increase in N_2 emissions at higher soil VWC (Wu et al., 2017; Ruser et al., 2006; Butterbach-Bahl et al., 2002), and the model does not take this into account. The model also disregards potential denitrification occurring at temperatures <15^{o}C, which is justified according to Avalakki et al. (1995), who reported low emissions on an Alfisol at 5°C. Lastly, the model used the highest observed denitrification rates for each field based on those cores with high residual soil NO_3^- concentration, and these rates were assumed to be applicable throughout the growing season. Given that residual soil NO_3^- decreases through the growing season, this assumption may over-estimate denitrification for events later in the season.

4.5 Conclusion

Denitrification estimates modelled by upscaling NFARM N_2O and N_2 measurements combined with soil environmental parameters was demonstrated to capture event-based dynamics and provide annual estimates of gaseous N loss from row crop fields. Denitrification from two Missouri fields cropped to corn or wheat accounted for up to 7.6% of total applied N fertilizer, showing that gaseous loss of N was a major transport pathway that may impact crop yields in some years. This approach used in this model development proposes an alternative to simulation models for field-scale estimations of denitrification by up-scaling NFARM data. Results showed that denitrification events were highly irregular in terms of the number and timing of events. This was consistent with the concept that hot moments control the magnitude of annual denitrification. It is possible that the processes used to develop this model can be used to upscale other plot measurements to the field-scale, and even to the watershed scale. However, the use of the LiDAR data in combination with soil mapping units and soil environmental data

are necessary to objectively upscale plot measurements to the watershed-scale. Extensive greenhouse gas sampling measurements should be obtained for these fields in the near future to determine the efficacy of the results and modelling techniques.

4.6 Acknowledgements

I would like to express appreciation and gratitude to the USDA-ARS and their staff for providing the relevant data and information for this study. I would also like to thank Dr. Peter Groffman and his research team at the Cary Institute of Ecosystem Studies for the analysis of the soil core samples and swiftly answering any question I had.

4.7 References

Almaraz, M., M.Y. Wong, and W.H. Yang. 2020. Looking back to look ahead: a vision for soil denitrification research. Ecology 101(1). doi: 10.1002/ecy.2917.

Alvalakki, U.K. W.M Strong, and P.G. Saffigna. 1995. Measurements of gaseous emissions from denitrification of applied nitrogen-15. II. Effects of temperature and added straw. Aust. J. Soil Res. 33:89-99.

Burgin, A.J., and P.M. Groffman. 2012. Soil O 2 controls denitrification rates and N 2 O yield in a riparian wetland. J. Geophys. Res. 117(G1). doi: 10.1029/2011JG001799.

Burgin, A.J., P.M. Groffman, and D.N. Lewis. 2010. Factors regulating denitrification in a riparian wetland. Soil Sci. Soc. Am. J. 74(5): 1826–1833. doi: 10.2136/sssaj2009.0463.

Butterbach-Bahl, K., G. Willibald, and H. Papen. Soil core method for direct simultaneous determination of N2 and N2O emissions from forest soils. : 12.

Crutzen, P.J. 1974. Photochemical reactions initiated by and influencing ozone in unpolluted tropospheric air. Tellus 26(1–2): 47–57. doi: 10.1111/j.2153-3490.1974.tb01951.x.

David, M.B., L.G. Wall, T.V. Royer, and J.L. Tank. 2006. Denitrification and the nitrogen budget of a reservoir in an agricultural landscape. Ecological Applications 16(6): 2177–2190. doi: 10.1890/1051-0761(2006)016[2177:datnbo]2.0.co;2.

Delgrosso, S., A. Mosier, W. Parton, and D. Ojima. 2005. DAYCENT model analysis of past and contemporary soil NO and net greenhouse gas flux for major crops in the USA. Soil and Tillage Research 83(1): 9–24. doi: 10.1016/j.still.2005.02.007.

Firestone, M.K., M.S. Smith, R.B. Firestone, and J.M. Tiedje. 1979. The influence of nitrate, nitrite, and oxygen on the composition of the gaseous products of denitrification in soil. Soil Sci. Soc. Am. J. 43(6): 1140–1144. doi: 10.2136/sssaj1979.03615995004300060016x.

Fischer, E.N., and S.C. Whalen. 2005. Rates and controls on denitrification in an agricultural soil fertilized with liquid lagoonal swine waste. Nutr Cycl Agroecosyst 71(3): 271–287. doi: 10.1007/s10705-004-6379-x.

Friedl, J., C. Scheer, D.W. Rowlings, H.V. McIntosh, A. Strazzabosco, et al. 2016. Denitrification losses from an intensively managed sub-tropical pasture – Impact of soil moisture on the partitioning of N 2 and N 2 O emissions. Soil Biology and Biochemistry 92: 58–66. doi: 10.1016/j.soilbio.2015.09.016.

Groffman, P.M., K. Butterbach-Bahl, R.W. Fulweiler, A.J. Gold, J.L. Morse, et al. 2009. Challenges to incorporating spatially and temporally explicit phenomena (hotspots and

hot moments) in denitrification models. Biogeochemistry 93(1–2): 49–77. doi: 10.1007/s10533-008-9277-5.

Grosso, S.J.D., S.M. Ogle, W.J. Parton, C. Nevison, W. Smith, et al. 2019. Modelling denitrification and N_2O emissions from fertilised cropping systems using Daycent. Climate change: 5.

Li, C., J. Aber, F. Stange, K. Butterbach-Bahl, and H. Papen. 2000. A process-oriented model of N 2 O and NO emissions from forest soils: 1. Model development. J. Geophys. Res. 105(D4): 4369–4384. doi: 10.1029/1999JD900949.

Liao, R., Y. Miao, J. Li, Y. Li, Z. Wang, et al. 2018. Temperature dependence of denitrification microbial communities and functional genes in an expanded granular sludge bed reactor treating nitrate-rich wastewater. RSC Adv. 8(73): 42087–42094. doi: 10.1039/C8RA08256A.

McClain, M.E., E.W. Boyer, C.L. Dent, S.E. Gergel, N.B. Grimm, et al. 2003. Biogeochemical hot spots and hot moments at the interface of terrestrial and aquatic ecosystems. Ecosystems 6(4): 301–312. doi: 10.1007/s10021-003-0161-9.

Nan, W., S. Yue, S. Li, H. Huang, and Y. Shen. 2016. Characteristics of N_2O production and transport within soil profiles subjected to different nitrogen application rates in China. Science of The Total Environment 542: 864–875. doi: 10.1016/j.scitotenv.2015.10.147.

Necpálová, M., R.P. Anex, M.N. Fienen, S.J. Del Grosso, M.J. Castellano, et al. 2015. Understanding the DayCent model: Calibration, sensitivity, and identifiability through inverse modeling. Environmental Modelling & Software 66: 110–130. doi: 10.1016/j.envsoft.2014.12.011.

Parton, W.J., M. Hartman, D. Ojima, and D. Schimel. 1998. DAYCENT and its land surface submodel: description and testing. Global and Planetary Change 19(1–4): 35–48. doi: 10.1016/S0921-8181(98)00040-X.

Philippot, L., S. Hallin, and M. Schloter. 2007. Ecology of Denitrifying Prokaryotes in Agricultural Soil. Advances in Agronomy. Elsevier. p. 249–305

Phillips, R., A. McMillan, T. Palmada, J. Dando, and D. Giltrap. 2015. Temperature effects on N 2 O and N 2 denitrification end-products for a New Zealand pasture soil. New Zealand Journal of Agricultural Research 58(1): 89–95. doi: 10.1080/00288233.2014.969380.

Portmann, R.W., J.S. Daniel, and A.R. Ravishankara. 2012. Stratospheric ozone depletion due to nitrous oxide: influences of other gases. Phil. Trans. R. Soc. B 367(1593): 1256–1264. doi: 10.1098/rstb.2011.0377.

Ramanathan,V.,Cicerone,R.J.,Singh,H.B.,andKiehl, J. T., 1985. Trace gas trends and their potential rolein climate change, J. Geophys. Res., 90, 5547–5566,https://doi.org/10.1029/JD090iD03p05547.

Ravishankara, A.R., J.S. Daniel, and R.W. Portmann. 2009. Nitrous Oxide (N2O): The dominant ozone-depleting substance emitted in the 21st century. Science 326(5949): 123–125. doi: 10.1126/science.1176985.

Ruddy, B.C. D.L. Lorenz, and D.K. Mueller. 2006. County-level estimates of nutrient inputs to the land surface of the conterminous United States, 1982-2001. National Water-Quality Assessment Program. Scientif Investigations Report 2006-5012. https://pubs.usgs.gov/sir/2006/5012/

Ruser, R., H. Flessa, R. Russow, G. Schmidt, F. Buegger, et al. 2006. Emission of N_2O, N_2 and CO_2 from soil fertilized with nitrate: effect of compaction, soil moisture and rewetting. Soil Biology and Biochemistry 38(2): 263–274. doi: 10.1016/j.soilbio.2005.05.005.

Seitzinger, S., J.A. Harrison, J.K. Böhlke, A.F. Bouwman, R. Lowrance, et al. 2006. Denitrification across landscapes and waterscapes: A synthesis. Ecological Applications 16(6): 2064–2090. doi: 10.1890/1051-0761(2006)016[2064:DALAWA]2.0.CO;2.

Seyfried, M.S., L.E. Grant, E. Du, and K. Humes. 2005. Dielectric loss and calibration of the Hydra probe soil water sensor. Vadose Zone Journal 4(4): 1070–1079. doi: 10.2136/vzj2004.0148.

Stanford, G., S. Dzienia, and R.A. Vander Pol. 1975. Effect of temperature on denitrification rate in soils. Soil Sci. Soc. Am. J. 39(5): 867–870. doi: 10.2136/sssaj1975.03615995003900050024x.

Thorburn, P.J., J.S. Biggs, K. Collins, and M.E. Probert. 2010. Using the APSIM model to estimate nitrous oxide emissions from diverse Australian sugarcane production systems. Agriculture, Ecosystems & Environment 136(3–4): 343–350. doi: 10.1016/j.agee.2009.12.014.

Tiedje, J.M. 1988. Ecology of denitrification and dissimilatory nitrate reduction to ammonium. In A.J.B. Zehnder (ed), Environmental Microbiology of Anaerobes. John Wiley and Sons, N.Y.

USEPA, 2018. Overview of greenhouse gas emissions. Available at https://www.epa.gov/ghgemissions/overview-greenhouse-gases Accessed on September 2, 2020.

Wang, J., D.R. Chadwick, Y. Cheng, and X. Yan. 2018. Global analysis of agricultural soil denitrification in response to fertilizer nitrogen. Science of The Total Environment 616–617: 908–917. doi: 10.1016/j.scitotenv.2017.10.229.

Well, R., M. Maier, D. Lewicka-Szczebak, J.-R. Köster, and N. Ruoss. 2019. Underestimation of denitrification rates from field application of the ¹⁵N gas flux method and its correction by gas diffusion modelling. Biogeosciences 16(10): 2233–2246. doi: 10.5194/bg-16-2233-2019.

Wu, D., L.M. Cárdenas, S. Calvet, N. Brüggemann, N. Loick, et al. 2017. The effect of nitrification inhibitor on N2O, NO and N2 emissions under different soil moisture levels in a permanent grassland soil. Soil Biology and Biochemistry 113: 153–160. doi: 10.1016/j.soilbio.2017.06.007.

Yu,H., Y. Fang, and R. Kang. 2020. Response of N2O and N2 emissions in forest soils to temperature change across China. EGU General Assembly Conference Abstracts.

4.8 Tables and Figures

Table 4.1: Areas for each landscape position for Field 1 and Field 3.

Field	Landscape Position	Area (ha)	Area Percentage of Field (%) (A)
1	Summit (S)	23.65	65.6
	Backslope (B)	6.19	17.2
	Toeslope (T)	6.22	17.2
3	Summit (S)	3.87	19.8
	Backslope (B)	13.11	67.1
	Toeslope (T)	2.56	13.1

Table 4.2: Actual N_2O and N_2 flux rates.

Field	Core Sampling Date/Event	Landscape	N_2O Flux Rate (g N ha^{-1} d^{-1})	N_2 Flux Rate (g N ha^{-1} d^{-1})
1	May 13, 2016	Summit	48.7	1017
		Backslope	4.25	95.2
		Toeslope	4.70	495
	March 17, 2017	Summit	14.1	333
		Backslope	0.328	447
		Toeslope	10.0	44.0
3	November 18, 2016	Summit	49.9	1394
		Backslope	25.0	1105
		Toeslope	141	574
	April 23, 2018	Summit	1.80	68.7
		Backslope	1.34	0
		Toeslope	2.55	804

Table 4.3: N_2O and N_2 rate equations for Fields 1 and 3 by landscape position.

Field	Landscape Position	N_2O Rate Equation (R) (g N ha^{-1} d^{-1})	N_2 Rate Equation (R) (g N ha^{-1} d^{-1})
1	Summit	$2.2899e^{0.0385T}$	$49.192e^{0.0385T}$
	Backslope	$0.1667e^{0.0385T}$	$19.781e^{0.0385T}$
	Toeslope	$0.5363e^{0.0385T}$	$19.659e^{0.0385T}$
3	Summit	$1.8863e^{0.0385T}$	$53.309e^{0.0385T}$
	Backslope	$0.9603e^{0.0385T}$	$38.788e^{0.0385T}$
	Toeslope	$5.225e^{0.0385T}$	$50.232e^{0.0385T}$

Note: N_2O and N_2 rates are dependent on the temperature (T).

Table 4.4: Parameters and conditions used to develop the denitrification model.

Parameter	Description	Value	Reference
θ_{crit}	Cut-off volumetric water content used for estimating denitrification.	0.395	--
T_{crit}	Cut-off temperature used for estimating denitrification.	15 °C	Liao et al., 2018
Q_{10}	Factor at which reaction rate changes every 10 °C increase in temperature.	2	Stanford et al., 1975; Phillips et al., 2015
A_{xy}	Area (%) for Field X (1,3), Landscape Y (Summit (S), Backslope (B), Toeslope (T)).	Table 4.1	--
R_{xy}	Rate (g N $ha^{-1}d^{-1}$) for Field X (1,3), Landscape Y	Table 4.2	--

Table 4.5: Cumulative precipitation amounts for each year.

Annual Period	Total Precipitation (mm)
Jan 1, 2016 - Dec 31, 2016	949
Nov 22, 2016 - Nov 21, 2017	851
Oct 18, 2017 - October 17, 2018	770
Jan 1, 2019 - Dec 31, 2019	1002

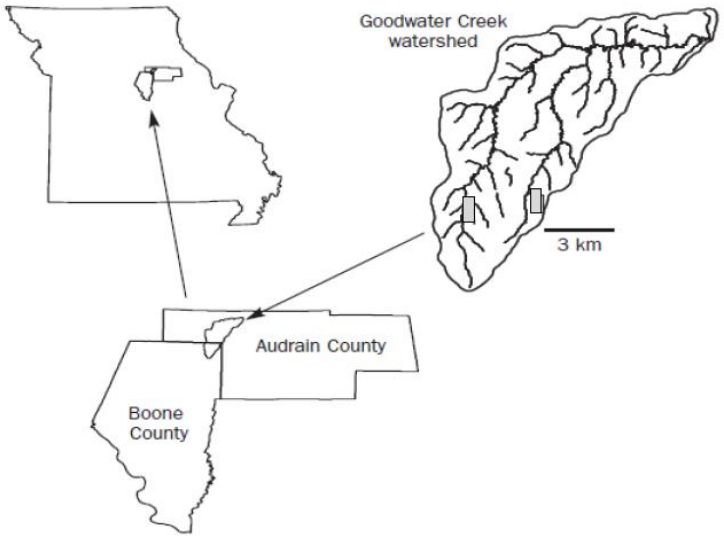

Figure 4.1: Location of study (Lerch et al., 2005; Sadler et al., 2015) in the Goodwater Creek watershed near Centralia, MO.

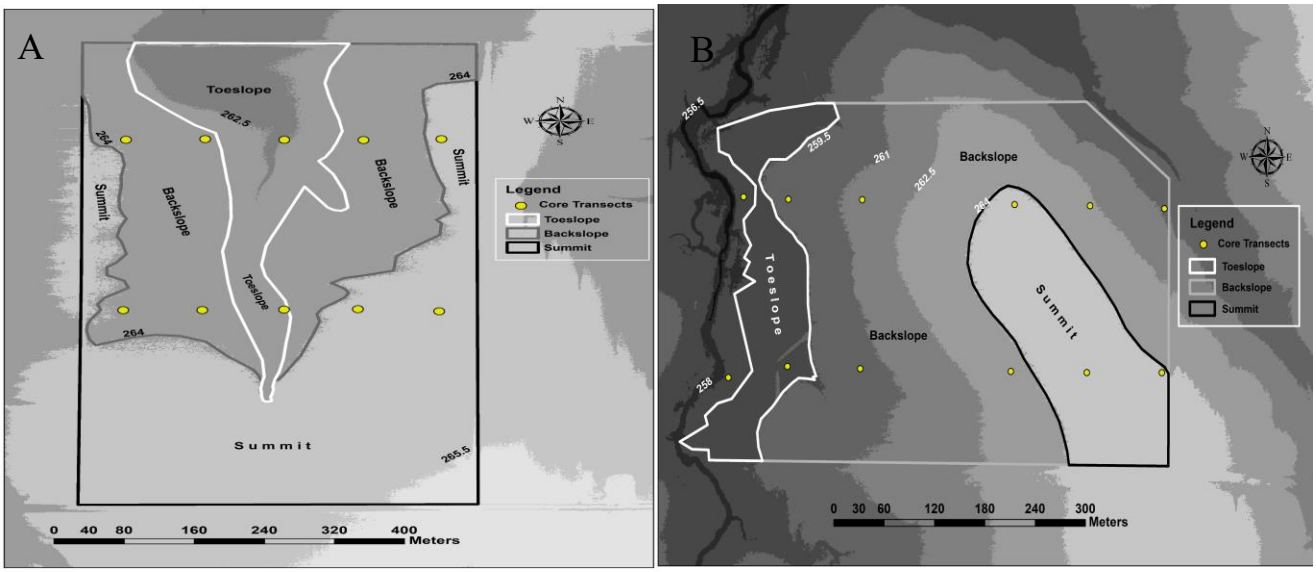

Figure 4.2 A&B: Core transect locations in identified landscape positions for Field 1(A) and Field 3 (B).

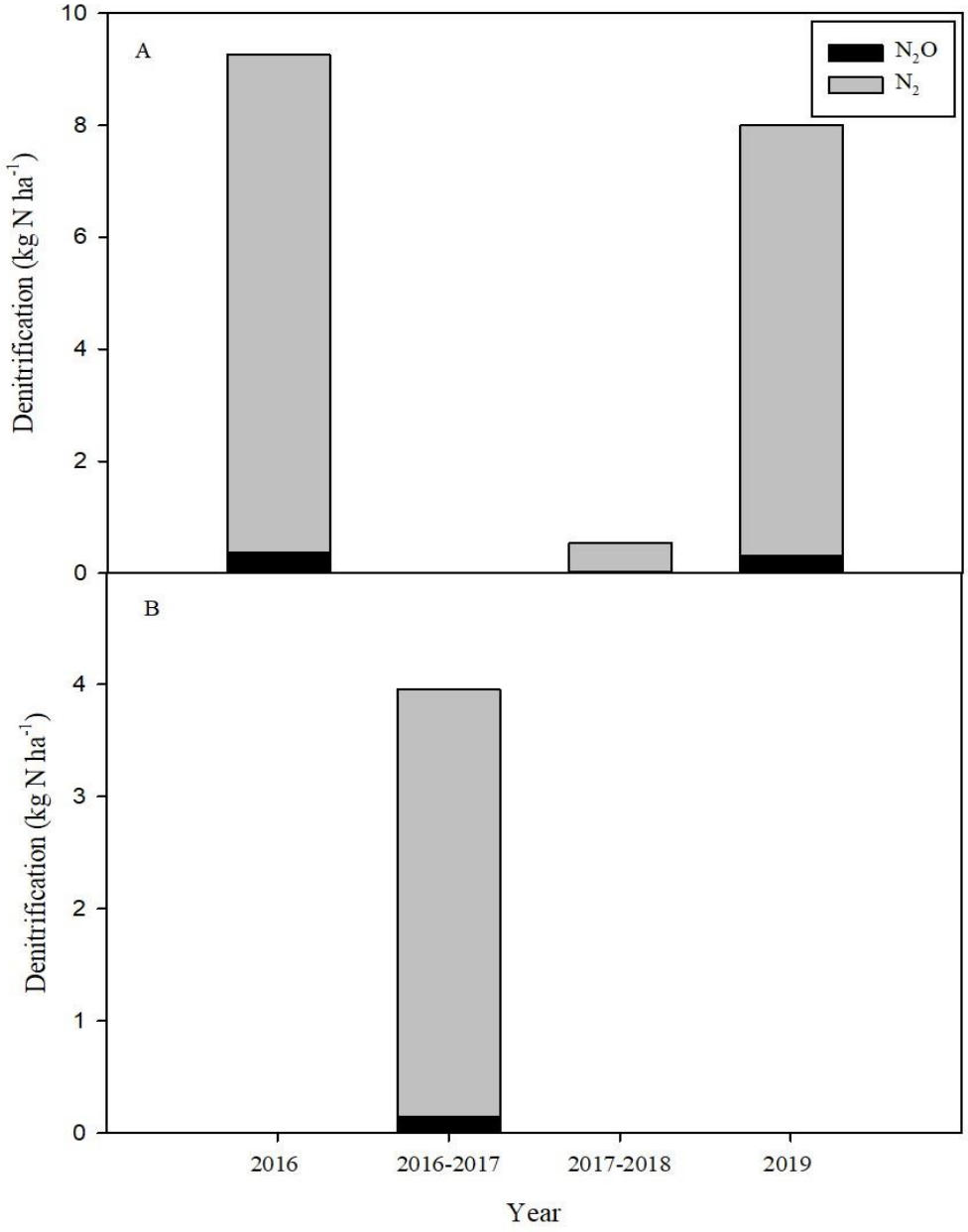

Figure 4.3 A&B: Annual denitrification estimates in 2016 – 2019 for Field 1 (A) and in 2016-2017 for Field 3 (B).

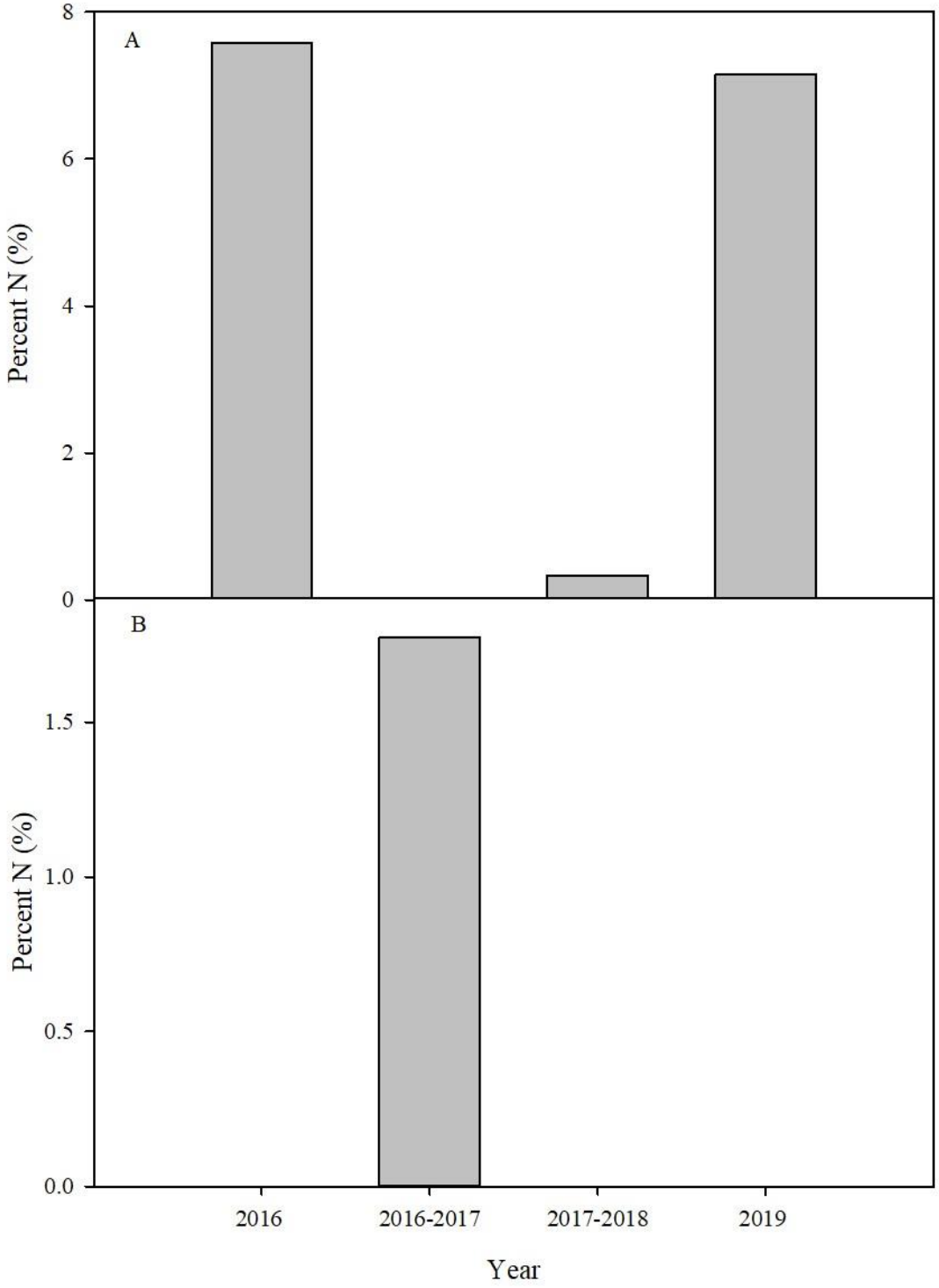

Figure 4.4 A&B: Percentage of applied N fertilizer lost annually through denitrification for Field 1 (A) and for Field 3 (B).

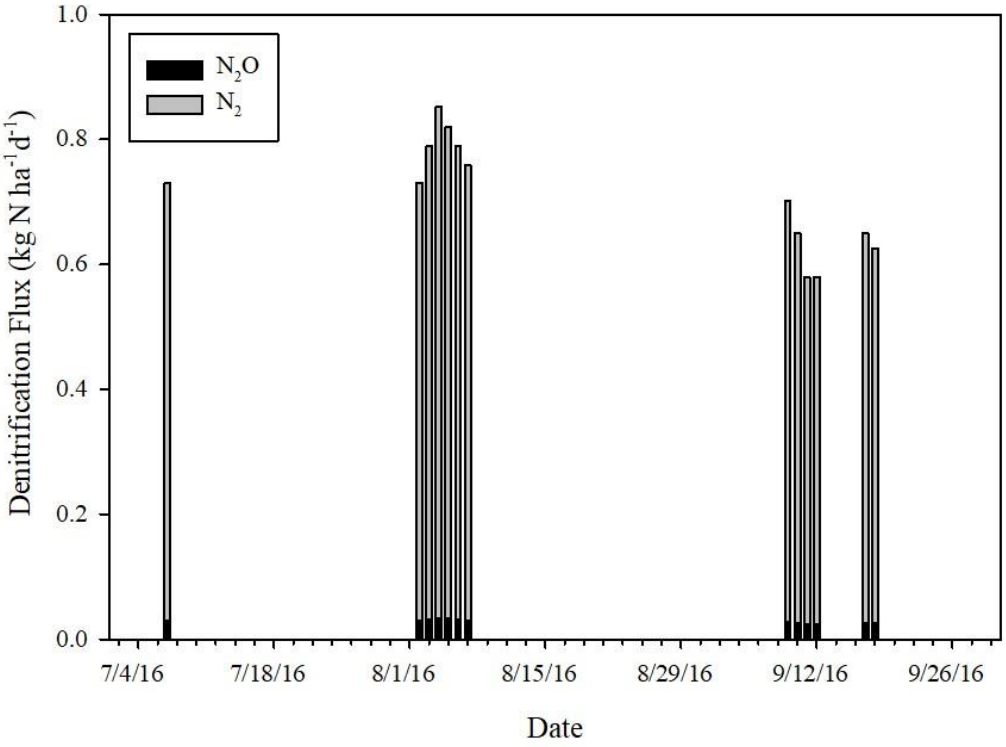

Figure 4.5: Daily total denitrification (N_2O+N_2) measurements for Field 1, grown under corn, in 2016.

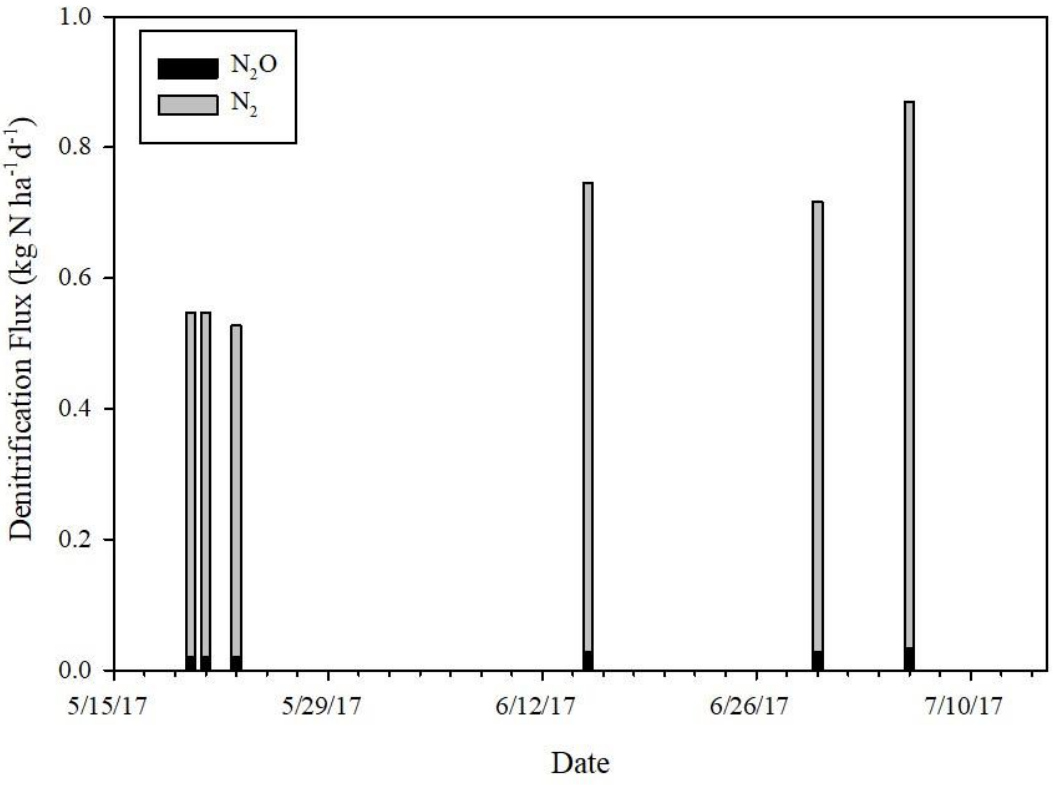

Figure 4.6: Daily total denitrification (N_2O+N_2) estimates for Field 3, grown under corn, in 2016-2017.

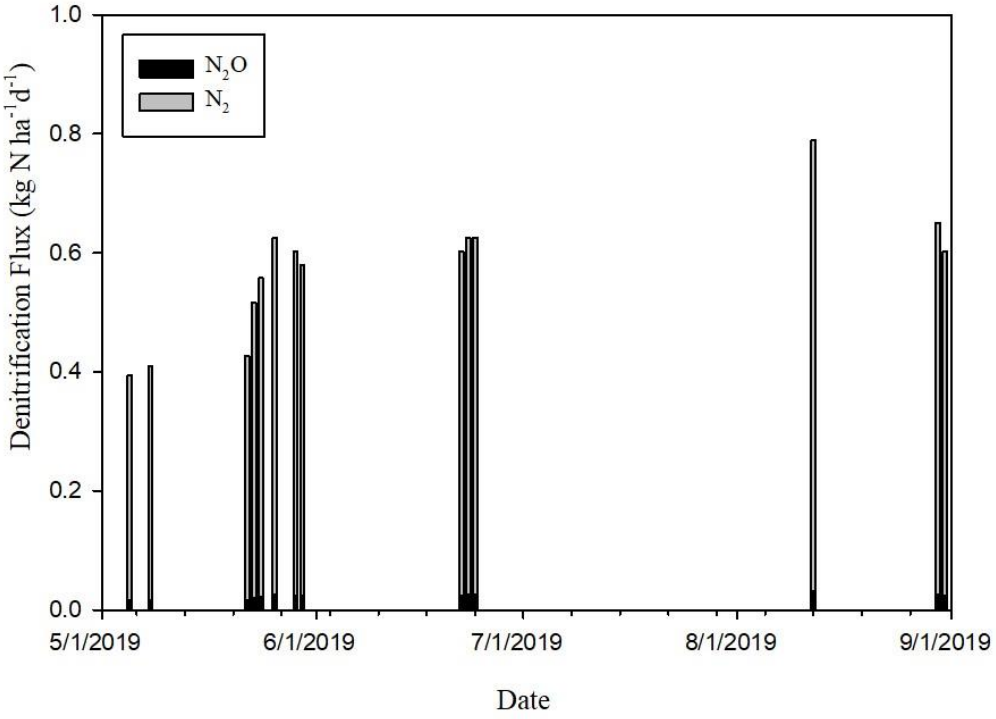

Figure 4.7: Daily total denitrification (N_2O+N_2) estimates for Field 1, grown under corn, in 2019.

CHAPTER 5

CONCLUSIONS

In general, high denitrification potential was expected to result in higher actual denitrification rates. This was not observed, but there were similar spatial patterns between the two. However, actual denitrification was much lower than denitrification potential across all landscape positions. This suggested that using denitrification potential alone may be an effective way to estimate actual emissions but may result in an over-estimation. It is also possible that some significant denitrification events were missed.

The measurements of *nos*Z abundance in combination with the denitrification potential and actual N_2O and N_2 measurements provided insight to the denitrifying community. Generally, gene abundance is associated with microbial activity. Regardless of sequencing method, there were no significant correlations between *nos*Z gene abundance and denitrification measurements. Reverse transcription qPCR, ddPCR, and nanostring sequencing technologies did not successfully capture the landscape dependence as expected and shown in denitrification measurements and other studies. Nanostring sequencing had the lowest *nos*Z abundance measurements and variability, suggesting high specificity for this analysis. It is possible with the use of other *nos*Z primers in combination with abundance measurements of other genes along the denitrification pathway, a significant relationship can be established between denitrifying gene abundance and denitrification flux measurements. Since nanostring sequencing technology allows for the detection of multiple genes, it may be a useful tool when measuring multiple denitrification genes. However, the gene sequencing technology was not correlated to potential or actual denitrification and these methods are of limited utility in their current state.

Many complex denitrification models exist and require several inputs to make estimates. This study demonstrated a unique way to develop a simple model estimating field-scale denitrification using N_2O and N_2 measurements from the NFARM in combination with daily soil moisture and temperature data to estimate annual denitrification flux. This model has an advantage of identifying hot moments, which has proven difficult to incorporate in other models. These estimates were used to determine the importance of denitrification to the N-budget of agricultural systems. With losses accounting for up to 7.2% of applied N fertilizer, the model supported the conclusion the gaseous N loss was a major transport pathway in these claypan fields. It is possible that the processes used to develop this model may be useful in upscaling plot-scale and field-scale measurements to the watershed scale. Using co-kriged estimates, as illustrated in chapter 2, is another way to approach estimating daily and annual denitrification flux as the co-kriged estimates were more conservative and similar to actual denitrification than kriged estimates from the DEA data. To verify our results, extensive daily in-field soil N_2O flux sampling should be conducted to allow the accurate determination of denitrification over multiple growing seasons. It would also aid in developing an efficient way to incorporate the identification and utilization of hot spots and hot moments into this model and many others.

Overall, this study highlights the complexities of denitrification research. Results here illustrate denitrification differences are more likely associated with soil characteristic differences across landscape position rather than crop management in agricultural systems. Although nosZ abundance measurements did not correlate with other measured variables, RT-qPCR, ddPCR, and nanostring sequencing may be useful tools in understanding the genetic component of denitrification. Other molecular sequencing techniques should be investigated to determine the

best method to measure genes involved in denitrification. This study was performed on poorly drained claypan soils, and could yield different results in other soils. Utilizing this information can aid in our scientific understanding of denitrification and the inter-relationships between soil properties, environmental variables, and denitrifying genes and expression in agricultural system, and indicates the need to implement strategies to reduce N_2O emissions.

APPENDIX A

Percent difference between TDR and FDR sensors as a function of time.

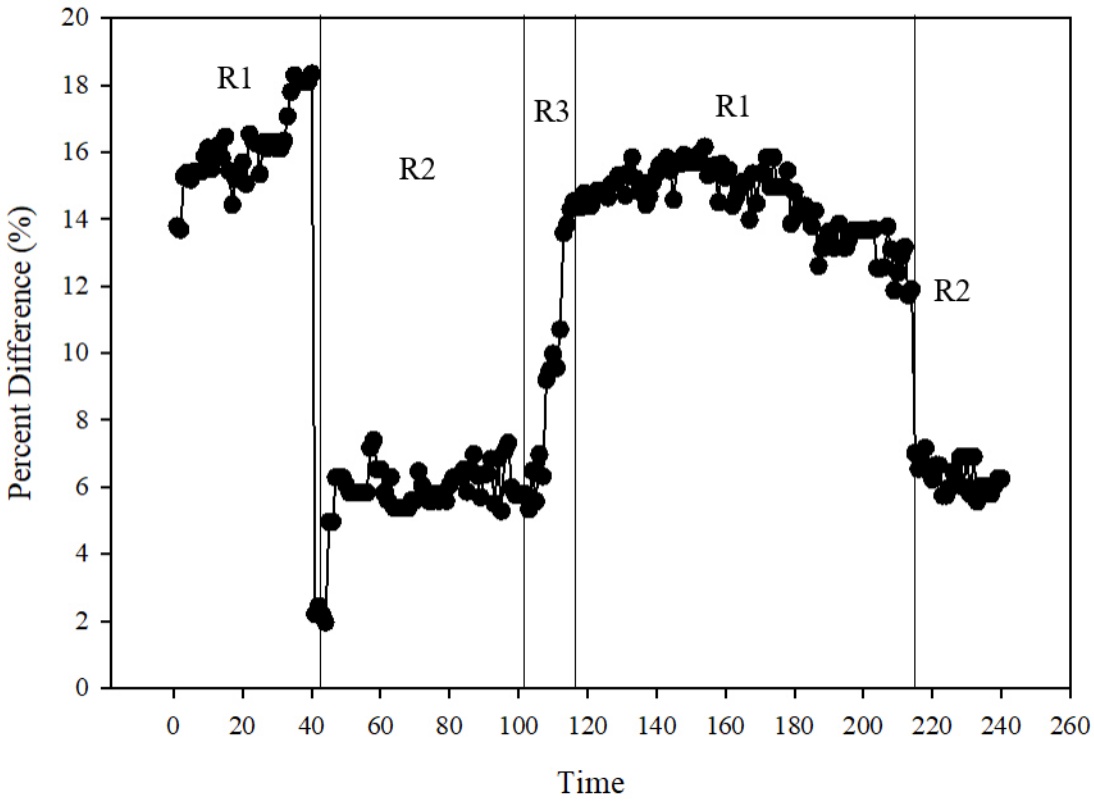

APPENDIX B

Linear relationship used comparing percent difference between FDR and TDR sensors.

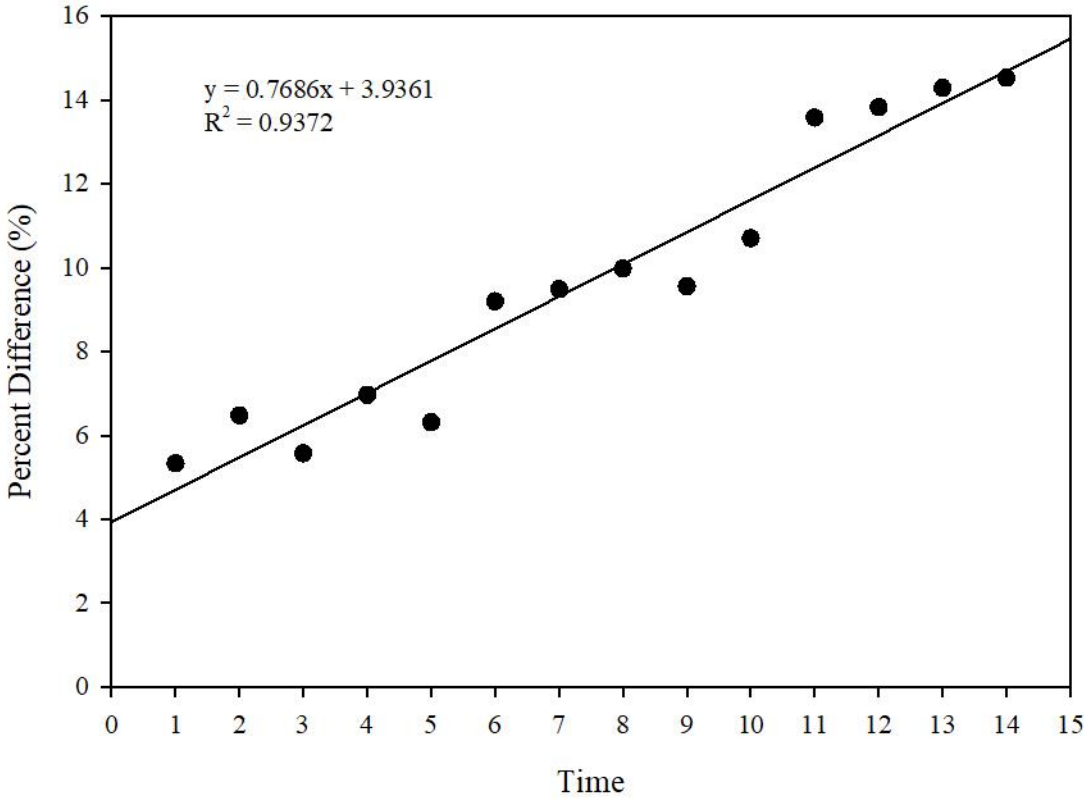

VITA

Frank E. Johnson, II was born in Phoenix, Arizona on July 3rd, 1991. Before starting kindergarten, he and his family moved to Kansas City, Missouri. As an African-American child growing up in Kansas City, he became interested in science because he was intrigued by natural environmental phenomena, such as severe ice storms and tornadoes that occur in the region. The sense of awe and wonderment from those experiences spurred him to learn more about science and how the environment functions. Frank has always sought to excel in science within and outside of academia, but while doing so, tries to remain steadfast in helping others in the community, as well as pursue his interest in music. As exemplified by many great scientists, his pursuits of science, social awareness and the arts are not incompatible and provide him with a unique perspective to contribute to science and society as a scholar.